USGS
science for a changing world

Relations Between Well-Field Pumping and Induced Canal Leakage in East-Central Miami-Dade County, Florida, 2010–2011

Prepared in cooperation with the
Miami-Dade Water and Sewer Department

Scientific Investigations Report 2015–5095

U.S. Department of the Interior
U.S. Geological Survey

Relations Between Well-Field Pumping and Induced Canal Leakage in East-Central Miami-Dade County, Florida, 2010–2011

By Katherine Nemec, Dominick Antolino, Michael Turtora, and Adam Foster

Prepared in cooperation with the
Miami-Dade Water and Sewer Department

Scientific Investigations Report 2015–5095

U.S. Department of the Interior
U.S. Geological Survey

U.S. Department of the Interior
SALLY JEWELL, Secretary

U.S. Geological Survey
Suzette M. Kimball, Acting Director

U.S. Geological Survey, Reston, Virginia: 2015

Suggested citation:
Nemec, Katherine, Antolino, Dominick, Turtora, Michael, and Foster, Adam, 2015, Relations between well-field pumping and induced canal leakage in east-central Miami-Dade County, Florida, 2010–2011: U.S. Geological Survey Scientific Investigations Report 2015–5095, 65 p., http://dx.doi.org/10.3133/sir20155095.

ISSN 2328-0328 (online)

Contents

Figures

Tables

Conversion Factors and Datums

SI to Inch/Pound

Multiply	By	To obtain
	Length	
millimeter (mm)	0.03937	inch (in.)
centimeter (cm)	0.3937	inch (in.)
meter (m)	3.281	foot (ft)
kilometer (km)	0.6214	mile (mi)
	Area	
square meter (m^2)	10.76	square foot (ft^2)
square kilometer (km^2)	0.3861	square mile (mi^2)
	Volume	
cubic meter (m^3)	264.2	gallon (gal)
cubic meter (m^3)	0.0002642	million gallons (Mgal)
cubic meter (m^3)	35.31	cubic foot (ft^3)
	Flow rate	
cubic meter per second (m^3/s)	70.07	acre-foot per day (acre-ft/d)
meter per second (m/s)	3.281	foot per second (ft/s)
meter per day (m/d)	3.281	foot per day (ft/d)
meter per year (m/yr)	3.281	foot per year ft/yr)
cubic meter per second (m^3/s)	35.31	cubic foot per second (ft^3/s)
cubic meter per day (m^3/d)	35.31	cubic foot per day (ft^3/d)
cubic meter per day (m^3/d)	264.2	gallon per day (gal/d)
cubic meter per second (m^3/s)	22.83	million gallons per day (Mgal/d)
	Hydraulic conductivity	
meter per day (m/d)	3.281	foot per day (ft/d)
	Transmissivity*	
meter squared per day (m^2/d)	10.76	foot squared per day (ft^2/d)

Inch/Pound to SI

Multiply	By	To obtain
	Length	
inch (in.)	2.54	centimeter (cm)
inch (in.)	25.4	millimeter (mm)
foot (ft)	0.3048	meter (m)
mile (mi)	1.609	kilometer (km)
	Flow rate	
gallon per minute (gal/min)	0.06309	liter per second (L/s)

Temperature in degrees Celsius (°C) may be converted to degrees Fahrenheit (°F) as follows: °F=(1.8×°C)+32.

Vertical coordinate information is referenced to the National Geodetic Vertical Datum of 1929 (NGVD 29).

Horizontal coordinate information is referenced to North American Datum of 1983 (NAD 83).

Elevation, as used in this report, refers to distance above the vertical datum.

Concentrations of chemical constituents in water are given either in milligrams per liter (mg/L) or micrograms per liter (µg/L).

Abbreviations and Acronyms

C-2	Snapper Creek Canal
CHD	Time-Variant Specified-Head (Package)
CSS	composite-scaled sensitivities
ET	Evapotranspiration
GHB	General Head Boundary (Package)
GMWL	Global Meteoric Water Line
MAE	Mean average error
MNW	Multi Nodal Well (Package)
SL_DOWN	Downstream Snapper Creek Canal Side Looker
SL_MID	Middle Snapper Creek Canal Side Looker
SL_UP	Upstream Snapper Creek Canal Side Looker
USGS	U.S. Geological Survey
VSMOW	Vienna Standard Mean Ocean Water

Acknowledgments

This report was a collaborative effort accomplished with the cooperation of many individuals and organizations. The authors would like to thank Virginia Walsh, Maria MacFarlane, and Sonia Villamil of the Miami-Dade Water and Sewer Department for providing data and logistical support throughout the study.

Several staff members from the U.S. Geological Survey (USGS) Caribbean-Florida Water Science Center, Davie office, contributed to this report. Christian Lopez collected groundwater-level and index velocity data during regular site visits. Mike Oliver constructed the canal monitoring sites so that the sites could be pulled in and out of the canal during canal cleaning operations. Michael Wacker provided hydrogeologic insight and guidance used in the groundwater model. Michele Markovits performed data collection at the well-field. Jeffrey Robinson assisted with the initial well-field drilling and data collection. Richard Westcott developed the 3-dimensional geomodel used for the model grid delineation. Barclay Shoemaker provided significant assistance and insight in many areas of the initial project development. Eve Kuniansky of the USGS Water Science Field Team Groundwater Specialist for Southeast Region, provided guidance that improved the groundwater model. Brian Katz, formerly of the USGS Caribbean-Florida Water Science Center, provided guidance with the isotope analysis, and David Sumner of the USGS Caribbean-Florida Water Science Center provided assistance describing the evapotranspiration data collection. John Williams of the USGS New York Water Science Center also provided insight and guidance on hydrogeology used in the groundwater model.

Relations Between Well-Field Pumping and Induced Canal Leakage in East-Central Miami-Dade County, Florida, 2010–2011

By Katherine Nemec, Dominick Antolino, Michael Turtora, and Adam Foster

Abstract

An extensive canal and water management system exists in south Florida to prevent flooding, replenish groundwater, and impede saltwater intrusion. The unconfined Biscayne aquifer, which underlies southeast Florida and provides water for millions of residents, interacts with the canal system. The Biscayne aquifer is composed of a highly transmissive karst limestone; therefore, canal stage and flow may be affected by production well pumping, especially in locations where production wells and canals are in proximity.

The U.S. Geological Survey developed a local-scale, transient, numerical groundwater flow model of a well field in Miami-Dade County to (1) quantify relations between well-field pumping and C-2 Canal (herein referred to as the Snapper Creek Canal) leakage, (2) determine primary controls on canal leakage variability, and (3) summarize results that could simplify characterization of canal/well-field interactions in other locations. In addition to the groundwater model development, stable isotope data from water-quality samples were used to characterize the relations between production well pumping and canal leakage. The results from the groundwater model and the isotope data were used to refine the conceptual flow model of the study area.

The groundwater flow model MODFLOW-NWT was used for simulating groundwater flow and quantifying interactions between pumping from the well field and Snapper Creek Canal leakage. Input data for the groundwater model included precipitation, evapotranspiration, pumping, canal stage, and regional groundwater elevation. The inverse modeling tool UCODE and groundwater data from June 2010 to July 2011 were used to calibrate the model. Parameter sensitivity analyses were performed with UCODE. Model sensitivities to geologic heterogeneity, non-laminar flow, and changes in the regional flow boundary were evaluated. The groundwater model generally fits the calibration criteria well within estimated error ranges for groundwater elevations and canal leakage values. The mean average error for heads simulated with the model was 0.19 meter, and head residuals were generally randomly distributed.

The model simulated groundwater flow under ambient conditions without production well pumping to establish background leakage. Groundwater flow also was simulated with production well pumping to estimate induced leakage from the Snapper Creek Canal that occurs in response to pumping.

Canal leakage was quantified as a percentage of total canal leakage. The percentage of leakage during pumping increased non-linearly with pumping rate, indicating a decreasing sensitivity of canal leakage to pumping at relatively large pumping magnitudes. The results for Snapper Creek Canal may serve as an upper limit for well-field interaction with surface-water features in Miami-Dade County, given the proximity (about 50 meters) of the pumping wells in this study to the Snapper Creek Canal.

The isotopic compositions of hydrogen (H) and oxygen (O) in groundwater samples were used to distinguish sources for groundwater within the study area and to assess the extent of natural mixing and pumping-induced mixing with water in the Snapper Creek Canal. Water-level data and water-quality samples were collected from monitoring well clusters, production wells, and the Snapper Creek Canal during discrete sampling events under ambient and pumping conditions. Trends in the isotope data generally follow the regional west-to-east hydraulic gradient across the study area. Data collected within the monitoring-well clusters in closest proximity to the canal indicate that groundwater/surface-water interactions are greatest within the shallow flow zone of the aquifer, especially during pumping conditions. The isotopic composition of samples collected within the study area indicates that the shallow, highly transmissive preferential flow zone receives substantial recharge from the canal. The isotope data from the production wells, which are open to the deeper flow zone within the aquifer, indicate only traces of mixing with a ^{2}H- and ^{18}O-enriched source, suggesting little canal admixture with waters of the deeper flow zone.

Results from the groundwater model and the stable isotope data analysis indicate the importance of considering geologic heterogeneity when investigating the relations between pumping and canal leakage, not only at this site, but also at other sites with similar heterogeneous geology. The model results were consistently sensitive to the hydrogeologic framework and changes in hydraulic conductivities. The model and the isotope data indicate that the majority of the groundwater/surface-water interactions occurred within the shallow flow zone. A relatively lower-permeability geologic layer occurring between the shallowest and deep preferential flow zones lessens the interactions between the production wells and the canal.

Introduction

Groundwater pumping in the Biscayne aquifer may cause large losses of water as leakage from the extensive surface-water canal system in south Florida. The Biscayne aquifer is a highly transmissive karst limestone aquifer that contains permeable flow zones in the shallow and deep parts of the aquifer and is designated by the U.S. Environmental Protection Agency as a sole-source aquifer in the region (U.S. Environmental Protection Agency, 2013). The high-permeability flow zones likely provide the majority of water supply from the Biscayne aquifer in Miami-Dade County. The South Florida Water Management District uses the multipurpose surface-water canal system as a water-resource management tool to alleviate flooding during the wet season and to release water from the Everglades during the dry season to provide aquifer recharge and maintain groundwater levels sufficient to inhibit saltwater intrusion. The canal system commonly intersects the shallowest flow zone of the Biscayne aquifer. This intersection provides a pathway for interactions between the Biscayne aquifer and the surface-water canals.

To address concerns about leakage of canal water to the surrounding aquifer as a result of groundwater pumping, the U.S. Geological Survey (USGS), in cooperation with the Miami-Dade Water and Sewer Department, initiated a comprehensive study in 2008 to evaluate the contribution of surface water in the canal system to pumped groundwater. A production well field area was selected for study due to its proximity to a primary canal. A hydrologic budget was calculated for the aquifer to account for inflows and outflows, including exchanges between the surface-water and groundwater systems, and hydrologic properties that control the flows and exchanges within the system were quantified. The study included multiple components in an effort to better understand the hydrologic interactions at the site. Cores and lithologic and borehole geophysical data were collected to characterize the stratigraphy; canal discharge, precipitation, and evapotranspiration (ET) data were collected for use in hydrologic budget calculations; hydraulic testing was done to estimate hydraulic conductivity; a well-field-scale groundwater flow model was developed to simulate flow at the well field; and stable-isotope data were collected to identify groundwater sources and pathways. Snapper Creek well field in east-central Miami-Dade County was selected for the comprehensive study because it is divided by the Snapper Creek Canal (fig. 1); production wells at the well field are located near the canal. The canal is likely more strongly affected by groundwater pumping than other canal reaches located farther away from production well fields in Miami-Dade County, Florida; therefore, the configuration at this location may represent an upper-limit case for well-field interactions with surface-water features.

As part of the overarching objective of the study to quantify groundwater-canal exchange, a hydrogeologic framework of the Biscayne aquifer in Miami-Dade County was developed, as documented in Wacker and others (2014). Flow zones were identified and hydraulic properties were estimated, allowing a detailed characterization of the distribution and connectivity of flow zones, hydrogeologic characteristics of these flow zones, and flow pathways existing between the flow zones and production wells.

Purpose and Scope

The purpose of this report is to describe the effects of well-field pumping on groundwater flux between the canal and the aquifer. Groundwater modeling was used to calculate a flow budget that accounts for flows into and out of the aquifer during the study period and to estimate differences in canal leakage with and without groundwater pumping at the well field. Hydrogen and oxygen stable isotope data from the canal, monitoring wells, and production wells were used to characterize pathways of surface water and local groundwater to pumping wells. These data were then used to estimate contributions of surface-water recharge to the aquifer within the study area.

This report documents the numerical model that was developed to simulate groundwater flow at the study area during June 2010–July 2011 to evaluate the relation between well-field pumping and canal leakage. The numerical model incorporates all significant aspects of the conceptual flow at the study area (fig. 2). Data used to construct and calibrate the model are described, and the fit of the model to hydrologic data is quantified. Flow budgets and a quantification of canal leakage response to pumping are presented. Model results using an alternate set of boundary conditions and using a simplified hydrogeologic realization are presented and compared with the calibrated model. A model sensitivity test incorporating non-laminar flow is also described, and limitations of the analysis are discussed.

This report also presents water-quality data collected from October 2008 to November 2011 for evaluation of the relation between groundwater and surface water in the Snapper Creek study area. The isotopic composition of water samples were analyzed in relation to canal stage and groundwater levels to describe the hydrologic conditions during

ambient, non-pumping conditions. The effects of production well pumping on the local system are discussed based on two separate sampling events conducted in November 2010. A simple mixing analysis was used to estimate the mixing contributions of two identified end-members within the sampled wells.

Description of the Study Area

The study area includes about 2.19 square kilometers (km^2) of land in east-central Miami-Dade County, the Snapper Creek well field, and a section of the Snapper Creek Canal (fig. 1). The study area is flat with a land surface elevation of approximately 2.3 meters (m) above the National Geodetic Vertical Datum of 1929 (NGVD 29). Sand and rock fill constitute the topsoil in the well field, which has a cover of bahiagrass. Urban residential neighborhoods and commercial areas surround the well field, which was built and began operating in 1976. The Snapper Creek Canal traverses the well field from northwest to southeast; production pumping wells S-3011 and S-3012 are northeast of the canal, and production wells S-3013 and S-3014 are southwest of the canal. Each production pumping well can withdraw about 38,000–45,000 meters cubed per day (m^3/d).

The study area receives about 155 centimeters (cm) of precipitation annually (Renken and others, 2005). The majority of the rainfall occurs during the wet season (June–September) and recharges the canal and the well field; much of the rainfall is eventually lost to ET, and a small amount is lost to runoff. During the dry season, canal control structures release water upstream of the study area to maintain sufficient stage (water level) in the canal to promote groundwater recharge. The water that reaches the aquifer from rainfall through pervious surfaces and canal recharge mixes with the regional groundwater already present in the aquifer. The groundwater that is withdrawn from the aquifer is a mixture of recharge through pervious surfaces, regional flow, and water that leaks out of the surface-water canal.

The geology of the Biscayne aquifer underlying the study area is heterogeneous and karstic. At the well field, multiple flow zones have been identified in the aquifer, and the production wells are open to multiple flow zones, resulting in spatially varied responses in groundwater flow patterns induced by pumping. Evidence for non-laminar flow within the Biscayne aquifer has been reported by Parker and Glass (1951), DiFrenna and others (2008, and Cunningham and others (2009).

Hydrogeologic Framework

The Biscayne aquifer in east-central Miami-Dade County is composed of the Miami Limestone and Fort Thompson Formations (fig. 3). The Miami Limestone extends about 20 feet (ft) (6.1 m) below land surface and is underlain by the Fort Thompson Formation. The Tamiami Formation lies beneath the Fort Thompson Formation and generally marks the base of the Biscayne aquifer.

The hydrogeologic framework of the Biscayne aquifer at the study area has been characterized by using a variety of geophysical techniques, core analyses, and hydraulic tests (Wacker and others, 2014). Borehole geophysical data were collected from six continuously cored test holes within the study area. Flowmeter data were collected by measuring the vertical fluid flow in the coreholes. Borehole fluid data were obtaining by using acoustic borehole imaging to visualize borehole geometry. Both data types were collected during scheduled periods of non-pumping. These data were used to estimate hydrologic properties of the aquifer, characterize lithologic and stratigraphic units, and identify the base of the Biscayne aquifer. The 6 test holes were converted to monitoring wells, and an additional 17 monitoring wells were constructed, yielding a total of 23 monitoring wells in 6 clusters (fig. 1*B*). The naming system used in this report for the monitoring wells and clusters can be found in appendix 1 (table 1–1). Because of errors in elevation data at cluster 4, the data from that cluster were not used in this study. The majority of the monitoring wells remained open holes after completion, with the exception of several that were screened to prevent infilling (Wacker and others, 2014). Monitoring well construction information can also be found in appendix 1 (table 1–1).

Data from the coreholes were used to determine that production and monitoring wells in the Biscayne aquifer in the study area are open to two predominant types of flow zones, which are characterized by differences in porosity. One type consists of dense limestone or sandstone and is characterized by primarily interparticle, or "matrix," porosity (Wacker and others, 2014); the permeability is relatively low (fig. 4). Flow zones of this type are henceforth referred to as matrix flow zones. The second type of flow zone is more permeable than the first type and is mainly composed of highly burrowed limestone with large hydraulic conductivity values (Wacker and others, 2014). Flow zones of this type are henceforth referred to as preferential flow zones. Hydraulic conductivity values for preferential flow zones can be two orders of magnitude or greater than those of the matrix flow zones (Wacker and others, 2014).

The Snapper Creek Canal is cut into a shallow preferential flow zone in the study area and is separated from additional preferential flow zones at the base of the aquifer by a leaky matrix flow zone. Relative to the preferential flow zone type, the matrix flow zone type acts as a semi-confining unit, although some flow does occur in the matrix flow zones.

Additionally, horizontal and vertical dissolution cavities are present in the study area (fig. 2; vertical solution pipes). These dissolution cavities may serve to breach the leaky matrix flow zone and provide a more direct pathway for canal water to leak into the production zone (Wacker and others, 2014).

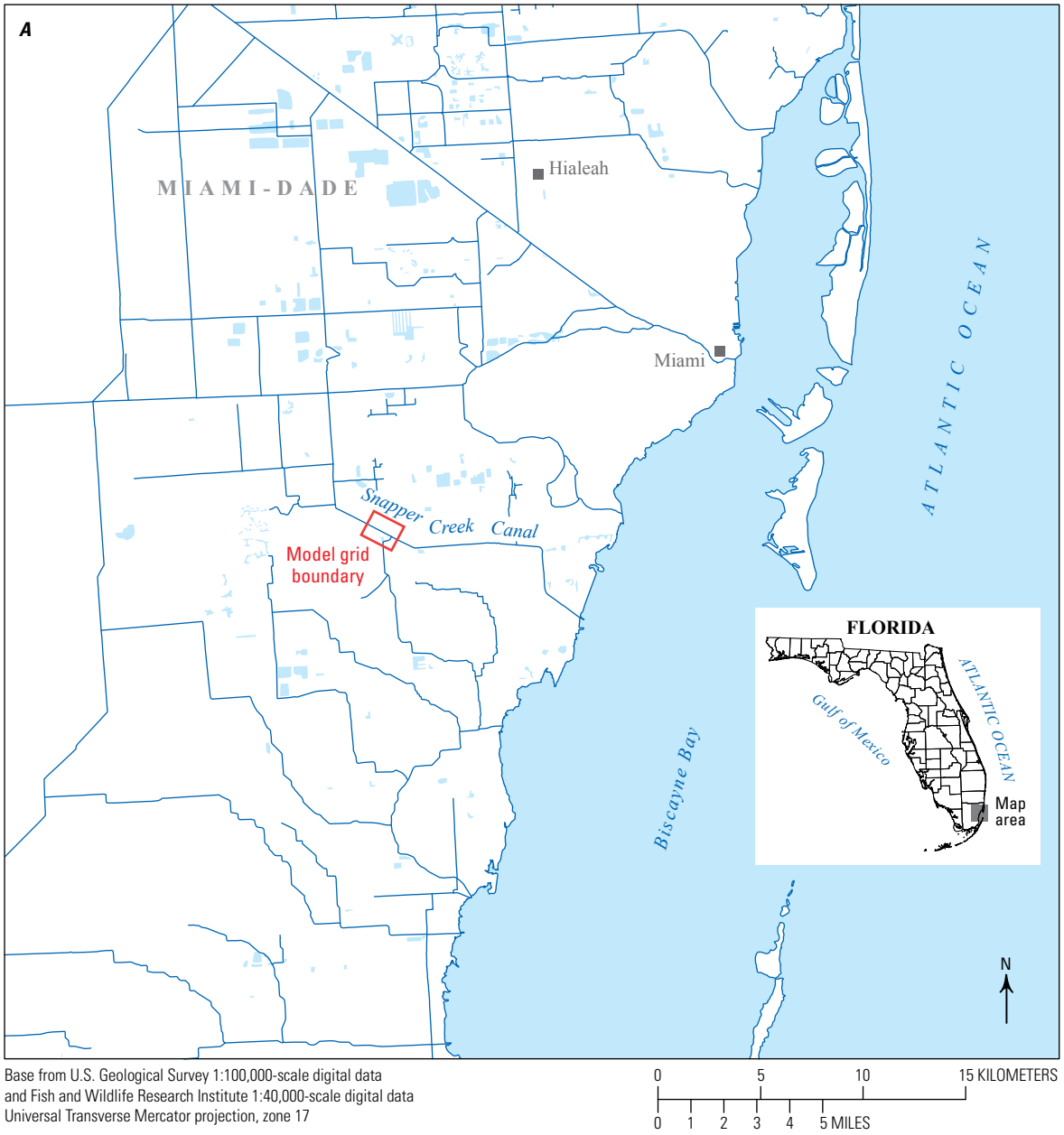

Figure 1. Locations of (*A*) the Snapper Creek well field in Miami-Dade County and (*B*) the Snapper Creek Canal and production pumping and monitoring wells at the Snapper Creek well field.

Conceptual Model of Groundwater Flow within the Study Area

The Snapper Creek Canal intersects the uppermost preferential flow zone within the Biscayne aquifer (fig. 2). At the Snapper Creek well field, the canal sides are in direct contact with the preferential flow zone, whereas the bottom of the canal is in contact with the less permeable matrix flow zone; therefore, more groundwater exchange is likely to occur through the canal sides than through the canal bottom. The matrix flow zone underlying the canal acts as a semi-confining layer, restricting flow between the upper and lower preferential flow zones, although some flow does occur in the matrix flow zone. Vertical dissolution cavities that have been observed in the study area also have the potential to greatly enhance flow through the matrix and allow hydraulic connection between the upper and lower preferential flow zones. Production well pumping in the deeper zone creates a vertical hydraulic gradient that induces flow downward through the Biscayne aquifer, either through the matrix and preferential flow zones, or through the vertical solution pipes that exist within the aquifer. Flow through the base of the Biscayne aquifer to underlying formations is negligible.

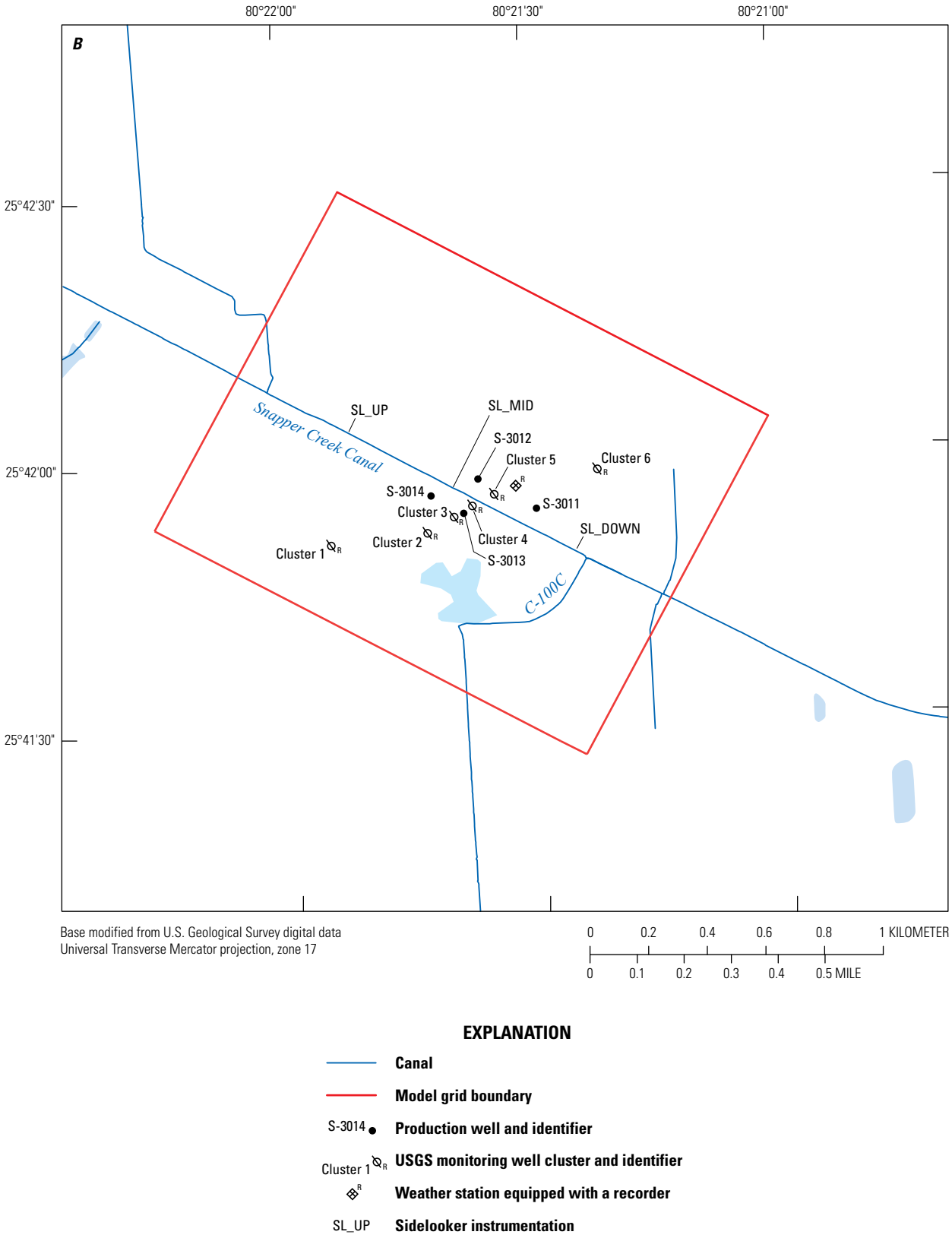

Figure 1. Locations of (*A*) the Snapper Creek well field in Miami-Dade County and (*B*) the Snapper Creek Canal and production pumping and monitoring wells at the Snapper Creek well field. —Continued

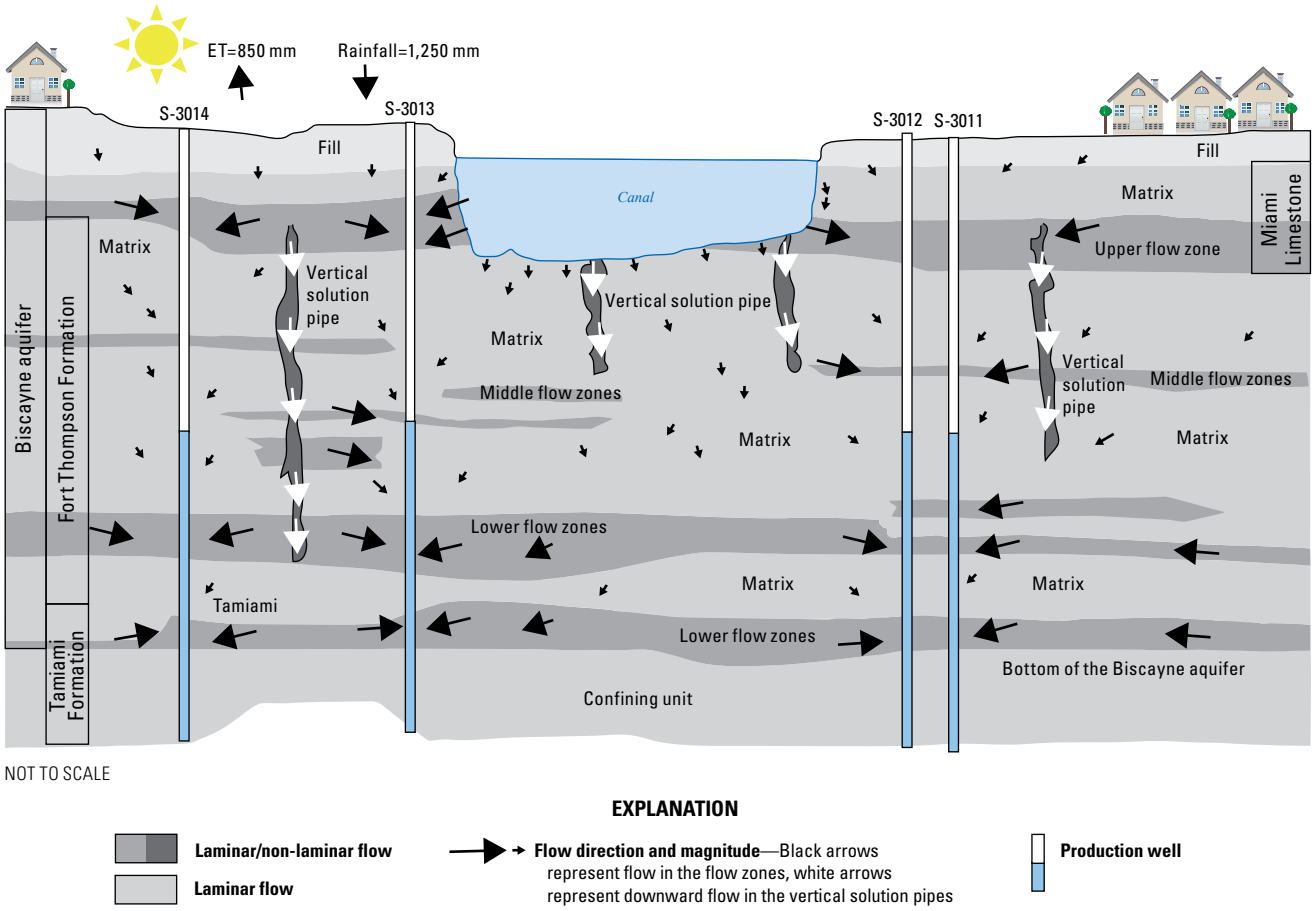

Figure 2. Conceptual hydrogeologic cross section and flow patterns at the Snapper Creek Canal study area, Miami-Dade County, Florida. [ET, evapotranspiration; mm, millimeters]

Groundwater recharge within the study area occurs through precipitation, canal losses, and regional groundwater flow into the model area (fig. 5). Stresses to the system causing a loss of water at the local study-area scale include production well pumping, evapotranspiration, runoff, discharge into the canal during gaining conditions, and regional groundwater flow out of the model area. These inputs and stresses vary depending on atmospheric conditions, groundwater levels within the model area, canal stage, and groundwater elevation outside of the model boundaries. While the period of study is 14 months, canal discharge data are missing for the months of June and July 2010 and February 2011; therefore, only 11 months of canal discharge data are used in this study.

Previous Studies

Meyer (1971) and Swayze (1988) quantified flow between canals and water conservation areas in Florida. Meyer constructed hydrologic profiles to determine water movement and leakage at Lake Okeechobee by using water-level, chloride-concentration, and water-temperature data. The study indicated that the majority of the leakage occurred under the dike through shell and limestone beds. Swayze quantified the flow between a canal in Broward County and the underlying aquifer by finding the difference between upstream and downstream flow in the canal. Results were reported as volumetric flow per unit canal length per unit head difference between the canal and each respective water conservation area, and the results indicated water from the aquifer was recharging the canal.

Chin (1990) derived analytical canal leakage estimates that depended upon drawdown in the aquifer on both sides of a canal (asymmetric water table distributions). The analytical solutions presented in Chin (1990) are only accurate when aquifer thickness is less than 3 canal widths and drawdowns are measured beyond 10 canal widths from the center of the canal (Bouwer, 1965; Chin 1990). The well field that is the focus of this study contains production wells that are located less than 10 canal widths from the center of the Snapper Creek Canal, which violates limitations of existing analytical solutions.

Sherwood and Leach (1962) and Sunderland and Krupa (2007) quantified Snapper Creek Canal leakage in response to control structure operations and well-field pumping. Sherwood

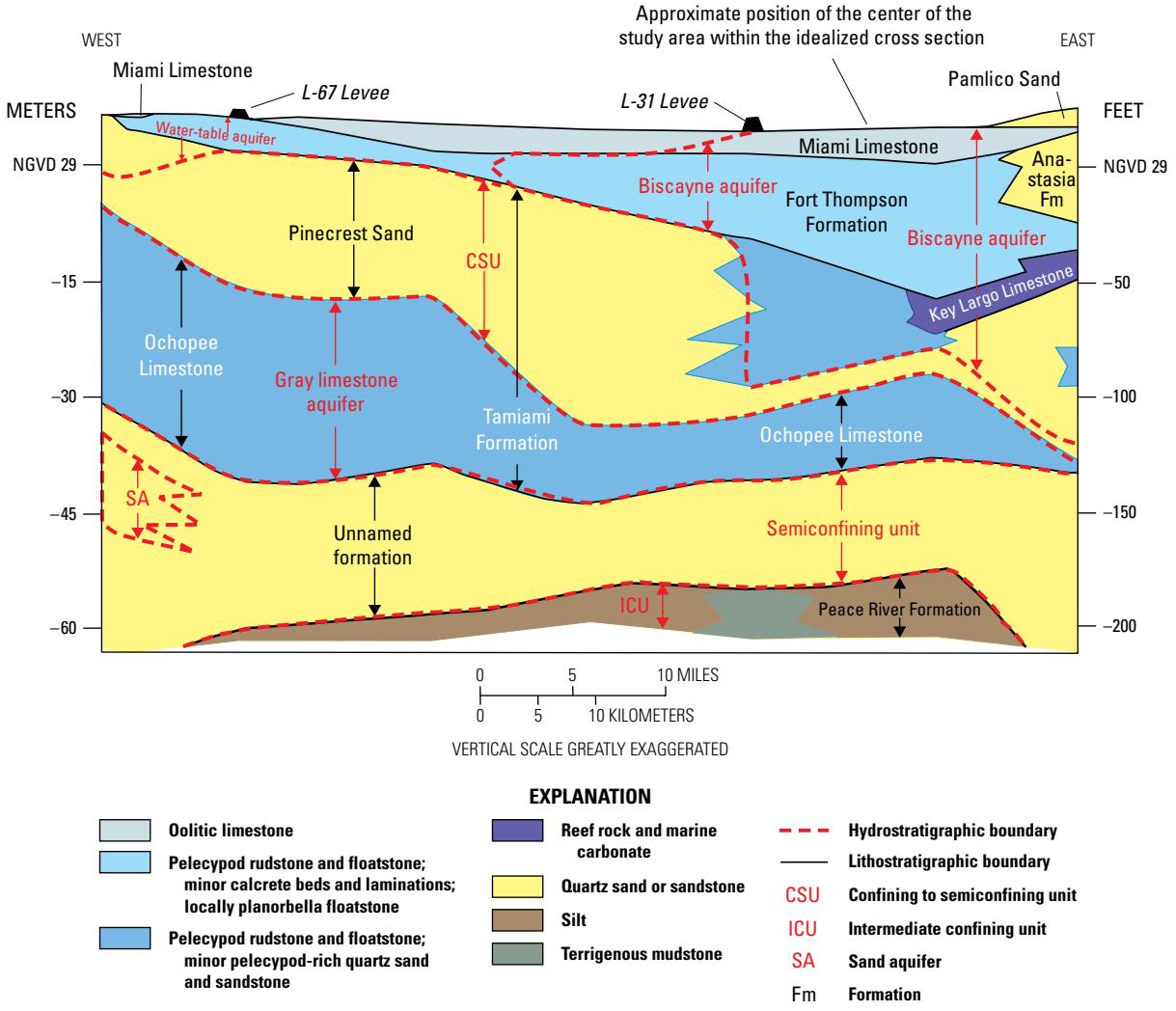

Figure 3. Relation of geologic and hydrogeologic units of the surficial aquifer system across central Miami-Dade County, north of the Snapper Creek well field study area (Cunningham and others, 2006a; original modified from Reese and Cunningham, 2000).

and Leach (1962) indicated that during a severe drought, about 1.5 cubic meters per second (m^3/s) of surface-water flow would be necessary to maintain the canal stage at 0.83 m at the Snapper Creek Canal control structure. Sherwood and Leach (1962) also reported that during a severe drought a large part of the water withdrawn from local well fields would probably be derived from the Snapper Creek Canal. Sunderland and Krupa (2007) suggested that a portion of freshwater flow to Biscayne Bay from the Snapper Creek Canal is lost due to leakage caused by pumping from the Snapper Creek well field in Miami-Dade County. A loss of 0.56 m^3/s along the reach of the Snapper Creek Canal to the northwest of the well field was attributed solely to groundwater withdrawals of equivalent magnitude (0.56 m^3/s). Further study was recommended by Sherwood and Leach (1962) and Sunderland and Krupa (2007) due to changes in the canal system and uncertainties in canal leakage results created by wind, low canal-flow velocities, and inexact well-field pumping rates.

Model Simulation of Study Area Hydrology

A transient, three-dimensional, groundwater flow model was developed to evaluate the effects of well-field pumping on surface-water and groundwater interactions in the study area. The model was constructed with a detailed representation of the hydrogeologic framework. Sensitivity analyses were performed to guide calibration and identify parameters that are

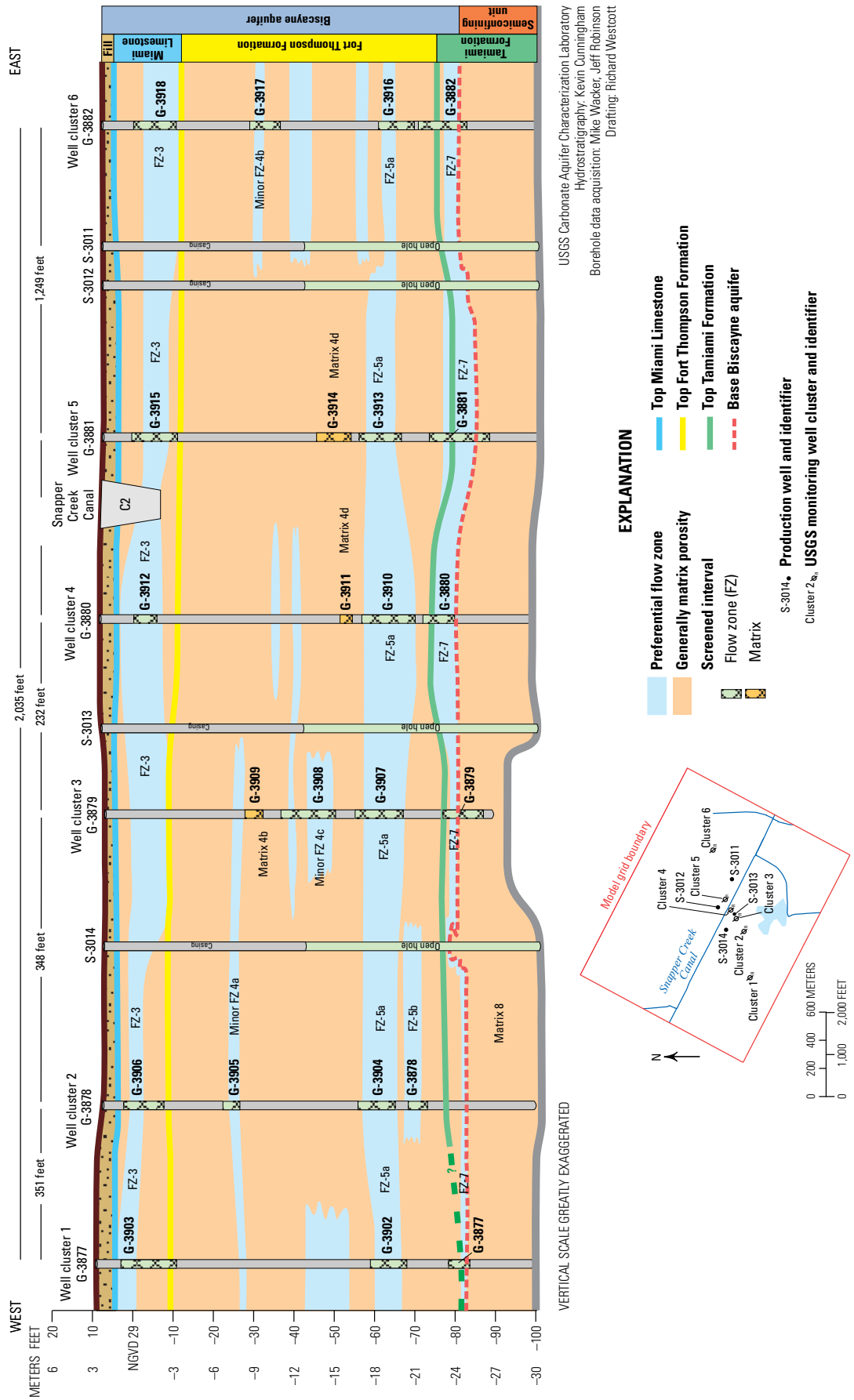

Figure 4. Hydrogeologic cross section of the Snapper Creek well field, Miami-Dade County, Florida.

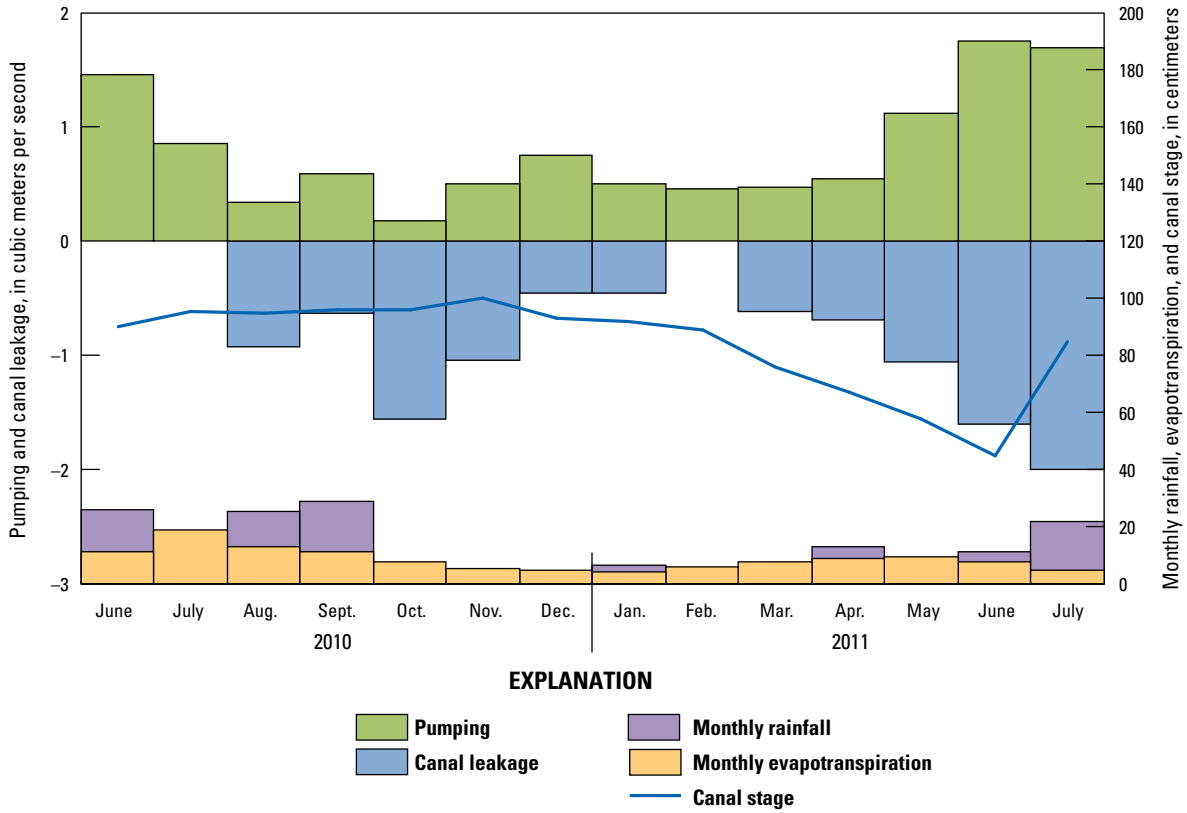

Figure 5. Mean monthly canal leakage, groundwater pumping, and canal stage and cumulative monthly rainfall and evapotranspiration near the Snapper Creek Canal, Miami-Dade County, Florida, 2010–2011.

most important for simulating groundwater levels and canal leakage. Additionally, conceptual model testing was performed to evaluate the model sensitivity to geologic heterogeneity and changes in the regional flow boundaries. The groundwater model was calibrated by adjusting the most sensitive parameters using "trial and error" and inverse-modeling methods (Poeter and others, 2005). Model fit was evaluated by using observed water levels and estimated canal leakage. Groundwater model simulations were completed with and without groundwater pumping to determine the effect of well-field pumping on canal leakage.

Numerical Model Construction

The groundwater model was constructed by using MODFLOW-NWT (Niswonger and others, 2011).

Governing Groundwater Flow Equation

MODFLOW-NWT (Niswonger and others, 2011) solves the following partial differential equation for groundwater flow:

$$\frac{\partial}{\partial x}\left(K_{xx}\frac{\partial h}{\partial x}\right)+\frac{\partial}{\partial y}\left(K_{yy}\frac{\partial h}{\partial y}\right)+\frac{\partial}{\partial z}\left(K_{zz}\frac{\partial h}{\partial z}\right)+W=S_s\frac{\partial h}{\partial t}\,, \qquad (1)$$

where

K_{xx}, K_{yy}, and K_{zz} are the values of hydraulic conductivity [L/T] along the x, y, and z coordinate axes, which are assumed to be parallel to the major axes of hydraulic conductivity;

h is the potentiometric head [L];

W is a volumetric flux per unit volume [1/T] representing sources and (or) sinks of water, with $W<0.0$ for flow out of the groundwater system, and $W>0$ for flow into the system;

S_s is the specific storage [1/L] of the porous material; and

t is the time [T].

Spatial and Temporal Discretization

A three-dimensional finite-difference model grid was designed with 60 rows, 83 columns, and 30 convertible layers, which are able to change from confined to unconfined conditions. The grid cell size increased as distance increased from the Snapper Creek Canal and surrounding production wells (fig. 6).

The largest cells were 50 m in length and width at the perimeter of the model grid. The smallest cells were 7 m

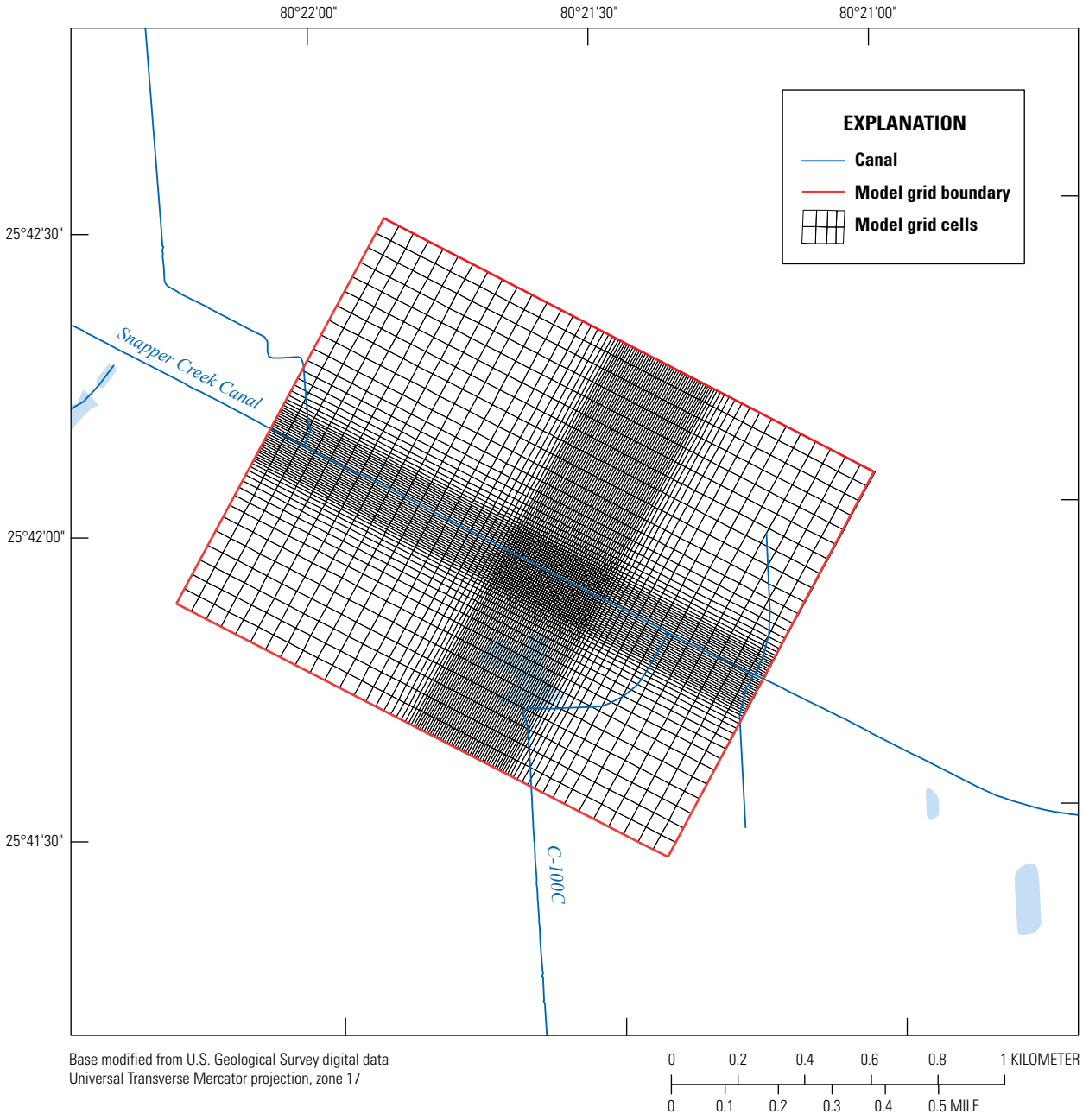

Figure 6. Model domain for the groundwater model showing model grid and perimeter boundary, Snapper Creek Canal study area, Miami-Dade County, Florida.

in length and width near the Snapper Creek Canal. Model layers 2 through 30 were uniformly 1 m thick. The thickness of layer 1 varied with land surface elevation. The thickness of the top layer was set equal to land surface elevation within each model cell. Land surface elevation varied from 4 to 6 ft (1.2 to 1.8 m) above NGVD 29. The model layers do not directly correspond to the flow units in the model. In most cases, the flow units extend through multiple layers vertically and may or may not be laterally extensive for each model layer that is intersected.

The study period from June 2009 to July 2011 was simulated by using 26 stress periods. Each stress period represented 1 month. Because errors in the initial head conditions can propagate into calibration stress periods and affect model estimates of water levels and flows in transient numerical models, the first 12 months are considered "warm-up" stress periods which were developed to minimize the consequences of errors in the initial head distribution. Hydraulic conductivity values for the Biscayne aquifer are comparable to those at the higher end of the range in the deeper Floridan aquifer

system. Sepulveda and others (2012) determined that error in initial condition with monthly stress periods was no longer present within model layers representing the Floridan aquifer after 7 months, thus a 12-month warm-up period was considered adequate for this model. Data collected from canals, pumping wells, a weather station, and groundwater wells were used to set the canal stage specified-head boundary condition, input pumping amounts, apply net recharge, and obtain head observations for the "warm-up" period by employing the same methods used for the calibration period described in the following sections. The final 14 months of the study period represented the calibration period. Each of the 26 stress periods was 1 time step, except for the first stress period of the calibration period, which was divided into 10 uniform time steps to facilitate convergence.

Assignment of Boundary Conditions

Boundary conditions are often based on natural hydrologic features such as rivers or groundwater divides. Pumping wells and net recharge from rainfall also can serve as boundaries. Where natural boundaries do not occur, they are imposed, such as inflows and outflows through the simulated boundary conditions from the external or regional groundwater system. Boundary conditions used in this model included no-flow, specified head, and head-dependent fluxes. These boundary conditions are implemented by using several MODFLOW packages and describe flow into and out of the groundwater system from canals, net recharge, and groundwater pumping and flow into and out of the aquifer from the regional aquifer system beneath the study area.

Canals

Exchange between the Snapper Creek Canal and the Biscayne aquifer was represented by the Constant-Head Boundary (CHD) Package (Leak and Prudic, 1991). Controlling heads for the CHD were derived from USGS stream gages located upstream (SL_UP), downstream (SL_DOWN), and within (SL_MID) the study area (fig. 1*B*) for each stress period. Canal stage data were collected at these three locations at 15-minute intervals using side-scan acoustic Doppler velocity meters. Mean daily and monthly canal stage from June 2010 to July 2011 (fig. 5) was computed as the average of instantaneous stage measurements taken every 15 minutes.

Groundwater Pumping

Pumping stresses were applied in cells that contained production wells. The Multi-Nodal Well Package (MNW) (Konikow and others, 2009) was used to distribute pumping according to the hydraulic conductivity of formations that intersect a well's open-hole interval. Flow between the aquifer and borehole can vary greatly along a borehole length that penetrates formations with different hydraulic conductivities. Most of the pumping is drawn from preferential flow zones with relatively large hydraulic conductivity. Production well construction information was referenced to accurately represent the production wells in the groundwater model and can be found in table 1–2. Daily pumping data were provided by the well-field operators and used to calculate the total monthly pumping assigned using the MNW Package. The largest withdrawals typically occurred during the summer months (fig. 5).

Rainfall and Evapotranspiration

Net recharge was applied to the top active layer of the model in all cells. Net recharge was calculated on a monthly basis as the difference between monthly summations of rainfall and ET. Although impervious area occurs within the study area (Hughes and White, 2014), runoff was not included in the recharge calculations because it was assumed to be relatively small. The effects of this exclusion are addressed in the limitations section. The MODFLOW Recharge Package was used to apply this boundary condition to the model (Harbaugh, 2005). Rainfall and ET were measured at a weather station constructed within the study area (fig. 1*B*). The values measured by two tipping-bucket rain gages were averaged and used to estimate rainfall. Daily rainfall was calculated by combining the totals of the 15-minute rainfall data, and daily rainfall was combined to estimate the monthly rainfall totals. The seasonal rainfall patterns in the study area are consistent with the regional patterns in south Florida; the majority of the rainfall occurs in the wet summer months of June–September (fig. 5). ET was estimated by using micrometeorological data and eddy covariance methods for the non-irrigated, mowed bahiagrass land cover in the vicinity of the weather station. ET of areas covered with non-irrigated bahiagrass is likely somewhat different from ET of the residential areas (irrigated grass, buildings, parking areas, roads) surrounding the well field. The eddy covariance method (Baldocchi and others, 1988) relies on high-frequency (10 hertz) measurements of vapor density and wind speed (three-dimensional). These data were collected at a height of 2.6 m by using an open-path infrared gas analyzer and a sonic anemometer, respectively, and half-hour composites of ET were computed by using the eddy covariance method. Monthly rainfall and ET data are listed in table 1–3.

Regional Groundwater Flow System

The regional groundwater flow system surrounding the model domain affects local water levels beneath the study area. Regional groundwater flow to and from the study area was represented by using a head-dependent flux. Groundwater-level data collected at eight monitoring wells surrounding the well field were used to define a water-level surface that represents the regional groundwater flow system state (fig. 7). Sampling frequency for these eight sites ranged from seconds to days. To keep the monthly average from being biased towards higher frequency sampling periods, a hierarchical time-averaging method for computing mean monthly water levels was used to estimate monthly average water levels.

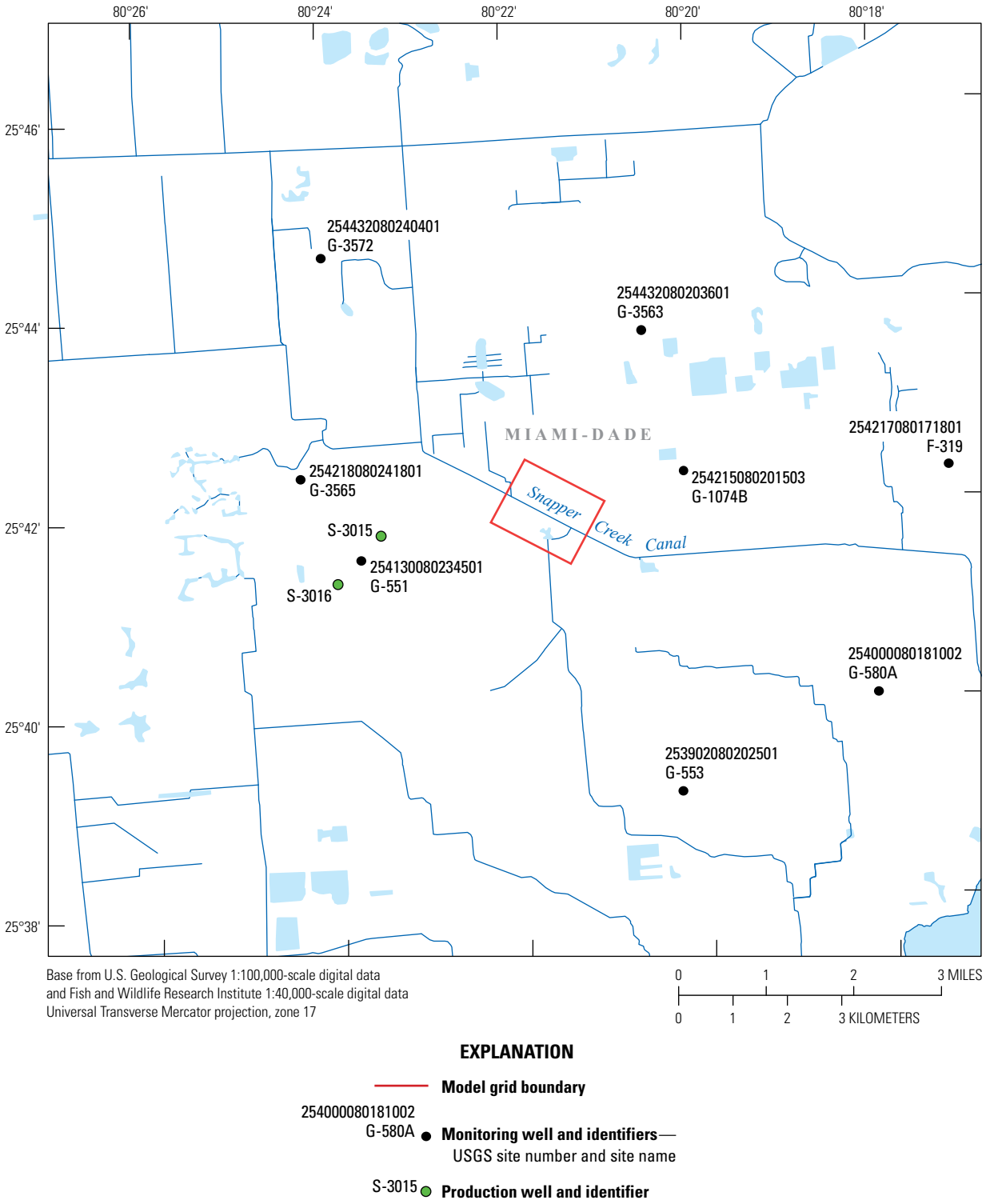

Figure 7. Location of monitoring wells used to develop the head-dependent flux boundary condition and the location of production wells S-3015 and S-3016, Snapper Creek Canal study area, Miami-Dade County, Florida.

First, sub-minute data were averaged to obtain an average value for each minute. Minute, hourly, and daily values were likewise averaged to obtain hourly, daily, and monthly values. Mean monthly water levels at these eight wells were then interpolated for each model stress period by using the SAS default 3D interpolation method (SAS Institute Inc., 2010). The SAS default 3D interpolation method applies a fifth-degree polynomial within each triangle obtained from a tessellation of the plane based on the observation locations. Grid centroids of all model cells at the model perimeter (rows 1 and 60; columns 1 and 83; layers 1 to 30) were intersected with the interpolated regional groundwater-level surfaces for each stress period to obtain controlling head values for the head-dependent flux boundary, as assigned with the MODFLOW General Head Boundary (GHB) Package (McDonald and Harbaugh, 1988). The model boundary was assumed to have vertically uniform head values from the base to the top of the Biscayne aquifer. These boundary heads along with conductance values are used to calculate flow to and from the GHB boundary for the groundwater model.

The magnitude of groundwater flux through the perimeter boundary is dependent upon the hydraulic conductance value defined for the perimeter cells within the GHB. Hydraulic conductance is defined by the relation

$$C = \frac{KA}{L}, \tag{2}$$

where

C is the conductance [L^2/T];
K is the hydraulic conductivity assigned to the cell [L/T];
A is the cross-sectional area of the flow path [L^2]; and
L is the length of the flow path [L].

The appropriate conductance values were calculated and assigned for the cells representing the perimeter boundary condition by using the hydraulic conductivity value in each of these cells with equation 4. Grid cells with similar dimensions and hydraulic conductivity values were assigned similar calculated conductance values; conductance values of multiple cells were grouped and averaged in the different flow zones on each side of the model. This resulted in four conductance values for the locations where the preferential flow zones intersect each side of the rectangular model domain and a uniform value for conductance within the matrix cells along the perimeter. These grouped averaged values that were commensurate with the hydraulic conductivities along the perimeter were used as the initial values for the parameter estimation of the boundary conductance values. Once these perimeter conductance values were assigned, the sensitivities of the hydraulic conductivities were re-tested. The most sensitive hydraulic conductivities were refined further by using parameter estimation to obtain a better fit for groundwater levels and canal leakage. The perimeter boundary conductances were then also refined by using parameter estimation.

Assignment of Hydraulic Properties

Aquifer horizontal hydraulic conductivity was specified for each cell within the model area based on the understanding of the hydrogeologic framework within the study area. By using the point data for the flow zone horizons from the monitoring wells and the interpreted hydrogeologic cross section at the well field (Wacker and others, 2014), flow zones were mapped in three dimensions within the model grid (fig. 8). Specifically, in Wacker and others (2014), the Biscayne aquifer is divided into three major hydrogeologic zones: (1) the shallow, highly transmissive uppermost flow unit; (2) the semi-confining matrix unit, which contains discontinuous flow zones; and (3) the deep, highly transmissive flow unit in the lower Fort Thompson Formation and upper Tamiami Formation, which contains multiple stratiform flow zones. For the purpose of this report, the deep, highly transmissive preferential flow zone was divided into two zones, A and B, for ease of delineation within the groundwater model and discussion purposes. Distinct differences between flow properties of preferential flow zones and matrix flow zones (as identified by using borehole flowmeter data, optical images, and slug testing; Wacker and others [2014]) were represented in the model by assigning values of hydraulic conductivity that were up to two orders of magnitude higher in the preferential flow zones than in the matrix flow zones.

Borehole and hydraulic property data also indicated that flow properties within preferential flow zones varied spatially across the study area. The variability, both vertically and laterally, is demonstrated by varying responses within a flow unit to stresses such as production well pumping. For example, the drawdown response of the monitoring wells at cluster 2 during the months of May–July 2011, when the production wells were pumping, illustrates the vertical variability within the cluster (fig. 9*A*). The deepest monitoring wells of clusters 3 and 5, monitoring wells G-3881 and G-3879, are open to the second unit of the lowest preferential flow zone and are each near production wells (figs. 4 and 9*B*). When the pumping was equal at all of the production wells during the last 2 months of the simulation period, a large difference in drawdown response was observed. Some of the variability may be explained by differences in distances to the canal and production wells, but the differences in drawdown may also suggest lateral variability. Variability was also observed during the slug testing and flowmeter testing at the study area (Wacker and others, 2014). For example, the hydraulic conductivity values estimated from the slug testing varied more than an order of magnitude within the deepest preferential flow zone (Wacker and others, 2014).

In order to represent the spatial variability of hydraulic properties within the preferential flow zones, each flow zone was divided into 24 hydraulic property zones of uniform hydraulic conductivity (fig. 10). The size of each hydraulic property zone is dependent on the grid cell size in that area. From these rectangular hydraulic property zones centered around the monitoring wells, the edges of the zones extended out in both directions to the model boundaries, with the

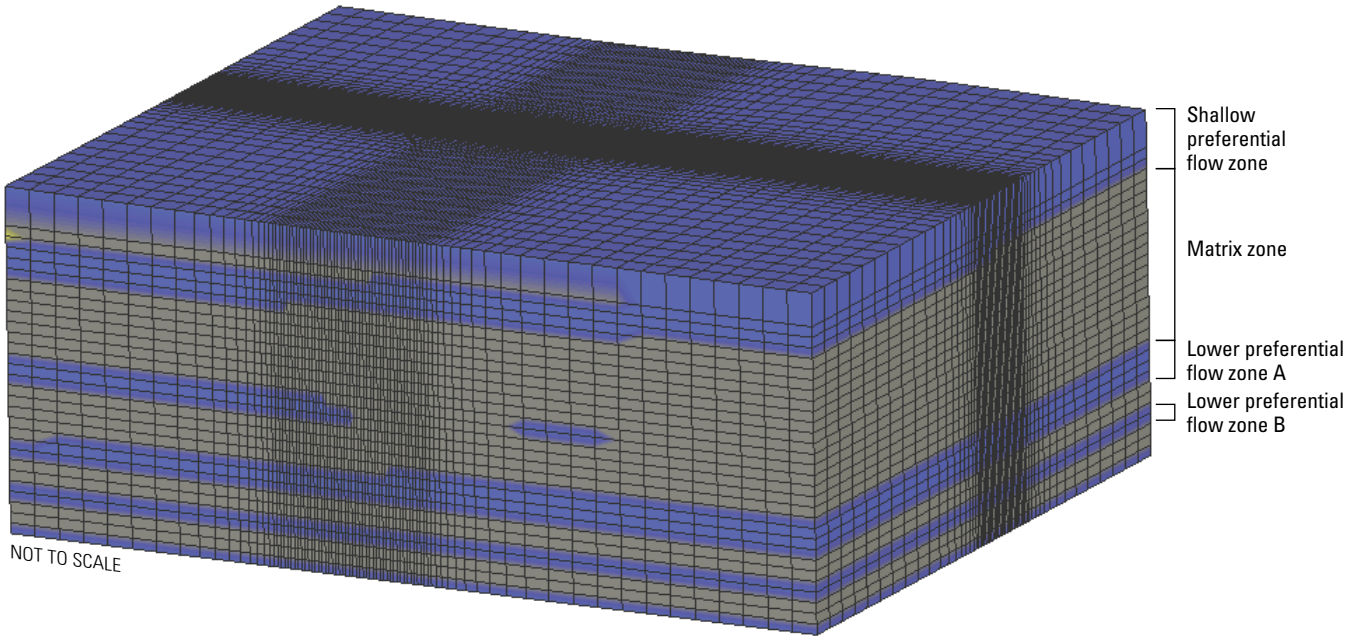

Figure 8. Spatial distribution of preferential flow zones and matrix flow zone for the Snapper Creek Canal study area groundwater flow model grid.

intersecting lines creating a grid of 24 hydraulic property zones (fig. 10). This zonation pattern was used for the preferential flow zones, but was not applied to the matrix zones. Additionally, this zonation pattern was not applied to the discontinuous preferential flow zone units that lie within the semi-confining matrix zone between the shallowest preferential flow zone and the deep preferential flow zones in the lower Biscayne aquifer flow unit. The hydraulic properties for the units to which the zonation was not applied remain uniform throughout those units.

Initial values used for calibrating hydraulic conductivity were obtained from slug and flowmeter data (Wacker and others, 2014). These values were also used as a way to verify that the final parameter estimates were within the same order of magnitude as the values from the testing. Final calibrated values of hydraulic conductivity are shown in figure 10.

Specific storage and specific yield were uniformly specified as 0.00001 m^{-1} and 0.2 (unitless), respectively, based on the results of aquifer hydraulic testing (Paillet and Reese, 2000; Bolster and others, 2001; R.S. Reese, U.S. Geological Survey, written commun., 2011).

Additionally, because flow from the base of the Biscayne aquifer to underlying formations is negligible, the base of the Biscayne was represented by a no-flow boundary in the groundwater model.

Calibration and Model Fit

The groundwater model was calibrated by adjusting sensitive parameters to fit groundwater elevation and canal leakage observations within the calibration criteria. Model fit was evaluated by comparing the simulated and observed groundwater elevation and canal leakage values. Residuals, which were defined as the simulated values minus the observed values, are examined spatially and temporally. Residual analysis reveals model strengths and weaknesses, including spatial and temporal biases in simulated groundwater-level distributions and canal leakage.

Calibration Data and Criteria

The groundwater flow model was calibrated to mean monthly (1) groundwater heads and (2) canal leakage. Specifically, 242 average monthly head elevations and 11 average monthly canal leakage observations were used during calibration.

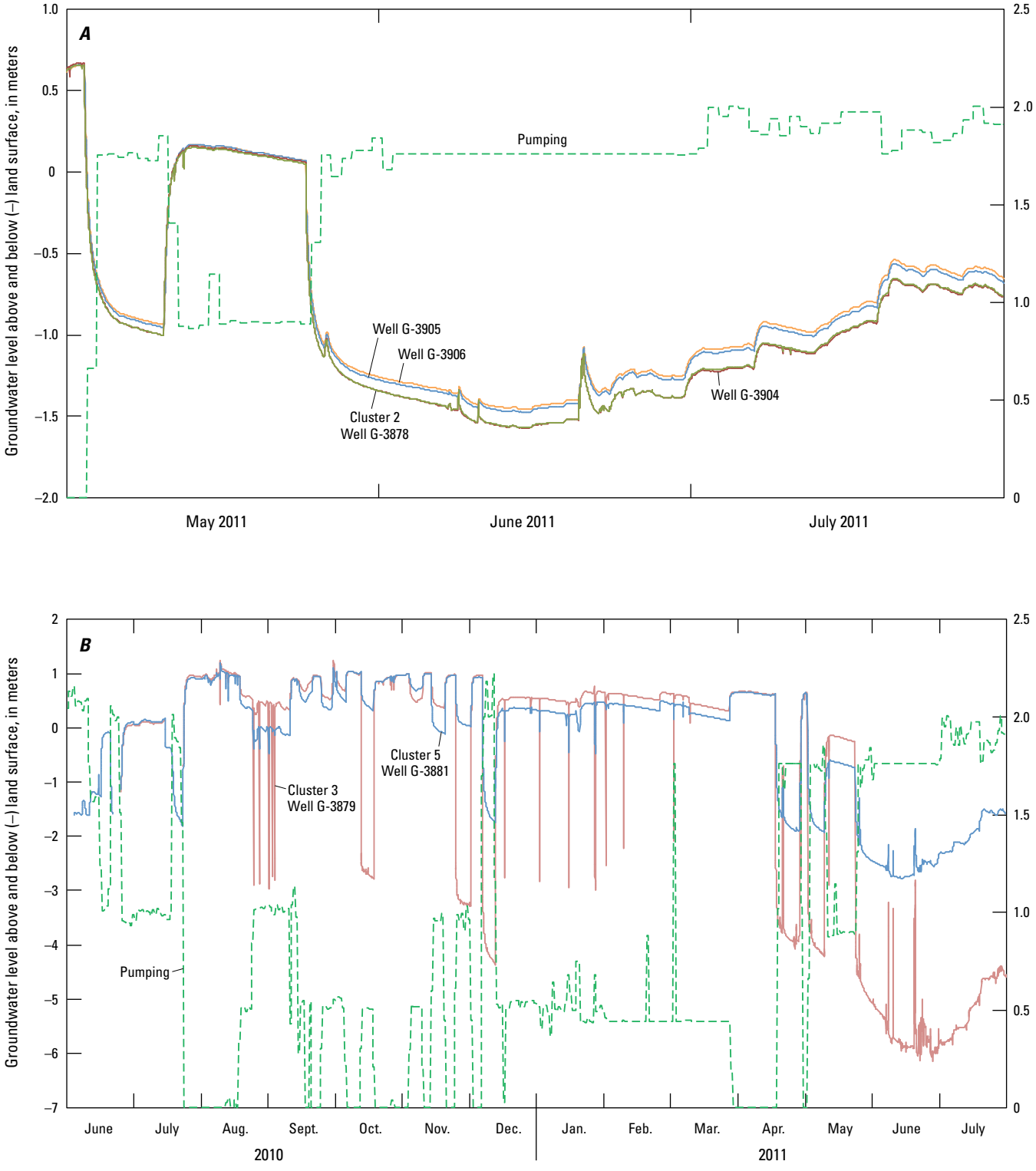

Figure 9. Hydrographs showing varying responses to production well pumping at (*A*) cluster 2 wells and (*B*) wells G-3881 and G-3879, Snapper Creek Canal study area, Miami-Dade County, Florida, 2010–2011.

Groundwater Levels

Groundwater-level data were recorded at the observation well clusters throughout the study area (table 1–4). A hierarchical time averaging method was applied to the groundwater-level observations to obtain mean monthly groundwater levels. Because of occasional equipment failures and the need to sample at higher frequencies during pumping tests, groundwater-level data were recorded at sampling intervals that varied from seconds to days. Hierarchical time averaging was used to obtain one value for every minute of the study period, and these 1-minute averages were then averaged for every hour. Hourly measurements were averaged to obtain daily averages, and the process was repeated to obtain monthly averages. These mean monthly groundwater levels were provided to the model using the Head Observation Package (Hill and others, 2000).

The groundwater levels for June and July 2011 for well G-3879 were removed from the dataset for calibration to eliminate potential bias caused by the influence of a cavity created by airlifting of material during the well construction process (Wacker and others, 2014). Under the highest pumping stresses, the drawdown pattern observed at well G-3879 was substantially different from patterns observed elsewhere in the well field.

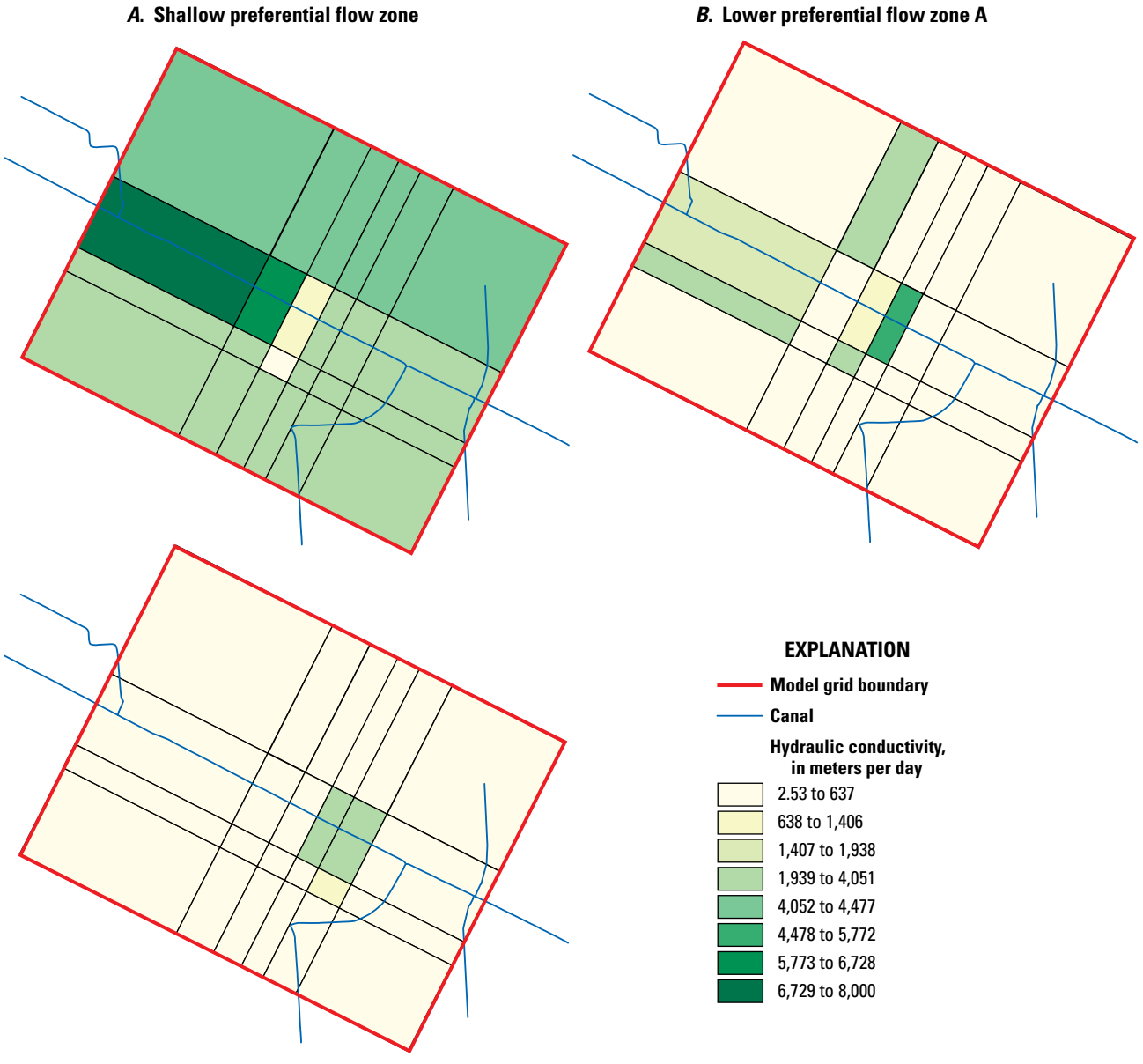

Figure 10. Zonation patterns used to represent heterogeneity in preferential flow zones with calibrated hydraulic conductivities: (*A*) shallow preferential flow zone, (*B*) lower preferential flow zone A, and (*C*) lower preferential flow zone B for the Snapper Creek Canal study area groundwater flow model.

Because error in the groundwater elevation measurements is generally small, the calibration criteria for groundwater elevation were defined by using the variability in the groundwater elevation measurements. At each well, the standard deviation of the groundwater elevations was calculated over the simulation period. The standard deviation value for each well was added and subtracted from the monthly observed means to obtain an acceptable range for the simulated groundwater levels. Simulated groundwater elevation values within this range were used as the calibration criteria for the groundwater elevation values. An alternative calibration criterion was developed by establishing a mean average error (MAE) that was less than or equal to 10 percent of the range in observed groundwater elevation values during the study period. Groundwater elevation values used in calibration ranged from –2.60 to 0.97 m, yielding an absolute total range of 3.57 m and resulting in a calibration criteria of an MAE of less than or equal to 10 percent of that range, or 0.36 m.

Canal Leakage

Canal leakage was calculated as the difference between canal discharge measured downstream and upstream of the study area. Changes in canal storage also were subtracted from the downstream flow and were calculated by using the distance between SL_DOWN and SL_UP (fig. 1*B*), the canal width, and the change in canal stage over each 24-hour period. Discharge data for the study period were acquired from the USGS National Water Information System (table 1). Evaporation from the Snapper Creek Canal is assumed to be minimal at the scale of this study and was not taken into account when calculating canal losses.

Table 1. Discharge data collection sites used for calculation of canal leakage, Snapper Creek Canal, Miami-Dade County, Florida.

Site name	USGS site identifier
SL_UP	254204080215600
SL_MID	254157080213800
SL_DOWN	254150080212500

Canal discharge was defined as the volume of water flowing through a canal cross-sectional area over a specified length of time:

$$Q_{CL} = Q_{UP} - Q_{DOWN} + Q_{STOR}, \quad (3)$$

where

Q_{CL} is the canal leakage [L^3/T];
Q_{UP} is the upstream volumetric flow [L^3/T];
Q_{DOWN} is the downstream volumetric flow [L^3/T]; and
Q_{STOR} is the canal storage change between the upstream and downstream locations [L^3/T].

Several factors made it difficult to quantify canal discharge measurements at the discharge and stage monitoring stations and could have contributed to possible measurement error and uncertainty in the leakage estimate. The canal bed gradient is low, which leads to flow rates below the lower limit of flow meter accuracy under certain conditions. Additionally, canal flow downstream is controlled by a gated structure that is open during parts of the year to allow the canal to discharge into Biscayne Bay. When the gated structure is open, the discharge data at the Snapper Creek monitoring station show tidal effects. The low canal bed gradient and structure-controlled flow can cause wind to affect the discharge rates and could also cause reversals of flow. Furthermore, canals in south Florida are subject to invasion by aquatic vegetation, which can grow rapidly during any season. Dense aquatic vegetation may impede flows, which can affect discharge measurements. Vegetation removal is not regularly scheduled at the Snapper Creek stations in the study area. Because of the difficulty quantifying the discharge measurements and the possible measurement errors, summary statistics for the measured discharge data were calculated (figs. 11 and 12).

The calibration criteria for canal leakage were defined by using a procedure similar to that described by Jones and Torak (2006). An upper limit for the target canal leakage range was calculated by using the following expression:

$$L_{\max} = Q25_d - Q75_u, \quad (4)$$

where

$L_{\max}$ is the upper limit of target leakage [L^3/T];
$Q25_d$ is the downstream 25-percent discharge value on a monthly basis [L^3/T]; and
$Q75_u$ is the upstream 75-percent discharge value on a monthly basis [L^3/T].

A lower limit for the target canal leakage range was calculated by using the following expression:

$$L_{\min} = Q75_d - Q25_u, \quad (5)$$

where

$L_{\min}$ is the lower limit of target leakage [L^3/T];
$Q75_d$ is the downstream 75-percent discharge value on a monthly basis [L^3/T]; and
$Q25_u$ is the upstream 25-percent discharge value on a monthly basis [L^3/T].

The simulated canal leakage values were compared to the calculated target ranges and observed leakage values to determine if the simulated results met the calibration criteria (table 2). Negative canal leakage values obtained with equations 4 and 5 represent a loss from the canal to the aquifer, and positive values represent recharge to the canal. This is opposite from the sign convention used in the remainder of this report, with a negative value representing recharge to the canal. Because of this, the signs of the values obtained from equations 4 and 5 were reversed as reflected in table 2.

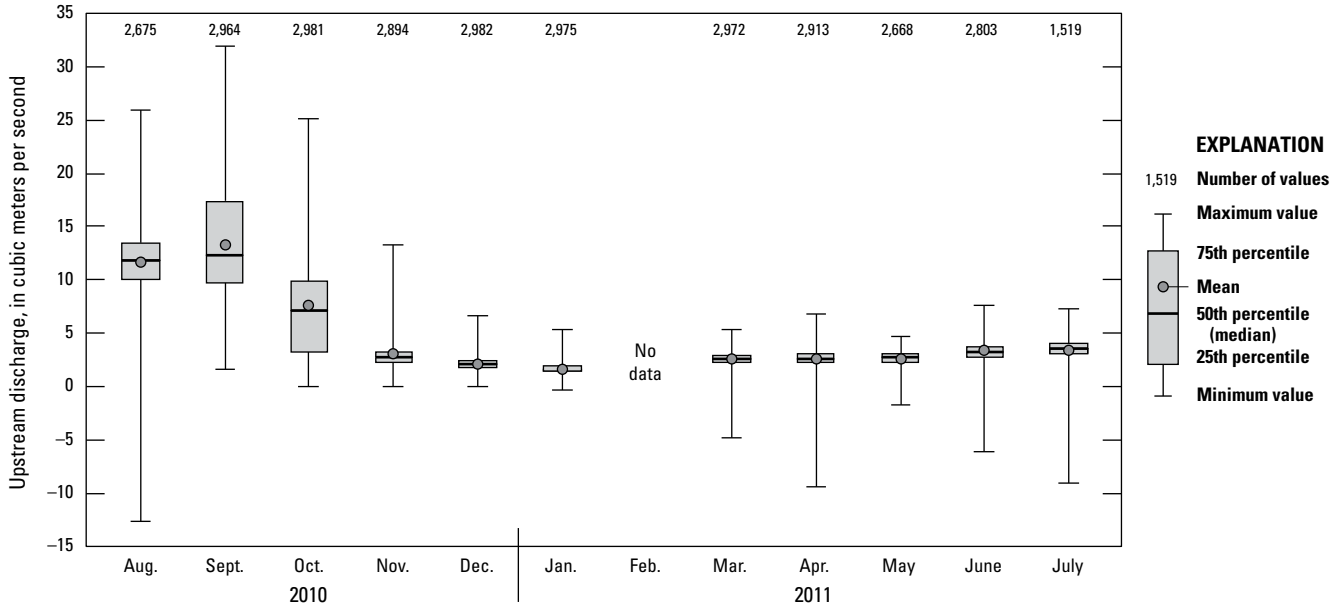

Figure 11. Summary of statistics for upstream discharge measurements, including mean, median, 75th-percentile, 25th-percentile, maximum, and minimum monthly values, for the 14-month calibration period for the Snapper Creek Canal groundwater flow model.

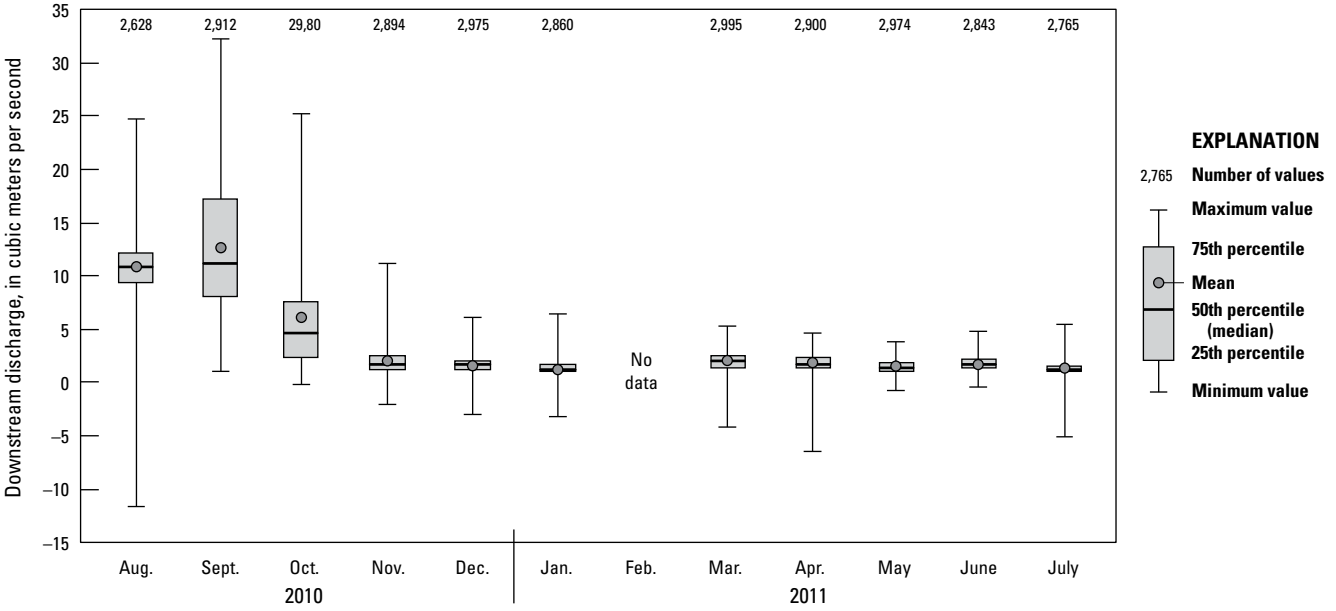

Figure 12. Summary of statistics for downstream discharge measurements, including mean, median, 75th-percentile, 25th-percentile, maximum, and minimum monthly values for the 14-month calibration period for the Snapper Creek Canal groundwater flow model.

Calibration Approach

The model was calibrated by using manual methods and the inverse modeling tool UCODE (Poeter and others, 2005). UCODE operates with any existing process model that has numerical input and output to perform sensitivity analyses, calibration, predictions, and uncertainty analyses. Sensitivity analyses guided calibration of the model. Specifically, composite-scaled sensitivities (CSS) (Hill and Tiedeman, 2007) were computed for parameters in each model to guide manual calibration and inversion. The CSS indicates how sensitive the model is at all of the observation locations to a change in a given parameter at a given value. Parameters with a large CSS value can be estimated more easily than parameters with a small CSS value. In order to save computational time and avoid over-parameterization, only parameters with relatively large CSS values were estimated during calibration. Parameters with a relatively small CSS were left at values that seemed reasonable based on field estimates, or assigned values that were consistent with adjacent parts of the model that possessed similar geologic characteristics. In addition to parameters with large sensitivity values, the hydraulic conductivities for the zones that contained monitoring wells and groundwater elevation data were also estimated by using parameter estimation.

Possible parameters include 74 hydraulic conductivity parameters and 12 perimeter conductance parameters. In order to simplify the sensitivity analysis presented in this report, but still illustrate which regions and hydrogeologic formations were most sensitive, some of the parameters were grouped for the sensitivity analysis (table 3). Although the sensitivities of all 74 hydraulic conductivity parameters were calculated and the results of these calculations were used during model calibration, they are not all presented in this report. In each flow zone, the 24 hydraulic conductivity parameters were grouped into 1 parameter group, resulting in 4 flow zone parameter groups. Likewise, the three parameters for the three matrix flow zones were grouped into a single parameter group. The sensitivities of the parameter groups are presented in figures 13 and 14. The unit that is labeled Kp2 for this sensitivity illustration is not a continuous flow zone; it is a group of minor discontinuous flow zones lying between the first and third continuous flow zones. The sensitivities of all the matrix flow zone hydraulic conductivities were grouped for this sensitivity illustration and represented as Km. Similarly, the perimeter conductance values were averaged for each side of the model study area, resulting in four perimeter conductance values.

CSS values were calculated to test the combined sensitivity of groundwater levels and canal leakage and the sensitivity of canal leakage to changes in parameter values. The parameter sensitivities were similar when calculated for all observations and for canal leakage alone. Model-simulated values of groundwater levels and canal leakage were consistently most sensitive to variations to the hydraulic conductivity values (figs. 13 and 14). When groundwater levels and canal leakage observations are considered, the model is most sensitive to changes to the matrix flow zone hydraulic conductivity, and the shallowest preferential flow zone (Kp) is the second most sensitive parameter (fig. 13). Parameter sensitivities to the canal leakage observations are greatest for the

Table 2. Canal leakage values and flow target ranges used for model calibration, August 2010–July 2011.

[All values in cubic meters per second; —, no data]

Month and year	Observed leakage	Lower limit of target leakage	Upper limit of target leakage
August 2010	0.92	–2.04	4.09
September 2010	0.63	–7.42	9.21
October 2010	1.55	–4.37	7.36
November 2010	1.03	–0.22	1.90
December 2010	0.46	–0.14	1.20
January 2011	0.45	–0.17	0.90
February 2011	—	—	—
March 2011	0.61	–0.20	1.54
April 2011	0.68	–0.14	1.74
May 2011	1.05	0.42	1.90
June 2011	1.60	0.64	2.44
July 2011	1.99	1.51	3.05

Table 3. Definition of sensitivity parameters used to determine flow zone and perimeter conductance sensitivities for the Snapper Creek groundwater model.

Sensitivity parameter	Definition
Km	Hydraulic conductivity value of matrix zone
Kp	Average hydraulic conductivity value of the shallowest preferential flow zone
Kp2	Average hydraulic conductivity value of the minor, discontinuous preferential flow zones
Kp3	Average hydraulic conductivity value of the lower preferential flow zone A
Kp4	Average hydraulic conductivity value of the lower preferential flow zone B
Sy	Specific yield
Ss	Specific storage
peri_cond1	Perimeter conductance for northeastern side of model
peri_cond2	Perimeter conductance for southeastern side of model
peri_cond3	Perimeter conductance for southwestern side of model
peri_cond4	Perimeter conductance for northwestern side of model

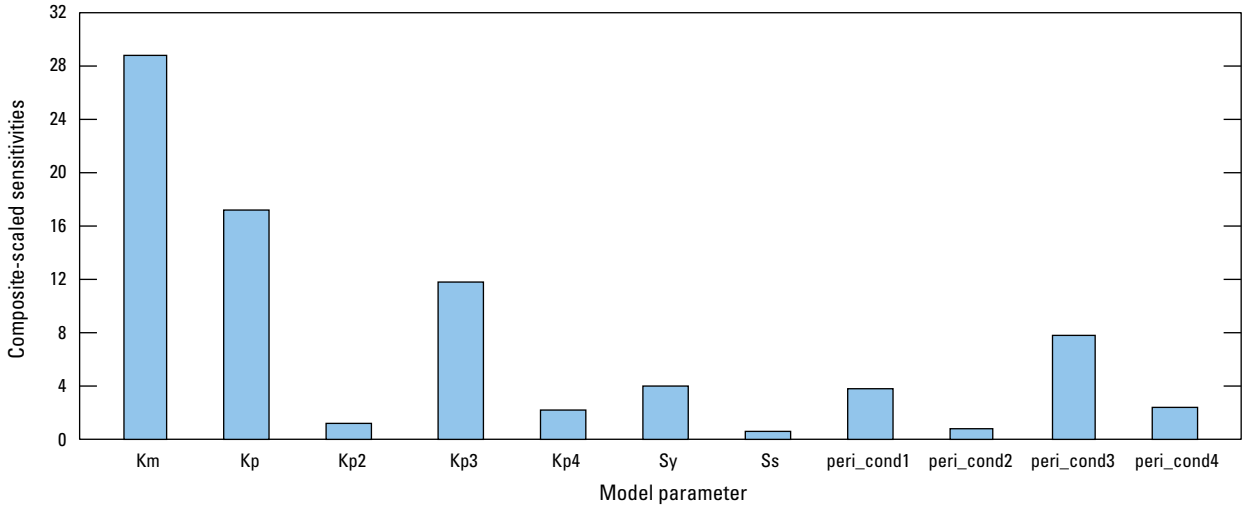

Figure 13. Composite-scaled sensitivities of leakage and groundwater elevation observations for the Snapper Creek Canal study area groundwater flow model.

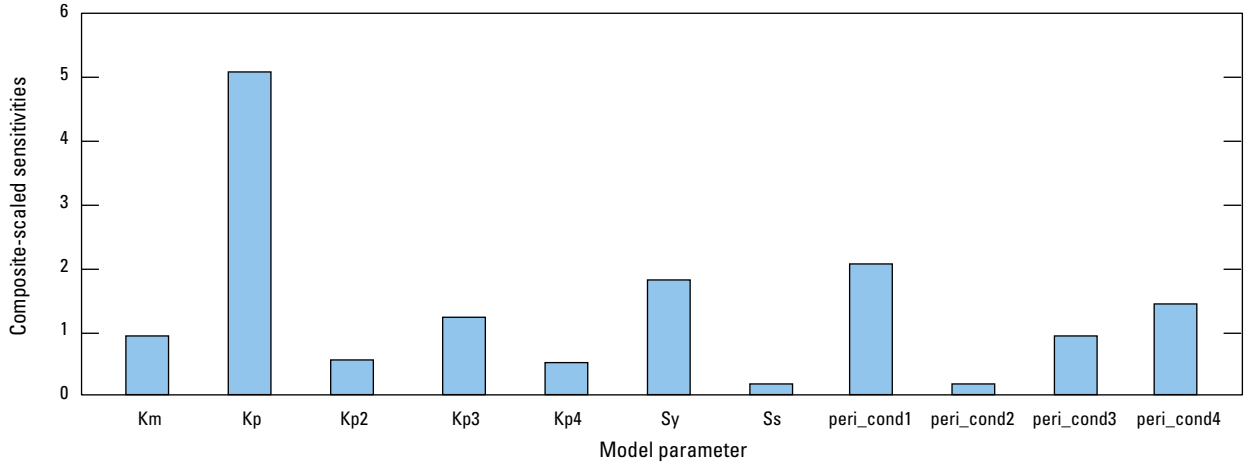

Figure 14. Composite-scaled sensitivities of leakage observations for the Snapper Creek Canal study area groundwater flow model.

shallowest preferential flow zone (fig. 14). Because the canal is cut directly into this shallow flow zone, variations to the hydraulic conductivities within this flow zone are expected to substantially change the canal leakage magnitude. Moreover, the model output is more sensitive to changes in perimeter conductance when canal leakage is considered alone than when the combined sensitivities to groundwater-level and canal leakage outputs are considered.

Model Fit

Model fit to observed groundwater levels and canal leakage was evaluated graphically and quantitatively. Model fit to groundwater levels was measured by using mean error, mean average error, various graphical comparisons of observed and simulated values, an analysis to determine if simulated groundwater levels fall within the target ranges at each well, and graphical examination of model residuals. Model fit to canal leakage was measured by using graphical comparisons of observed and simulated values, an analysis to determine if simulated canal leakage values fall within a target range, and graphical examination of model residuals. In general, differences were calculated by subtracting observed values from simulated values so that positive differences indicate that the model simulates values higher than observed values and negative differences indicate that the model simulates values lower than observed values.

Groundwater Levels

The overall mean error was –0.009 m, indicating that simulated water-level values are slightly lower than observed. In other words, simulated drawdown is slightly greater than observed, with the exception of the large drawdown events in the later months of the simulation period. The MAE of calibration was 0.19 m for the 242 average monthly water-level

observations, which was less than the calibration criteria of 0.36 m. About 60 percent of the monitoring wells have an absolute value of head residual less than or equal to 0.28 m, more than 80 percent of the monitoring wells have an absolute value of head residual less than or equal to 0.42 m, and 95 percent of the monitoring wells have an absolute value of head residual less than or equal to 0.85 m.

In general, the model simulates groundwater levels that are comparable to observed groundwater levels (fig. 15). Deviations from the fit generally increase with lower water levels, and simulated values tend to be higher than observed values. This indicates that the model tends to fit less closely for greater values of drawdown than for small drawdowns. At higher water levels, simulated values tend to be lower than observed values.

In addition to the groundwater-level calibration criteria, the simulated and observed groundwater elevation values were examined for individual monitoring wells. This was accomplished by using individual plots of measured and simulated groundwater elevation over the simulation time period for each monitoring well (fig. 16). The plots allow for analysis over time at each separate monitoring well, so that large deviations can be isolated in both time and space. Additionally, these plots illustrate whether or not the simulated groundwater levels are within the calibration target range.

The simulated groundwater levels at cluster 1 (wells G-3877, G-3902, and G-3903) are slightly outside of the lower range of the calibration targets for the first 5 months of the simulation period, indicating that the model is simulating too much drawdown in the early months at cluster 1. The excess drawdown may be due to the relative proximity of cluster 1 to the model boundaries. Moreover, at this cluster there is little variation in the observed groundwater levels, resulting in a smaller calibration target range. At wells G-3906, G-3917, and G-3918, the simulated groundwater level for June 2011 is slightly outside of the upper calibration target range. In response to production well pumping, a large amount of drawdown occurs during June 2011, and the model is not able to match the observed groundwater levels. Although there are other deviations from the observed and simulated groundwater levels at other groundwater wells and time periods, the simulated groundwater levels are within the calibration target for all other groundwater wells.

Another method to evaluate model fit is to examine residuals plotted against simulated values. Residuals are defined as the simulated values minus the observed values. An accurate and unbiased model would produce residuals that are random and normally distributed around the horizontal axis. A nonrandom distribution of residuals indicates either a model bias or model error (Hill and Tiedeman, 2007). Simulated groundwater levels and their residuals were plotted for June 2010 to July 2011 (fig. 17). Positive residuals indicate that simulated values are higher than the observed values, whereas negative residuals indicate that simulated values are lower than observed values. In general, there is a greater scatter of those residuals for lower simulated groundwater levels.

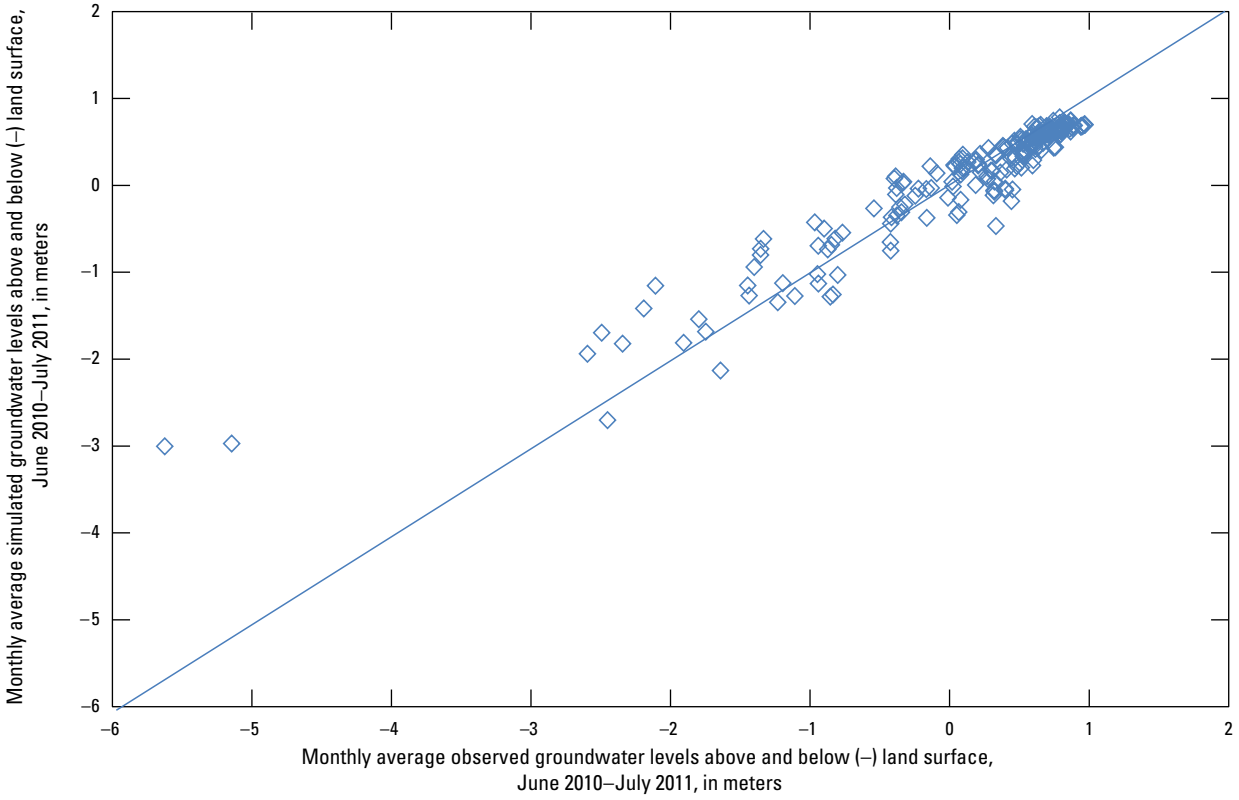

Figure 15. Model fit of observed and simulated groundwater elevations for the Snapper Creek Canal study area groundwater flow model.

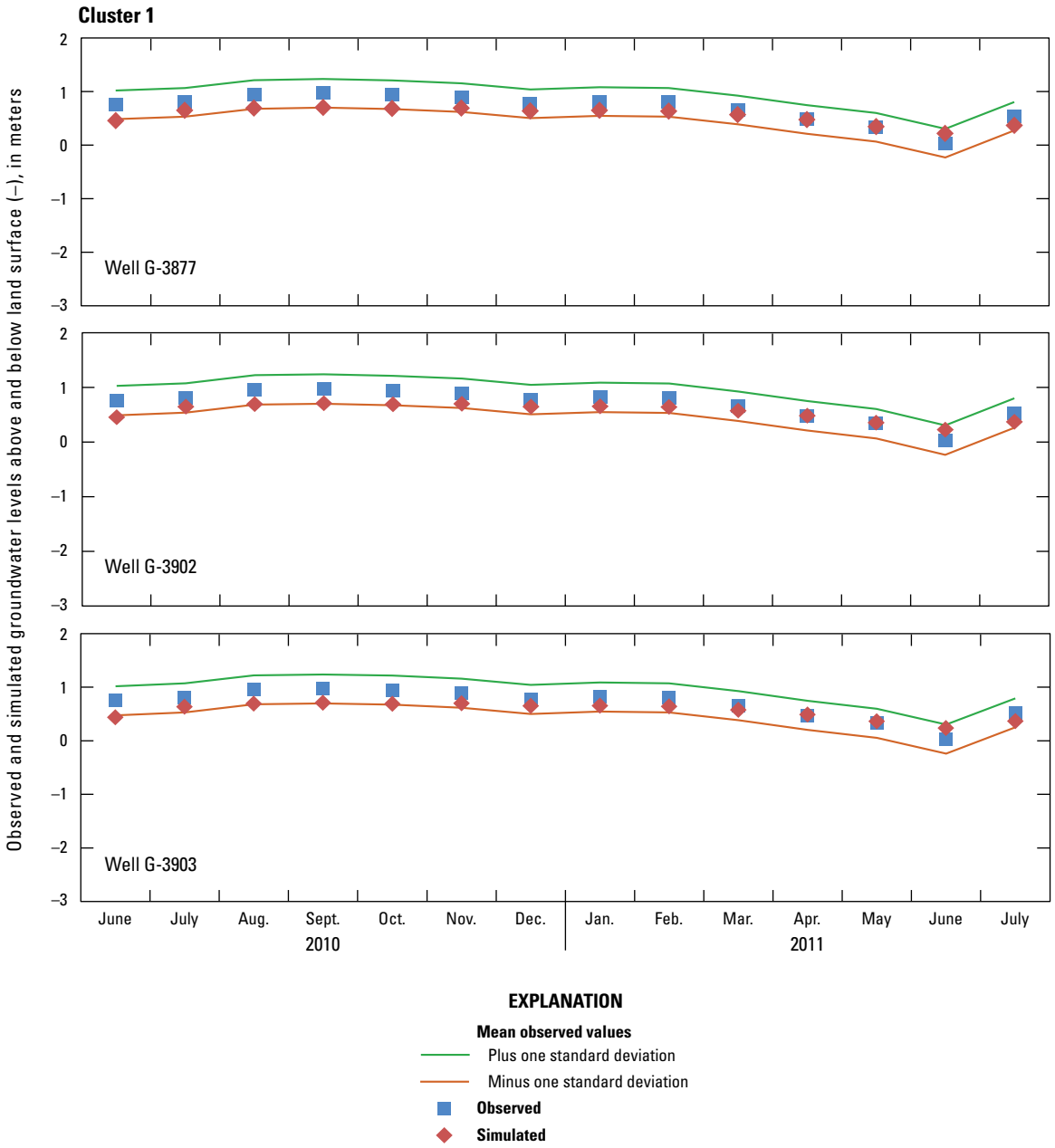

Figure 16. Simulated groundwater level, mean observed groundwater level, mean observed groundwater level plus one standard deviation, and mean observed groundwater level minus one standard deviation during the 14-month calibration period for the Snapper Creek Canal study area groundwater flow model.

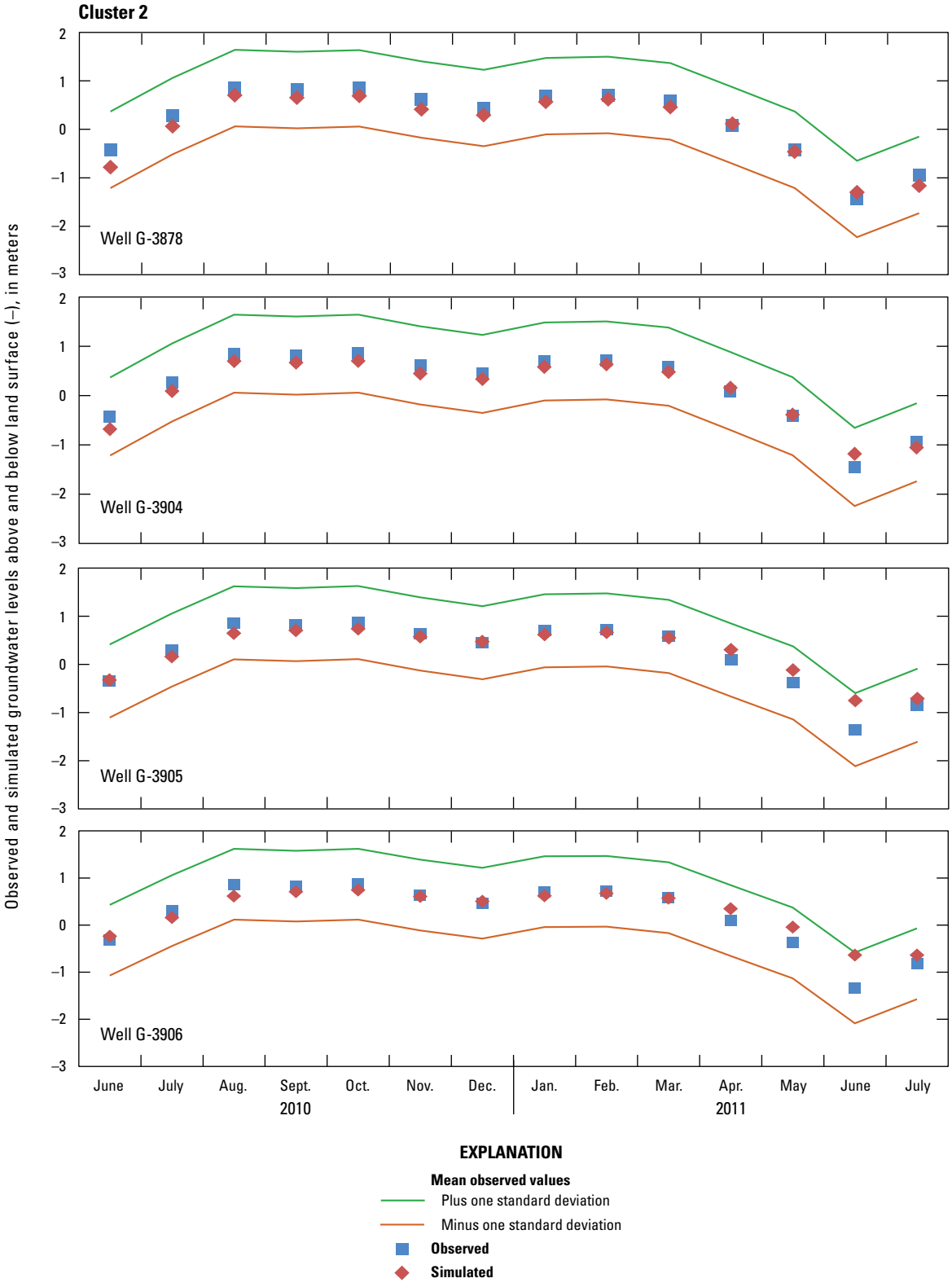

Figure 16. Simulated groundwater level, mean observed groundwater level, mean observed groundwater level plus one standard deviation, and mean observed groundwater level minus one standard deviation during the 14-month calibration period for the Snapper Creek Canal study area groundwater flow model. —Continued

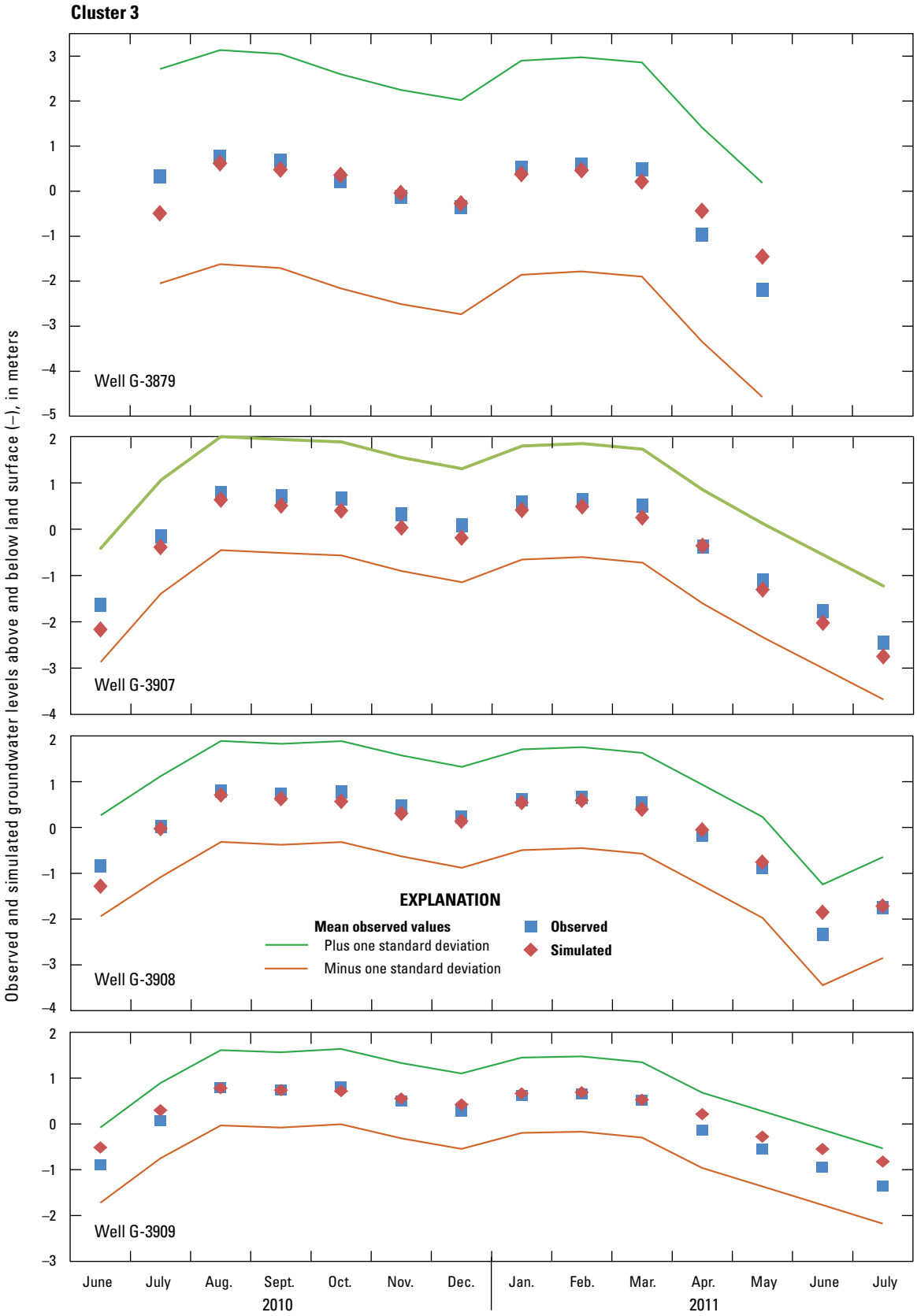

Figure 16. Simulated groundwater level, mean observed groundwater level, mean observed groundwater level plus one standard deviation, and mean observed groundwater level minus one standard deviation during the 14-month calibration period for the Snapper Creek Canal study area groundwater flow model. —Continued

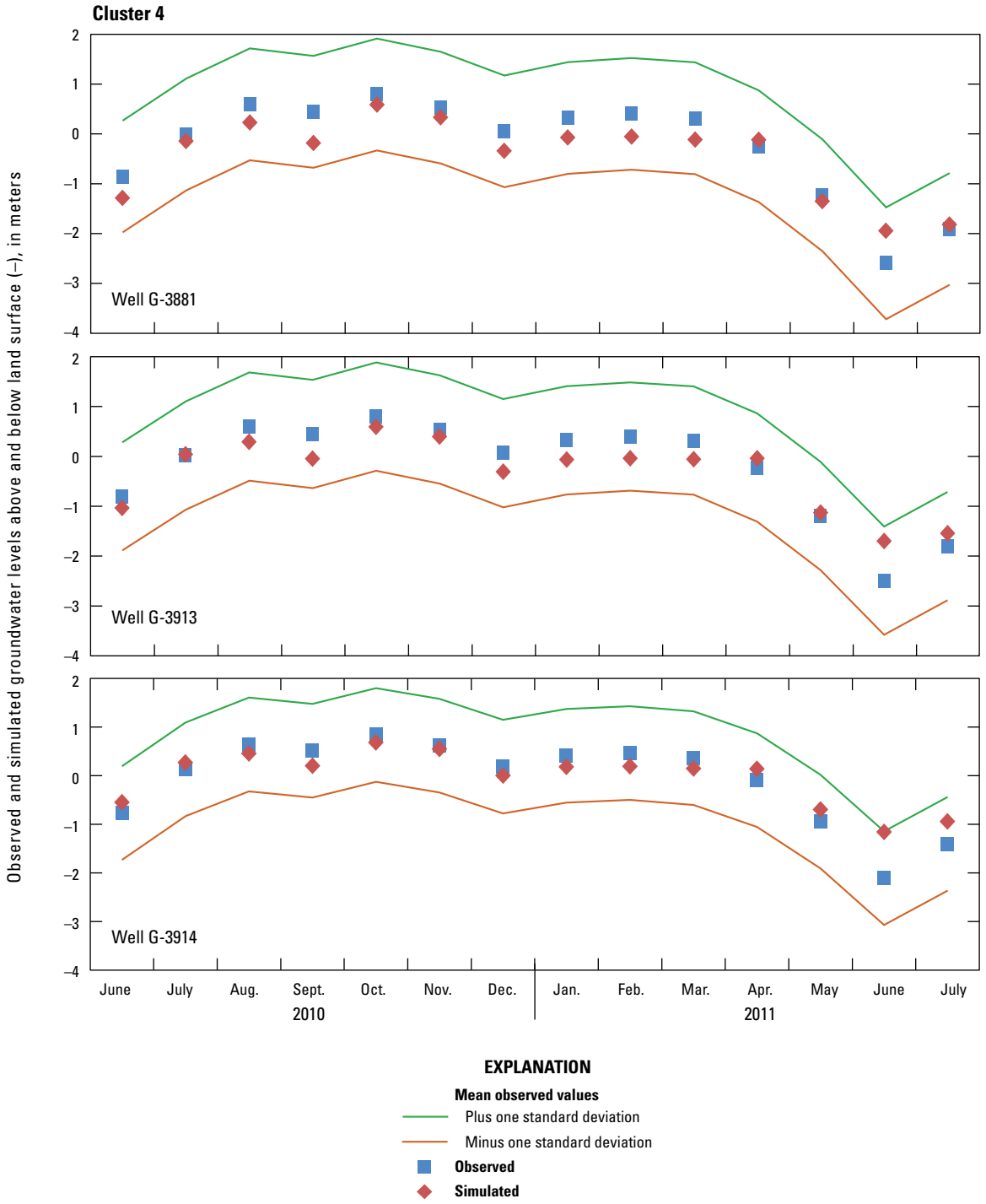

Figure 16. Simulated groundwater level, mean observed groundwater level, mean observed groundwater level plus one standard deviation, and mean observed groundwater level minus one standard deviation during the 14-month calibration period for the Snapper Creek Canal study area groundwater flow model. —Continued

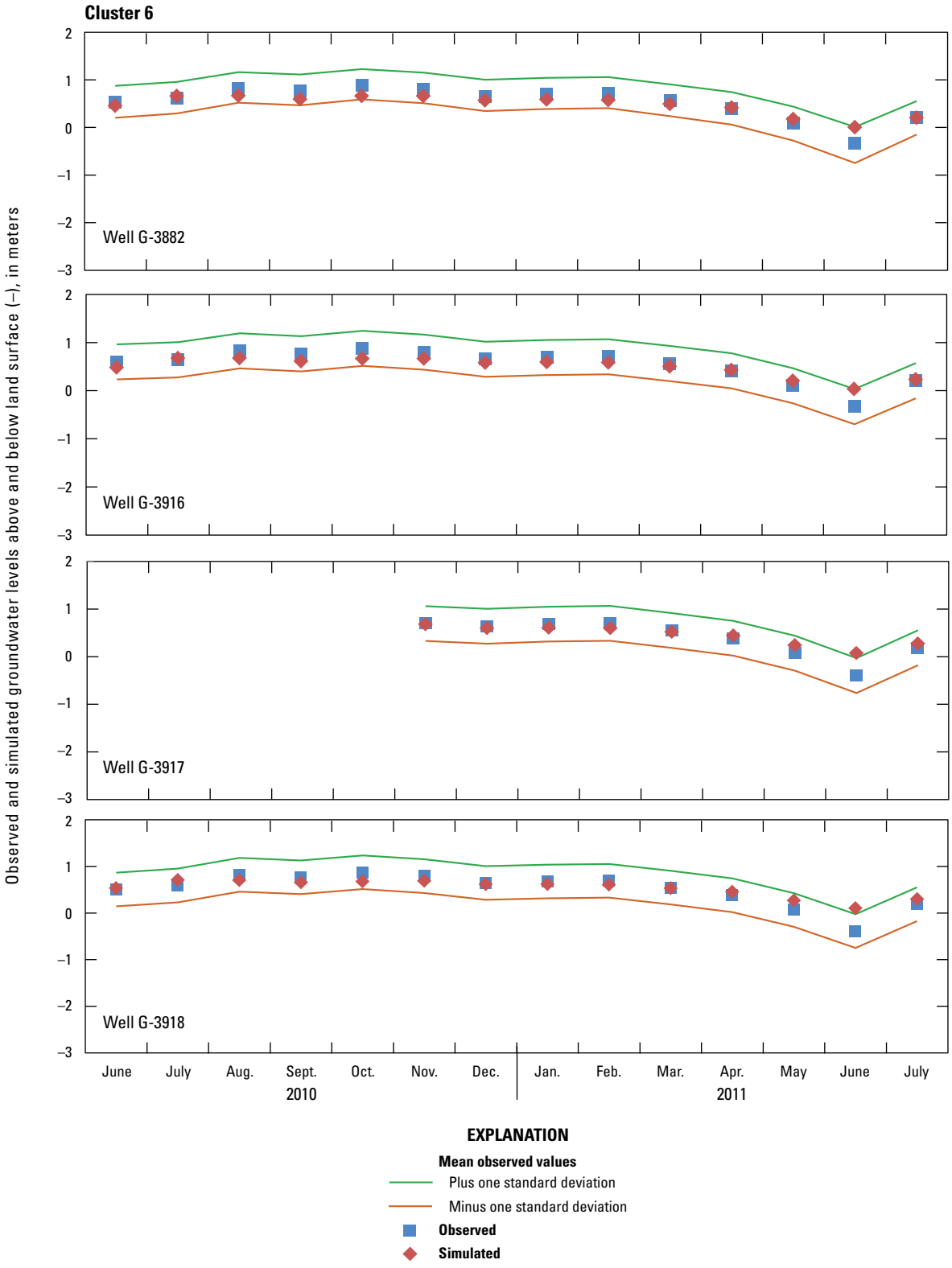

Figure 16. Simulated groundwater level, mean observed groundwater level, mean observed groundwater level plus one standard deviation, and mean observed groundwater level minus one standard deviation during the 14-month calibration period for the Snapper Creek Canal study area groundwater flow model. —Continued

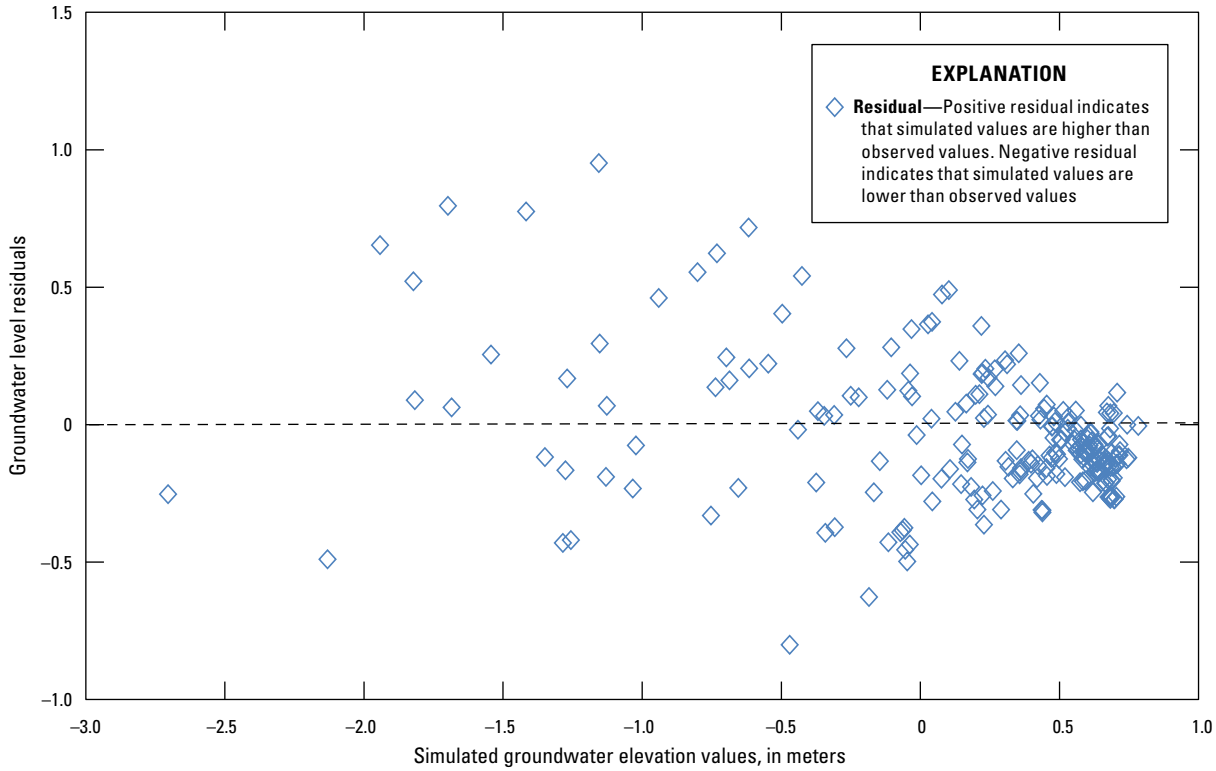

Figure 17. Simulated groundwater-level values and monthly groundwater-level residuals, June 2010–July 2011, Snapper Creek Canal study area, Miami-Dade County, Florida.

For simulated groundwater levels of –0.5 m or below, there are more positive than negative residuals, and the absolute values of the positive residuals in this range tend to be larger than the negative residuals. In contrast, for simulated groundwater levels of 0.5 m or above, there are more negative than positive residuals, and the absolute values of the negative residuals tend to be larger than the positive residuals.

Monthly mean error values for each well are also presented spatially across the study area (fig. 18). A mix of positive and negative monthly mean errors dispersed throughout the geologic cross section indicates randomness. Two of the groundwater clusters have positive and negative mean errors. The largest positive mean errors are mostly in the deeper preferential flow zones, and the negative mean errors tend to be in the shallower preferential flow zones. This pattern indicates that the model tends to simulate higher groundwater levels in the deeper preferential flow zones, and lower groundwater levels in the shallower preferential flow zones. One of the groundwater clusters (cluster 1) had all positive mean errors, indicating that the model simulates higher than observed water levels at this cluster. Conversely, clusters 2 and 3 had both positive and negative mean errors, indicating that the model simulates both higher and lower than observed water levels at these locations. This pattern indicates heterogeneity exists laterally between cluster 1 and clusters 2 and 3. No distinct systematic spatial patterns control the mean error distribution at the study area.

Canal Leakage

The fit of the simulated canal leakage is shown in figure 19. The majority of the plotted points cluster within 0.5 m^3/s of the line y=x, with the exception of data representing October 2010. During October 2010, a large amount of canal leakage was observed during a time of little pumping and precipitation (fig. 5). Daily data during October 2010 show periods with no pumping when the leakage continued to increase, indicating that processes other than local pumping can affect canal leakage. For example, a large decrease in barometric pressure occurred in the region at the end of September 2010, causing the canal stage and groundwater levels to spike. Canal stage and groundwater levels remained high through the beginning of October 2010 and then decreased after the beginning of the month. This “barometric event” and subsequent variability in canal stage and groundwater elevations may also have contributed to variations in canal leakage observed in October. Unusually high rates of groundwater pumping at neighboring well fields, although not documented in this study, could have caused changes in groundwater flow gradients that affected canal leakage.

The calibration target range for the simulated leakage values was defined by using the estimated maximum and minimum calculated observed leakage. The simulated leakage values all plot within this calibration target range (fig. 20). Note that the first 3 months of the calibration period have the

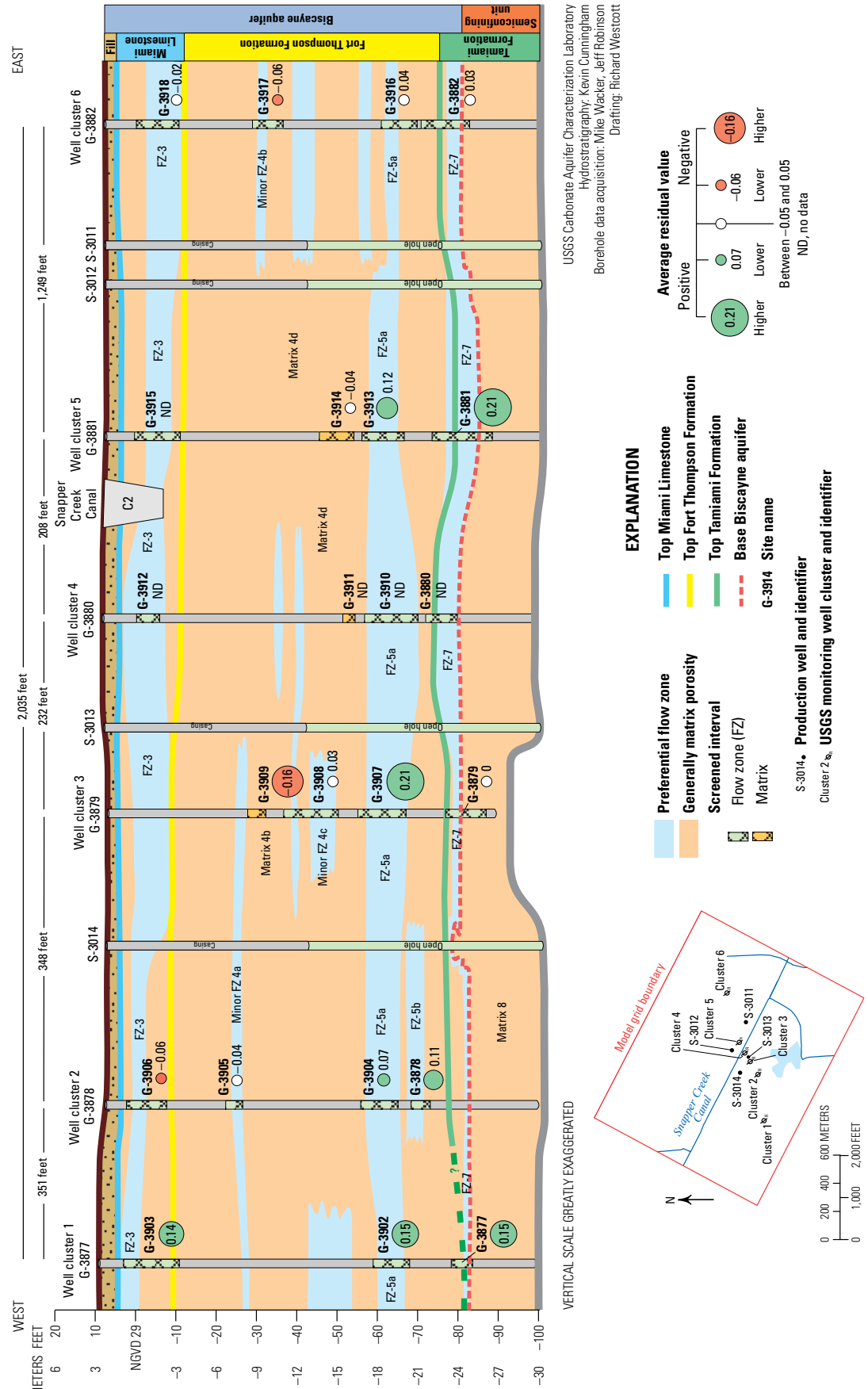

Figure 18. Conceptual hydrogeologic cross section showing monthly mean error values, by monitoring well, for June 2010–July 2011, calculated by using average monthly simulated and observed heads, Snapper Creek Canal study area, Miami-Dade County, Florida.

greatest variability in the measured discharge data (figs. 11 and 12), thus in leakage, and this results in the largest spread of the target flow range over the simulation period (fig. 20). Overall, the model can account for 87 percent of the 10.98 m^3/s of total cumulative observed leakage during the simulation period.

Leakage residuals were defined in the same manner as the groundwater-level residuals, with positive leakage residuals indicating an overestimate of canal leakage by the model and negative residuals indicating an underestimate. The calculated residuals appear to be normally distributed for the majority of the data, although it is somewhat uncertain with the small number of data points (fig. 21). The greater number of negative residuals than positive residuals indicates that in general the canal leakage values were slightly underestimated.

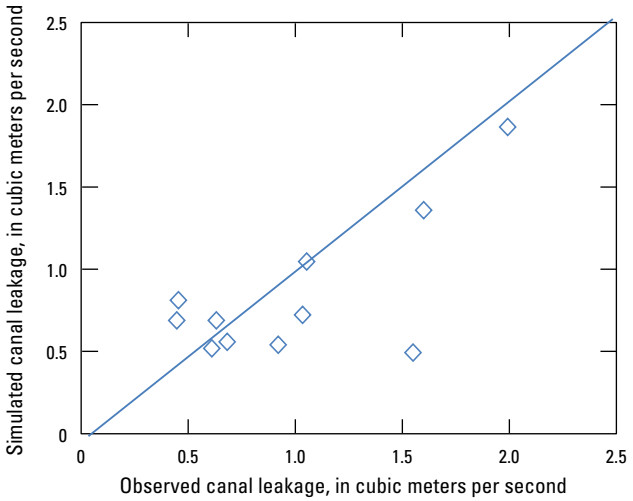

Figure 19. Model fit of observed and simulated canal leakage, Snapper Creek Canal, Miami-Dade County, June 2010–July 2011.

Groundwater Model Flow Budget

A groundwater flow budget was calculated for the study area to establish magnitudes of inflows and outflows from various sources and sinks (fig. 22). Groundwater inputs to the system occurred through the head-dependent boundaries, recharge, and canal leakage. Groundwater outflows from the system occurred through losses at the head-dependent boundaries, ET, canal seepage, or flow from the aquifer to the canal, and production well pumping. Production well pumping is represented with the term "net flow out of production wells" (fig. 22). Because the MNW package was used to simulate groundwater withdrawals, head gradients surrounding the pumping wells introduced a small amount of flow into the production wells, which also flows back out. This small amount of flow was subtracted from the flow out of the production wells, resulting in the net flow.

Canal leakage was the primary inflow, constituting about 97 percent of total flow into the groundwater system, and production well pumping and boundary outflow were the primary outflows, contributing 27 percent and 70 percent, respectively, of the total flow out of the groundwater system. The sum of production well pumping and boundary outflow

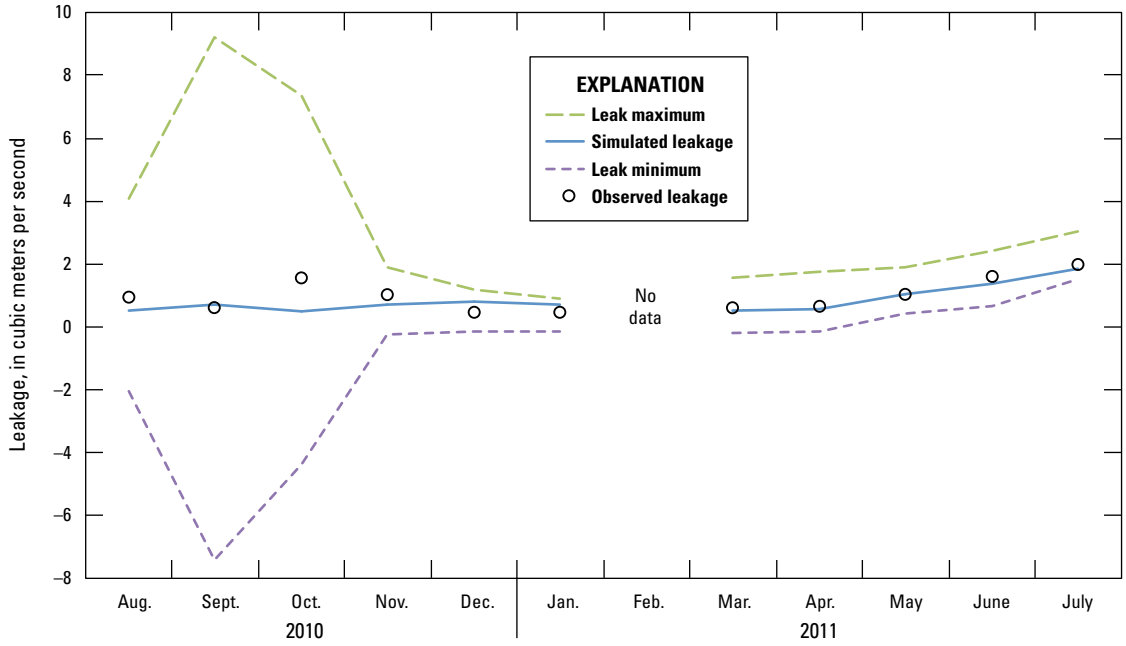

Figure 20. Model fit of observed and simulated canal leakage over the June 2010–July 2011 simulation period, Snapper Creek Canal study area, Miami-Dade County, Florida.

was essentially equivalent to canal leakage (97 percent). Cumulative groundwater flow into the system from general head boundaries was three orders of magnitude smaller than flow out of the boundaries. The groundwater levels were often higher within the study area than at the model boundaries because of large amounts of pumping in nearby production well fields that affected the groundwater levels at the boundary monitoring wells, thus causing a substantial amount of flow out of the model area through the boundaries and a smaller amount of inflow at the head-dependent boundaries. The amount of canal leakage recharging the aquifer was greater than the amount of canal seepage entering the canal, by five orders of magnitude. Input into the system from precipitation was greater than losses from evapotranspiration, but the magnitudes of these components were about an order of magnitude smaller than canal leakage, production well pumping, and boundary outflows.

Internal groundwater flow budgets were itemized to examine the amount of groundwater flux through each of the three continuous preferential flow zones into the matrix flow zone and the distribution of flux from the canal to the shallow preferential flow zone and the underlying matrix flow zone. Most of the cumulative canal leakage is into the shallow preferential flow zone through the canal sides; 57 percent occurs through the northeast side of the canal, and 39 percent occurs through the southwest side of the canal (fig. 23). Only 4 percent of the canal leakage occurs through the canal bottom into the underlying matrix flow zone. Overall, the net flux is from preferential flow zones into matrix flow zones. The net flux from the shallow flow zone into the underlying matrix flow zone is 97,030,000 m^3; the net fluxes from the middle preferential flow zone into the overlying and underlying matrix flow zones are 905,021 and 12,578,812 m^3, respectively; and the flux from the lowest preferential flow zone to the overlying matrix flow zone is 11,122,770 m^3 (table 4). This pattern indicates that the largest amount of flow occurs in the uppermost preferential flow zone, through recharge from precipitation and the canal as well as regional flow. This preferential flow zone is highly transmissive and acts to recharge the aquifer below the flow zone with vertically downward flow.

Table 4. Flow from preferential flow zones to matrix flow zones during simulation period.

Direction of flow	Flow, meters cubed
Shallow preferential flow zone to underlying matrix flow zone	97,030,000
Middle preferential flow zone to overlying matrix flow zone	905,021
Middle preferential flow zone to underlying matrix flow zone	12,578,812
Deepest preferential flow zone to overlying matrix flow zone	11,122,770

Flux through this top preferential flow zone to the rest of the Biscayne aquifer is substantially greater than the flux through any of the other preferential flow zones.

The cumulative flow budget was also calculated on a seasonal basis to highlight the differences in groundwater flow during south Florida's wet and dry seasons (fig. 24). For this study, the wet season was defined as occurring between June and September, and precipitation during the wet season accounted for 78 percent of the precipitation for the study period. The dry season was defined as occurring during October through May. From August 2010 through July 2011, production well pumping rates were greater during the wet season than during the dry season, which is unusual. Pumping rates are usually greater during the dry season because of less precipitation and available surface water. Because pumping was greater during the wet season for the time period representing the simulation period, the seasonal flow patterns observed may be atypical when compared with those from other years. During the dry season, the percentages of the flow budget that canal leakage and boundary outflows represent are greater than during the wet season. On a monthly scale, however, canal leakage is greater during the wet season than during the dry season, likely because of lower heads along the boundary and increased pumping during June and July 2011.

Relation Between Canal Leakage and Boundary Conditions

To better understand the relations between canal leakage and boundary conditions, two different scenarios were simulated. The controlling boundary heads along the perimeter of the model area were modified for the first scenario. For the second scenario, the production well pumping was turned off for the simulation period within the model so that the differences in canal leakage could be observed.

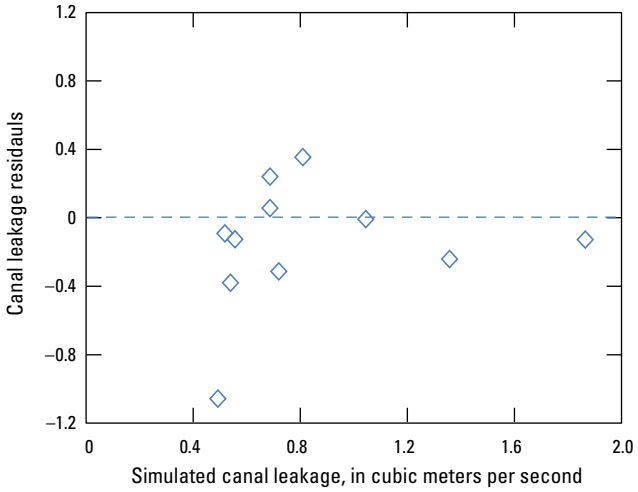

Figure 21. Simulated monthly average canal leakage and canal leakage residuals, June 2010-July 2011, Snapper Creek Canal study area, Miami-Dade County, Florida.

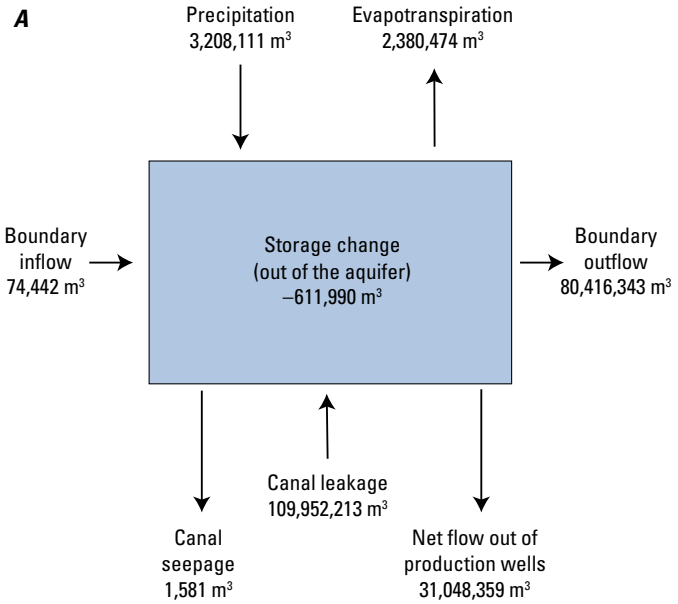

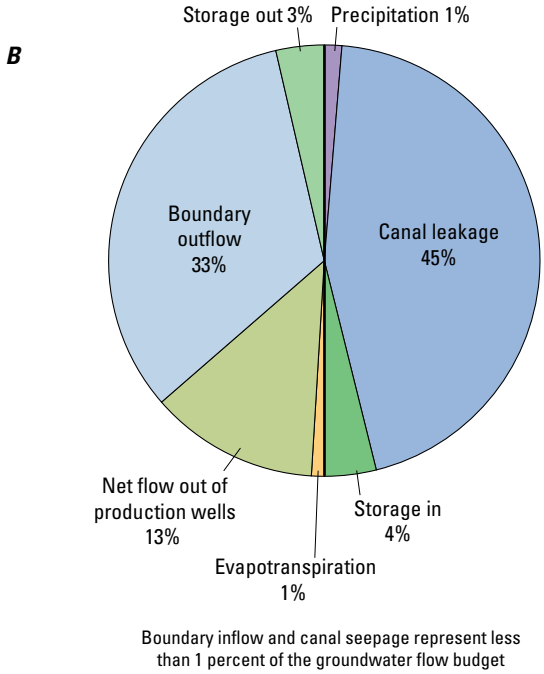

Figure 22. Cumulative groundwater flow budget for the Snapper Creek Canal study area, shown in (*A*) cubic meters (m^3) and (*B*) percentages.

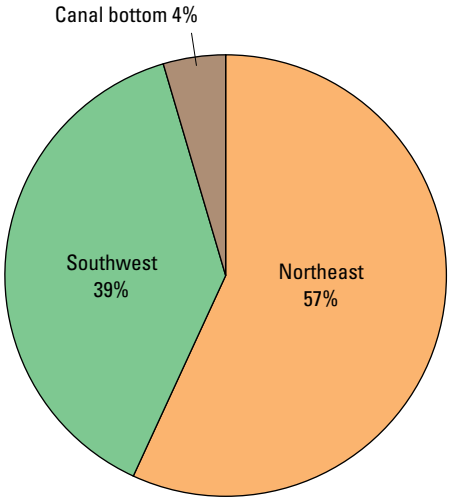

Figure 23. Distribution of canal leakage between canal bottom and the southwest and northeast sides, Snapper Creek Canal, Miami-Dade County, Florida.

Groundwater Flow with Modified Controlling Boundary Heads

The distribution of groundwater levels at the model boundary is uncertain. The study area is situated between two production well fields, and monitoring wells at those well fields demonstrate substantial drawdown during pumping. The water levels at the model boundaries likely are not as strongly affected as those of the well field's monitoring wells, but are likely still affected by the stresses at the neighboring well fields. To test the sensitivity of the model to the controlling heads at the model boundaries, a model realization using controlling heads not influenced by pumping at one of the neighboring well fields was simulated and compared with the calibrated model.

To generate the realization using controlling heads at the model boundary not influenced by pumping at the neighboring well fields, the GHB file was modified by sampling potentiometric surfaces generated without data from the two monitoring wells at a neighboring well field. Without wells G-3563 and G-1074B (fig. 7), the groundwater elevations at the perimeter boundary do not reflect as much drawdown as those used in the calibrated model, resulting in a smaller groundwater-level gradient from the canal stage to the groundwater levels at the boundaries. Therefore, the GHB file used for this realization generally resulted in higher water levels at the model boundaries.

Calibrating this realization resulted in a model fit similar to that of the calibrated model, with a slight linear bias, but the canal leakage was notably underestimated (figs. 25 and 26). For almost every month during the simulation, the simulated canal leakage was less than the observed canal leakage, and the leakage was underestimated relative to the calibrated model. Due to the increase in groundwater levels along

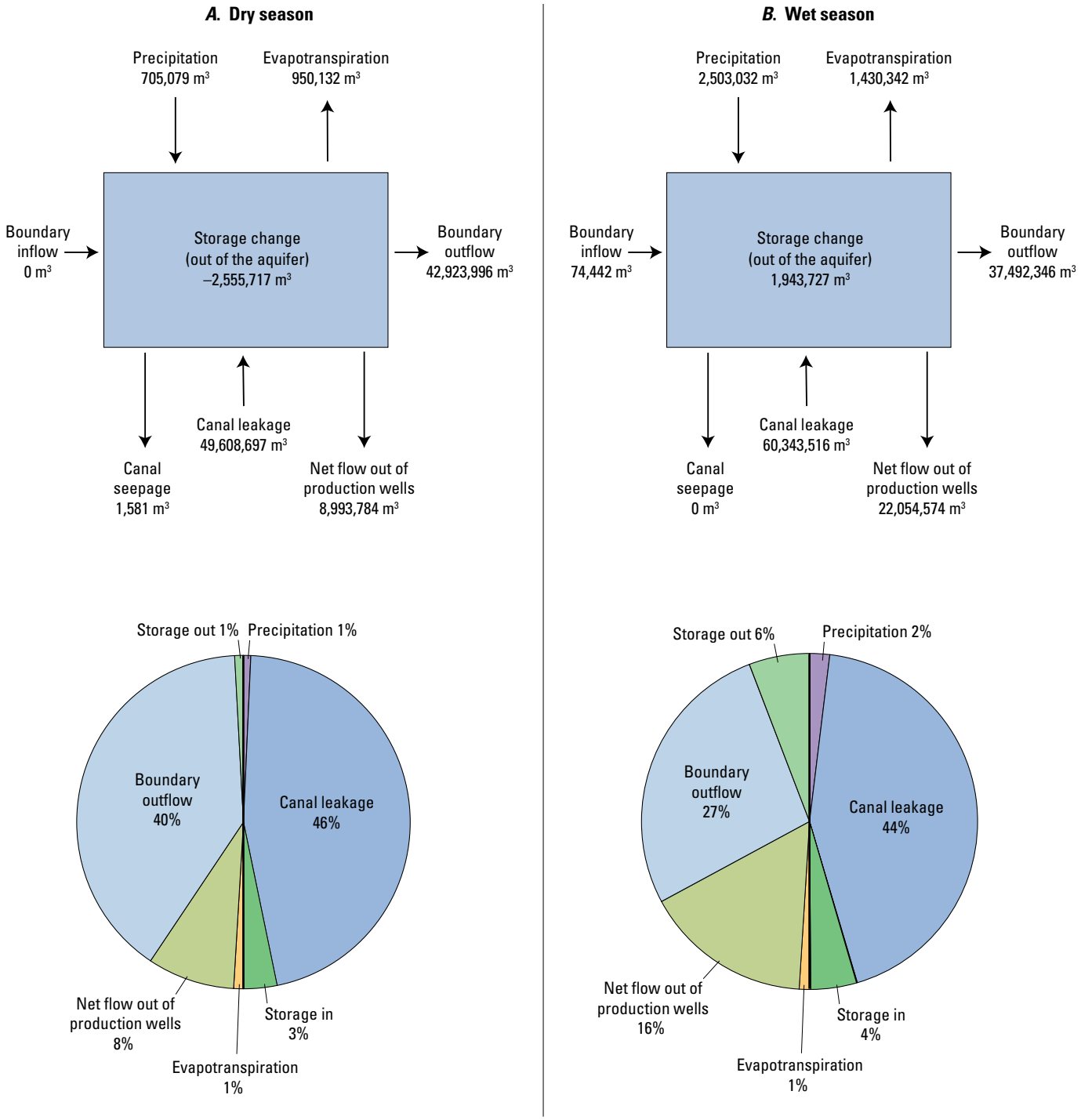

Figure 24. Cumulative groundwater flow budget for the dry and wet seasons for the Snapper Creek Canal study area, Miami-Dade County, Florida, June 2010–July 2011.

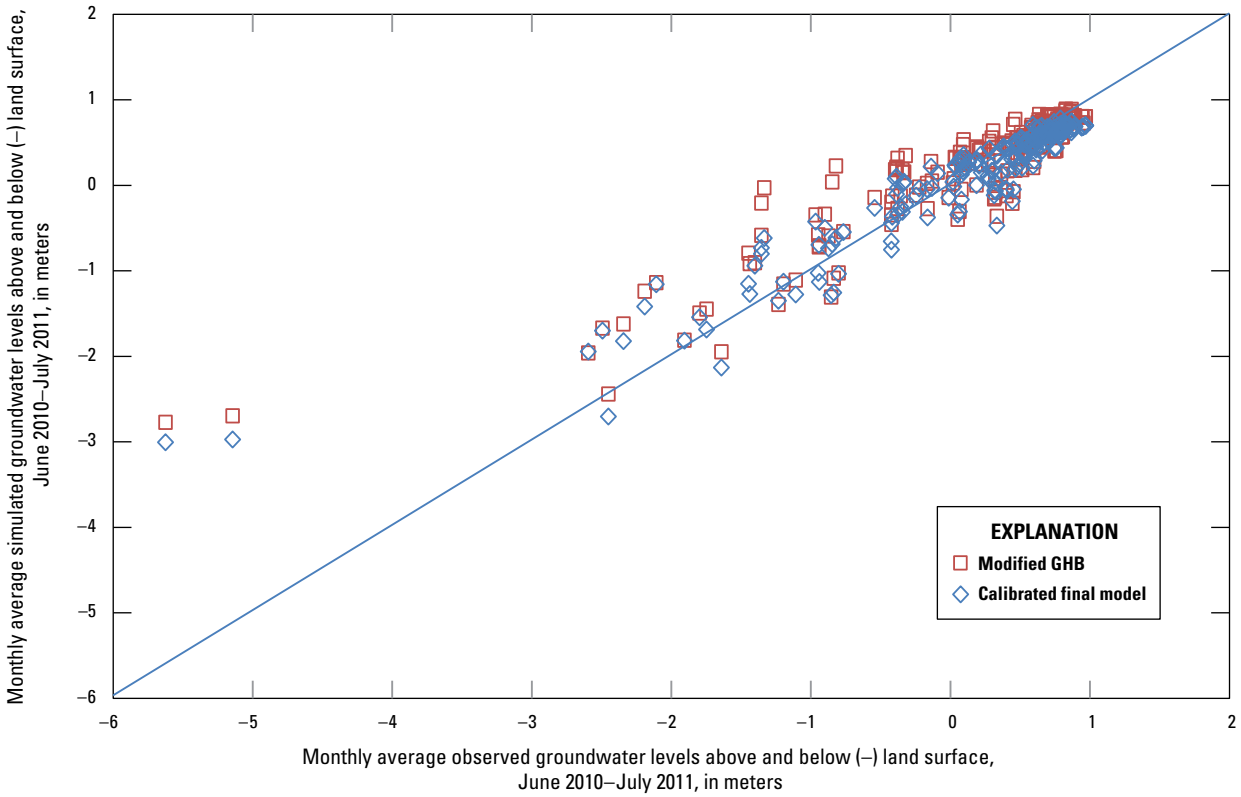

Figure 25. Monthly average simulated and observed groundwater levels, Snapper Creek well field, Miami-Dade County, Florida, June 2010–July 2011.

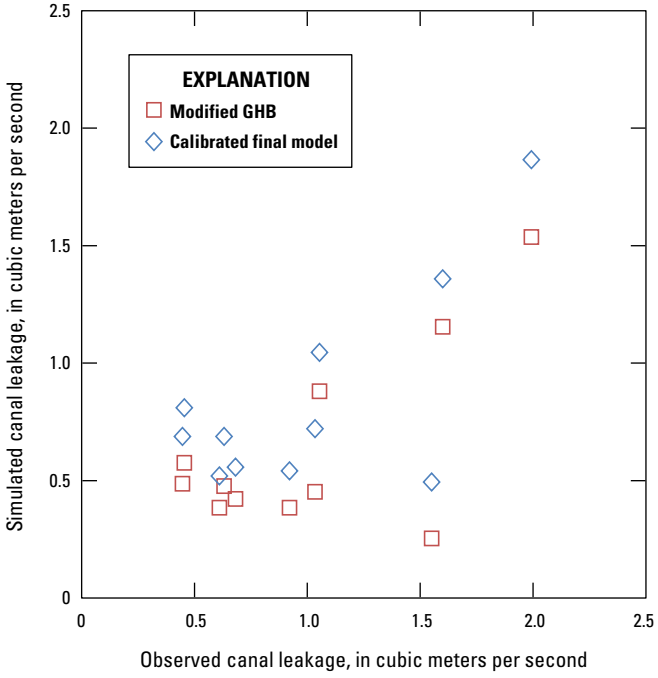

Figure 26. Observed and simulated canal leakage values used for the modified controlling heads realization in the groundwater flow model for the Snapper Creek Canal study area, Miami-Dade County, Florida.

the perimeter boundary when wells G-3563 and G-1074B were excluded, the magnitude of canal leakage was reduced (fig. 26). Without a substantial head gradient between the Snapper Creek Canal and the perimeter of the model area, the model was unable to simulate as much canal leakage as for the calibrated model. The model with the modified boundary condition was only able to capture 64 percent of the 10.98 m^3/s of observed cumulative leakage over the simulation period. These results indicate that the representation of the groundwater elevation distribution along the boundary of the model area is important and has the potential to substantially influence the simulated groundwater elevation and canal leakage values.

The mismatch between simulated canal leakage and observed canal leakage indicates the presence of another sink for the leakage other than pumping. This realization simulated with modified controlling heads at the model boundary indicates that lower groundwater levels outside of the study area can help match observed leakage. The simulation with the greater drawdown at model boundaries yielded larger amounts of canal leakage, suggesting that if groundwater levels were even lower at the model boundaries due to pumping at neighboring well fields or seasonal groundwater variations, obtaining the cumulative canal leakage observed at the study area would be possible. Periods of observed pumping at the study area well field often coincided with lowered groundwater levels along the perimeter boundary, suggesting that pumping at the neighboring well fields is affecting the canal leakage at Snapper Creek well field (fig. 27).

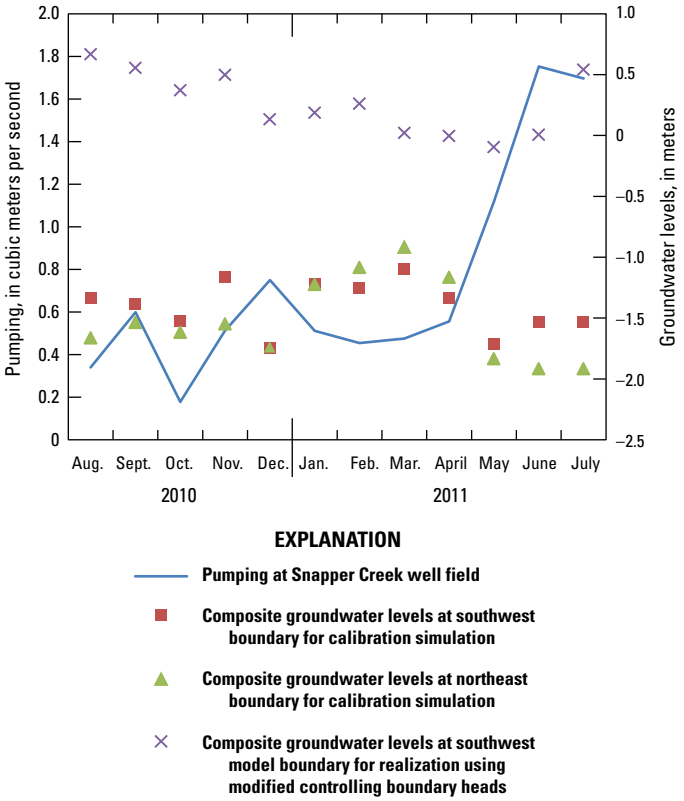

Figure 27. Simulated response of groundwater levels along the perimeter of the modeled study area during pumping of production wells, Snapper Creek Canal study area, Miami-Dade County, Florida, August 2010–July 2011.

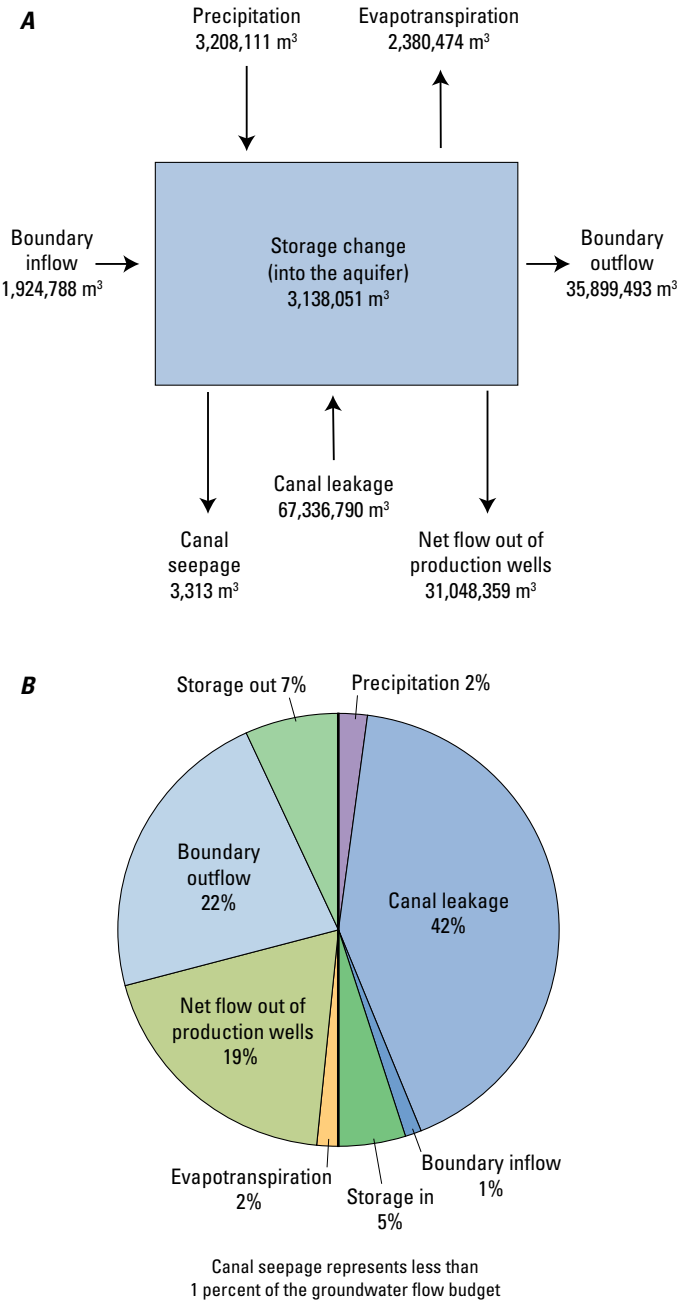

Figure 28. Cumulative groundwater flow budget calculated by using the modified controlling heads realization for the Snapper Creek Canal study area, shown in (*A*) cubic meters (m^3) and (*B*) percentages, June 2010–July 2011.

Using this modified controlling heads realization with wells G-3563 and G-1074B removed yielded a different groundwater flow budget than the one obtained when using the complete GHB file (figs. 22 and 28). The groundwater flow budget shows decreased outflow through the GHB by more than half (35,899,557 m^3 with modified GHB; 79,417,703 m^3 with complete GHB), and an order of magnitude greater inflow through the GHB (1,924,790 m^3 with modified controlling heads; 86,014 m^3 with complete GHB). Because the wells that had large amounts of drawdown due to pumping at the neighboring production well fields were removed, the groundwater-level gradient from the study area towards the boundaries was smaller than in the calibrated model. With this modified model, the amount of cumulative canal leakage recharging the aquifer is 62 percent of the amount of canal leakage in the calibrated model.

The cumulative groundwater flow budget with the modified boundary conditions was calculated on a seasonal basis (fig. 29), with June through September representing the wet season and October through May representing the dry season. Canal leakage is about the same percentage of the flow budget during the wet and dry season; however, the canal leakage rate on a monthly basis is greater during the wet season likely due to increased pumping during the wet season. During the wet season, the percentage of the flow budget represented by boundary outflow is less than half of the percentage represented by boundary outflow during the dry season. As illustrated in fig. 29, the average groundwater levels modeled by using the modified controlling heads were lower during the dry season than the wet season, causing more boundary outflow during the drier months.

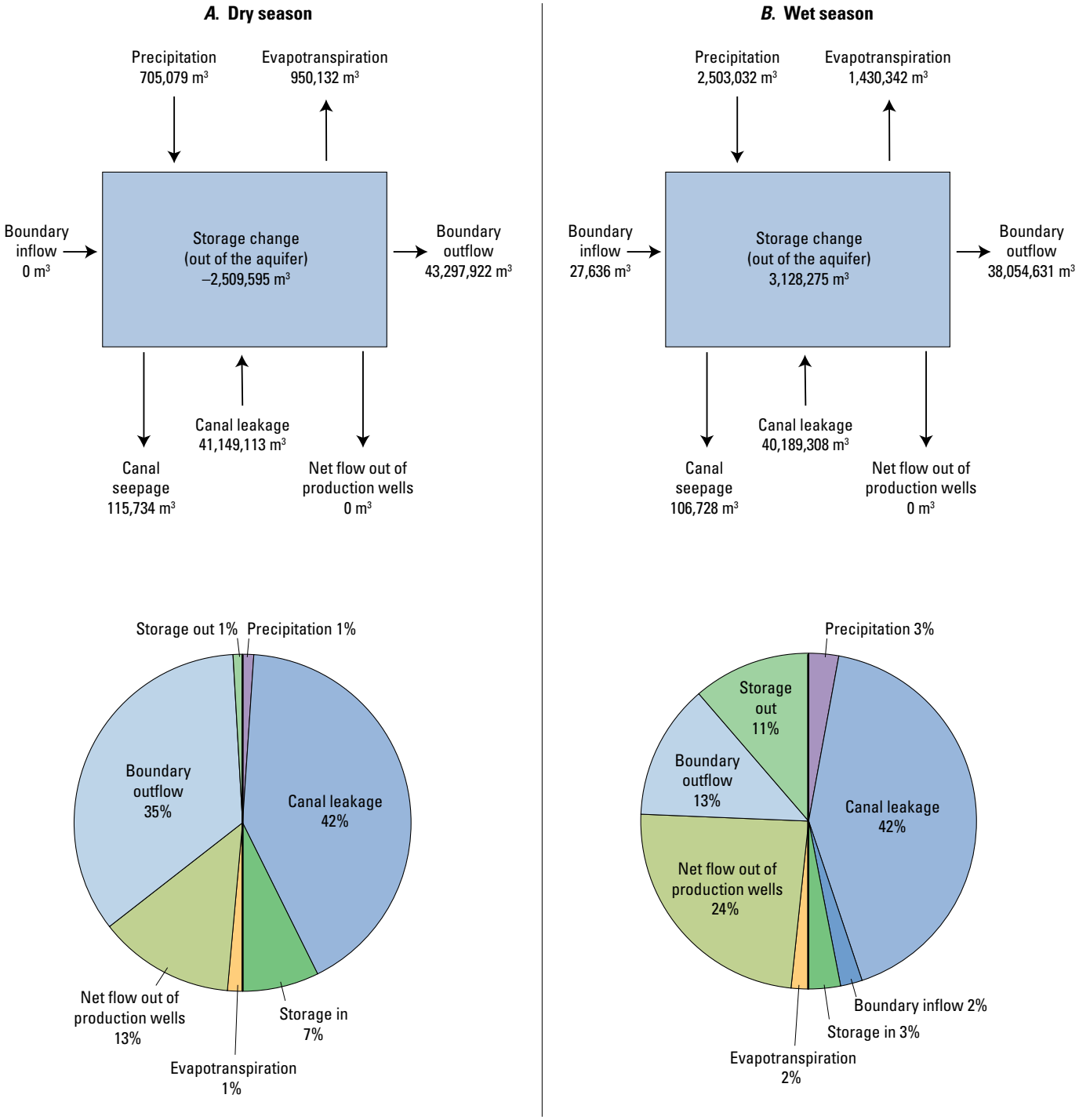

Boundary inflow (dry season) and canal seepage (dry and wet seasons) represent less than 1 percent of the groundwater flow budget

Figure 29. Cumulative groundwater flow budget calculated by using the modified controlling heads realization for the dry and wet seasons for the Snapper Creek Canal study area, Miami-Dade County, Florida, June 2010–July 2011.

Groundwater Flow for Non-Pumping Conditions

To quantify the relation between canal leakage and groundwater pumping, the calibrated model was run with and without pumping from the Snapper Creek well field to estimate the difference in canal leakage during production well pumping and the background leakage that occurs during non-pumping conditions (fig. 30). Background leakage was defined as the leakage that occurs within the system that cannot be attributed to local production well pumping. As such, background leakage was quantified from model runs without groundwater pumping. In the simulation, some background leakage was caused each month by natural and regional processes, and some leakage was induced by local pumping during each month.

The fraction of total canal leakage during pumping was examined as a function of local groundwater pumping by comparing the simulated difference in leakage with the pumps off to the amount of leakage occurring with the pumps on (fig. 31). Specifically, the term was calculated by using the following relation:

$$Leak_{pump} = \left[1 - \frac{sim_{NP}}{sim_{p}}\right] * 100\% , \quad (6)$$

where

$Leak_{pump}$ is the fraction of leakage during pumping;
sim_{P} is simulated leakage with pumping; and
sim_{NP} is simulated leakage without pumping.

The fraction of canal leakage during pumping is not linear with respect to pumping, which indicates that the amount of canal leakage caused by pumping varies with pumping magnitude (fig. 31). The results indicate that the increase over background leakage is about 6 to 45 percent in response to increased pumping magnitude. Specifically, when the pumping is about 0.5 m^3/s, the canal leakage during pumping is about 15 percent. When the pumping is about 1.9 m^3/s, the canal leakage during pumping is about 33 percent. These increases are, in effect, measures of the sensitivity of canal leakage to pumping and suggest decreasing sensitivity of canal leakage to pumping at relatively large pumping magnitudes. At the smaller pumping magnitudes, there are larger variations between fractions of leakage, and at larger pumping magnitudes, the fraction of leakage is not as sensitive to increases in pumping magnitude. The fraction of leakage begins to plateau around 0.4 suggesting that pumping greater than 0.9 m^3/s will not substantially increase the fraction of leakage during pumping.

The increase in leakage during production well pumping at the well field is not completely attributable to local pumping. During the dry season, months with large amounts of pumping at the study area coincide with increased pumping at the surrounding well fields. The increased pumping at the surrounding well fields results in increased drawdown at the model boundaries (fig. 27). Thus, the pumping in the surrounding well fields is causing additional canal leakage at the study area that occurs at the same time as large pumping

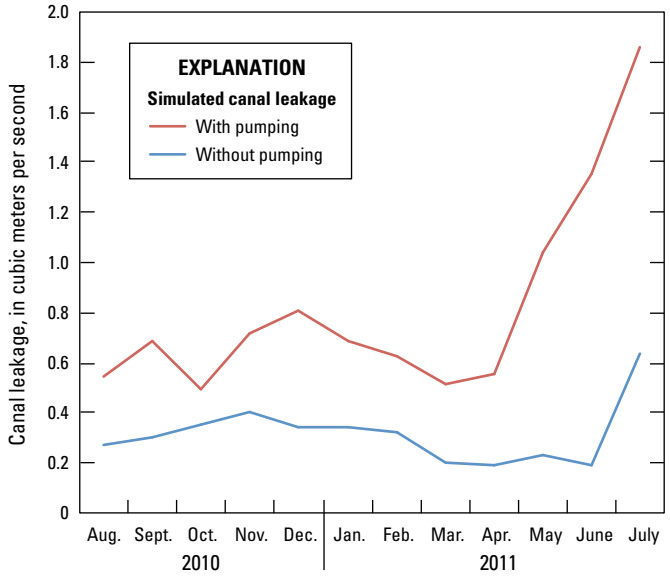

Figure 30. Simulated canal leakage with and without production well pumping, Snapper Creek Canal study area, Miami-Dade County, Florida, August 2010–July 2011.

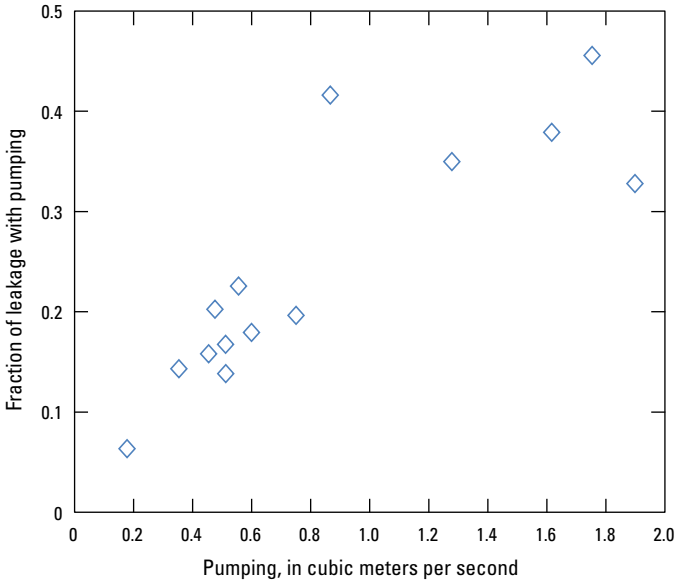

Figure 31. Fraction of canal leakage during pumping plotted as a function of pumping, Snapper Creek Canal study area, Miami-Dade County, Florida, August 2010–July 2011.

events at the study area, making it difficult to isolate the amount of induced leakage caused solely by local pumping at the study area.

The varied geology at the study area is likely responsible for somewhat dampening the relation between production well pumping and canal leakage. The semi-confining matrix zone that lies between the upper, highly transmissive preferential flow zone and the deeper, highly transmissive preferential flow zones containing the production wells buffers the pumping stresses on the canal. Without this semi-confining matrix flow zone between the highly transmissive zones, the production well pumping would likely induce a larger amount of canal leakage.

The cumulative groundwater flow budget was calculated for the simulation period under non-pumping conditions (fig. 32). Without the production well pumping, canal leakage and flow out of the model boundaries represent 43 and 44 percent, respectively, of flow within the model. The only other types of flow under non-pumping conditions were recharge from precipitation and losses through evapotranspiration, both of which were small in comparison to the magnitude of canal leakage and boundary outflows.

The seasonal groundwater flow budgets were calculated for the wet (June through September) and dry (October through May) seasons. The canal leakage is a slightly larger percentage of the flow budget during the dry season than during the wet season (fig. 33); however, the actual monthly rate of canal leakage is slightly greater during the wet season. The boundary outflows are also a greater percentage of the flow budget during the dry season than during the wet season. Because no production wells are pumping, these differences must be driven by the groundwater levels along the boundary.

The simulation with no pumping can be described as an "end member" analysis because of the proximity of the canal to the well field. The interactions between well-field pumping and induced canal leakage observed in this study are expected to be greater than the degree of interaction that would be observed at canals that are not as close to nearby pumping wells. Other factors, such as well depth, open interval depth, and geometry of the flow zones, affect the magnitude of canal leakage, but in this study, the proximity of the canal to the pumping wells magnifies their interaction. As distances between canals and well fields increase, the connection between well-field pumping and induced canal leakage would be dampened. Furthermore, at locations further from production well fields, the effects of additional processes would be relatively stronger than well-field pumping, making it more difficult to distinguish the direct relation between well-field pumping and canal leakage.

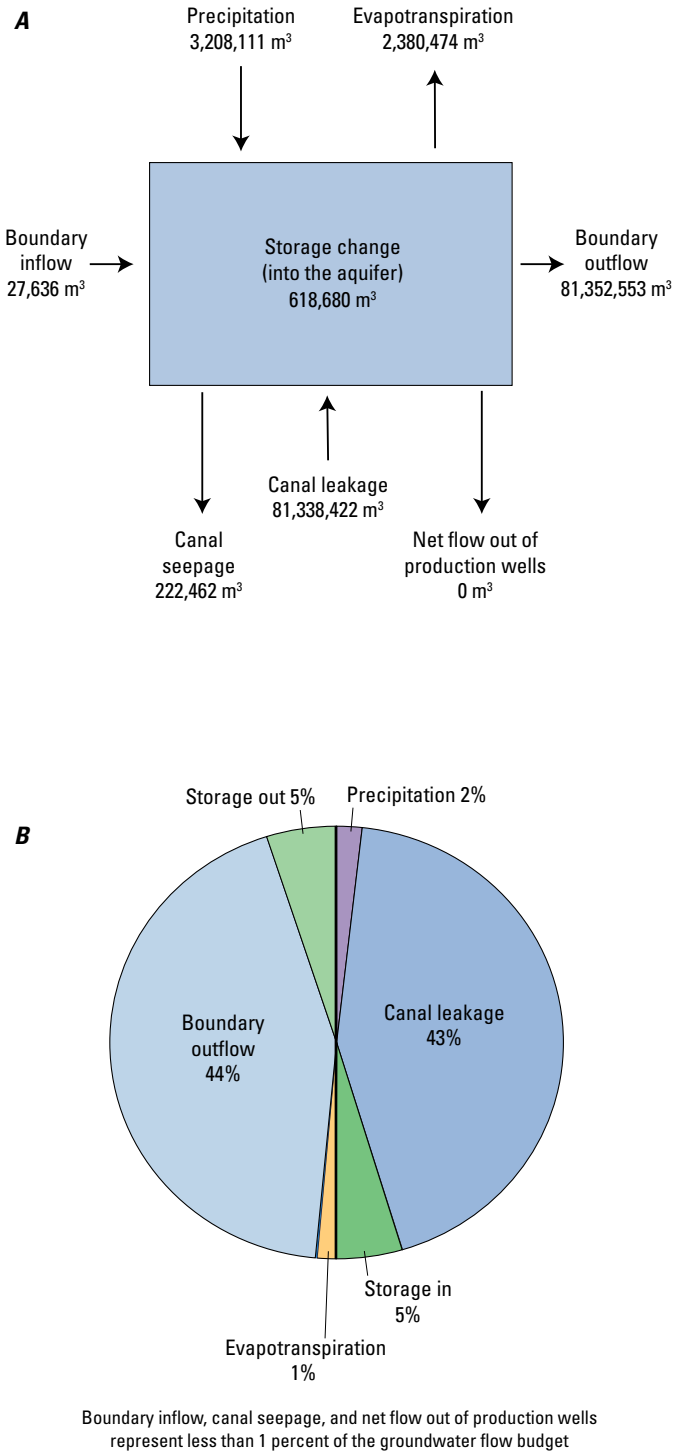

Figure 32. Cumulative groundwater flow budget under non-pumping conditions for the Snapper Creek Canal study area, shown in (*A*) cubic meters (m^3) and (*B*) percentages, June 2010–July 2011.

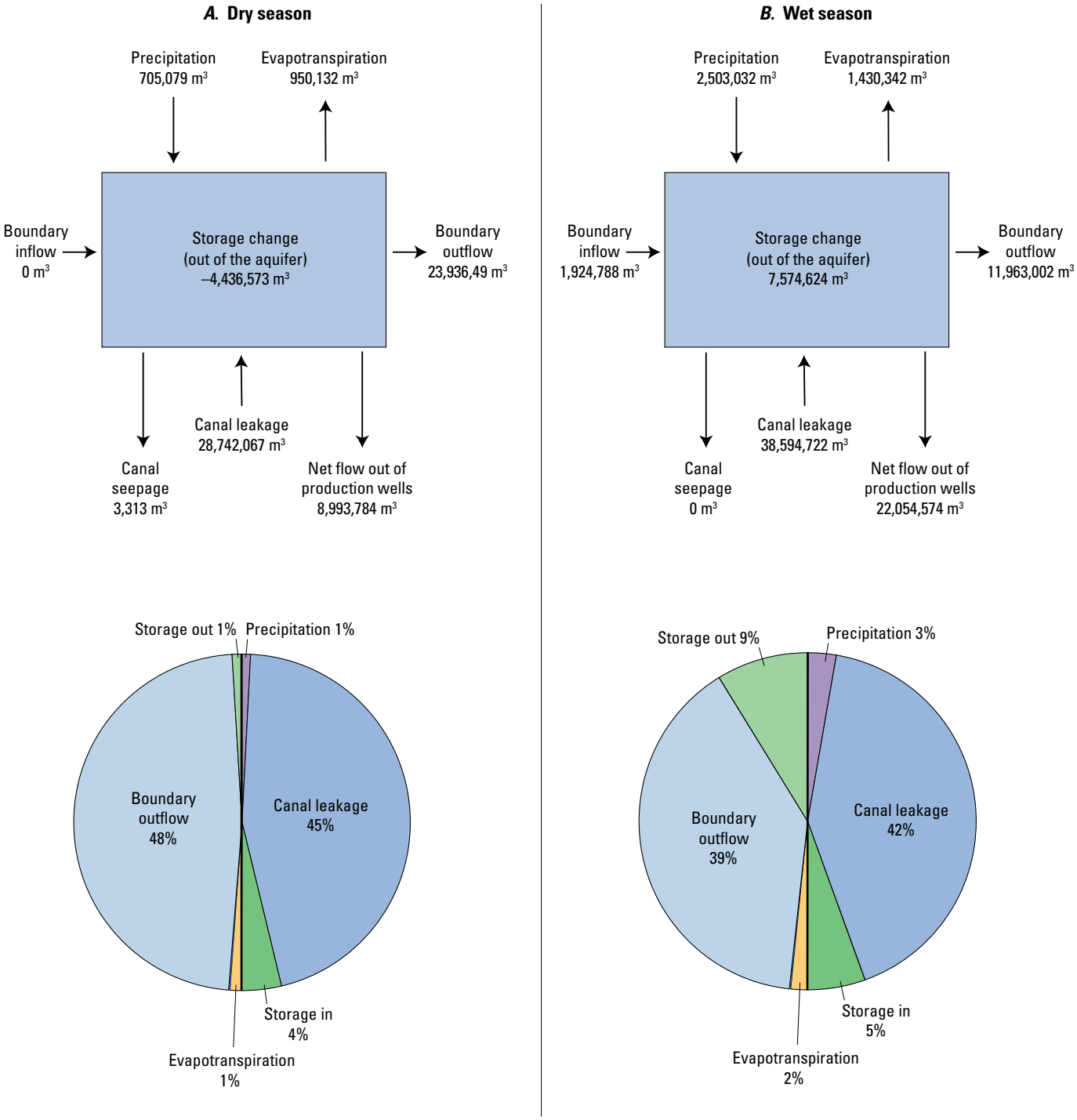

Boundary inflow, canal seepage, and net flow out of production wells represent less than 1 percent of the groundwater flow budget

Figure 33. Cumulative groundwater flow budget during non-pumping conditions for the (*A*) dry and (*B*) wet seasons for the Snapper Creek Canal study area, Miami-Dade County, Florida, June 2010–July 2011.

Isotope Chemistry

The stable isotopes of water are useful in distinguishing water samples from different sources based on variations caused by isotopic fractionation processes (Gibson and others, 2005). Hydrogen has two stable isotopes, protium (^{1}H) and deuterium (^{2}H, or D), and oxygen has three stable isotopes, ^{16}O, ^{17}O, and ^{18}O. Of the three stable oxygen isotopes, ^{16}O and ^{18}O are more naturally abundant. The isotopic fractionation process that occurs within the hydrologic cycle involves lighter water molecules (^{1}H and ^{16}O) preferentially evaporating, while leaving behind source water enriched in the heavier ^{2}H and ^{18}O isotopes. Additionally, during condensation, the heavier ^{2}H and ^{18}O isotopes preferentially condense and initially fall out as precipitation, leaving the remaining water vapor and subsequent precipitation more deplete in ^{2}H and ^{18}O. The repeated processes of evaporation, condensation, and precipitation alter the relative proportions of $^{2}H/\ ^{1}H$ and $^{18}O/\ ^{16}O$ and yield an isotopic signature that can be used to help distinguish water samples of different origins.

Oxygen and hydrogen isotopic compositions are reported relative to an established standard of average ocean water, referred to as the Vienna Standard Mean Ocean Water (VSMOW) (Clark and Fritz, 1997). Because of the large differences in natural abundance for each of the water isotopes, the ratios of $^{2}H/^{1}H$ and $^{18}O/^{16}O$ are conventionally expressed as δD and $\delta^{18}O$, respectively, as per mil deviations from VSMOW, where VSMOW is assigned δD and $\delta^{18}O$ values of 0 per mil. There is a linear relation between δD and $\delta^{18}O$ in global meteoric waters that have not undergone large amounts of evaporation (Craig, 1961). This relation can be expressed as the linear equation $\delta D=8*\delta^{18}O+10$ and is known as the Global Meteoric Water Line (GMWL). The slope of the GMWL equation reflects that fractionation processes are about eight times greater for hydrogen than for oxygen due to the significant size difference between ^{2}H and ^{1}H relative to that between ^{18}O and ^{16}O. The y-intercept value of 10 in the equation is because meteoric water is not in thermodynamic equilibrium with the ocean water it is sourced from and additional kinetic fractionation processes result in slightly more enrichment in deuterium (Kendall and McDonnell, 1998). A local meteoric water line can also be determined for a given geographic region using isotopic analyses of the local precipitation.

When the stable isotope compositions of water samples are compared to meteoric water lines and to each other, the source origin of the water (for example, surface water or groundwater) can be inferred and identified. Samples that have experienced some degree of evaporation will be enriched in ^{18}O and ^{2}H relative to local precipitation and will plot below the meteoric water line. By running a linear regression of these δD and $\delta^{18}O$ data for the water samples, an evaporation line can be constructed that yields a slope with a value that is less than that of the meteoric water lines. Samples with values that plot along this line can be assumed to have experienced evaporative processes or to have been mixed with water from a source that has experienced evaporative processes.

Methods

Samples were collected from the six groundwater well clusters that are roughly aligned from southwest to northeast through the study area (fig. 1*B*). Samples were collected from multiple monitoring wells and from matrix and preferential flow zones in the Biscayne aquifer. Wells completed in the deepest preferential flow zone had screened intervals, and the wells completed in the matrix and other preferential flow zones had open intervals (tables 1–1 and 1–2).

Beginning in October 2008, samples were collected monthly for the stable isotopes of water ($\delta^{2}H$ and $\delta^{18}O$) from four production wells (S-3011, S-3014, S-3015, and S-3016) and the Snapper Creek Canal. Two production wells, S-3011 and S-3014, are located within the study area (fig. 1*B*), whereas the other two production wells, S-3015 and S-3016 (fig. 7), are located approximately 3 kilometers (km) west of the study area.

In addition to the monthly sampling, four discrete water-quality sampling events were conducted during the summer and fall of 2010 and during the spring of 2011 under ambient (non-pumping) and pumping conditions (table 5). The first sampling event was conducted July 26–28, 2010. All production wells were turned off 3 days prior to the sampling event in order to obtain water-quality data under ambient conditions. All monitoring wells at all 6 well clusters, 23 wells in total, were sampled during this initial event. Because cleaning operations were being conducted within the Snapper Creek Canal, no concurrent surface-water sample was collected during this event. The second sampling event was conducted November 17–18, 2010, during which the two production wells on the north side of the Snapper Creek Canal (S-3011 and S-3012, fig. 1*B*) were turned on 4 days prior to and throughout the sampling. The third sampling event was conducted November 30, 2010, during which two production wells on the south side of the canal (S-3013 and S-3014) were turned on 6 days prior to and throughout the sampling. Due to the field logistics and pumping schedules involved, it was not possible to sample all clusters for either the second or third sampling events under pumping conditions. Therefore, only the active pumping wells (including S-3012, S-3013, and S-3014), well clusters closest to the canal (clusters 4 and 5), and the canal itself were sampled. Production well S-3011 was not sampled during the second and third sampling events because the well house was not equipped with the necessary infrastructure for the sampling at the time. The fourth sampling event was performed April 13–15, 2011. All of the production wells were turned off 14 days before the water-quality sampling began in order to achieve stable, ambient water levels within the study area. All monitoring well clusters, as well as the canal, were sampled during this event.

All water-quality samples within the study were collected according to USGS protocols (U.S. Geological Survey, variously dated). Water samples from the monitoring well clusters were collected by using a portable submersible pump with Teflon tubing. A minimum of three well-casing volumes of

water were purged from each well prior to sample collection, and water samples were collected only after field properties (temperature, pH, specific conductance, and dissolved oxygen) had stabilized. Water samples from the production wells were collected from spigots attached to each well while the well was pumping. Canal water samples were collected by using depth-integrated techniques consistent with USGS protocols (U.S. Geological Survey, variously dated). Samples were collected using a Teflon bottle and were composited together within a 14-L Teflon churn splitter.

Sample collection and preservation methods for the stable isotopes are described in the National Field Manual for the Collection of Water-Quality Data (U.S. Geological Survey, variously dated). Samples for stable isotope analysis (δ^2H and $\delta^{18}O$) were analyzed by using an isotope ratio-mass spectrometer with hydrogen gas water equilibration and carbon dioxide water equilibration techniques, respectively, at the USGS Stable Isotope Laboratory in Reston, Virginia. Values of δ^2H and $\delta^{18}O$ were reported in parts per thousand (‰) relative to VSMOW (Epstein and Mayeda, 1953; Coplen and others, 1991, 1994; Révész and Coplen, 2008) and normalized (Coplen, 1994) on scales such that the oxygen and hydrogen isotopic values of Standard Light Antarctic Precipitation are –55.5‰ and –428‰, respectively. The estimated expanded uncertainties of oxygen and hydrogen isotope results are 0.2‰ and 2‰, respectively.

Results and Discussion

The values of isotopic composition of all samples from the monitoring wells, production wells, and Snapper Creek Canal plot along a line that has a slope lower than that of the GMWL, indicating that some degree of evaporative fractionation has taken place in all samples (fig. 34). Previous research near the study area shows that the δD and $\delta^{18}O$ values for the groundwater samples collected in this study are within range of the values for groundwater samples collected in western Miami-Dade County and that the local meteoric water line for south Florida is consistent with the GMWL (Wilcox and others, 2004; Florea and McGee, 2010). The groundwater and canal samples from the study area plot along a regression line (also known as an evaporation line) of 5.28 $\delta^{18}O$ + 0.90 (r = 0.90), where, if extrapolated out, the intersection it makes with the GMWL approximates the isotopic signature of the original local precipitation source. The composition values of samples from production wells S-3015 and S-3016 also plot along the evaporation line because they share the same local precipitation source. Samples that contain a water composition exhibiting the effects of evaporative fractionation will plot away from the intersection point and further along the evaporation line (towards top right) as the evaporated component increases.

The canal water samples, with concentrations of δD ranging from –0.93 to 5.51‰ and $\delta^{18}O$ ranging from –0.26 to 0.89‰, generally have a more enriched isotopic composition compared to the groundwater samples in the study area. The δD and $\delta^{18}O$ concentrations in water samples from the monitoring well clusters range from –8.02 to 5.62‰ and –1.79 to 0.70‰, respectively, whereas δD and $\delta^{18}O$ concentrations in samples from the production wells range from –3.63 to 2.76‰ and –0.90 to 0.18‰, respectively. Production well S-3015 has a similar isotopic composition to that of the study area production wells, yet well S-3016 reflects a more depleted composition. The isotopic composition observed in well S-3016 may be related to the proximity of seepage ponds that are used to hold discharge from a nearby drinking water treatment processing plant. Vertical solution pipes within the shallow aquifer may bring rapid groundwater recharge from the surface seepage ponds.

The Snapper Creek Canal has a clearly enriched isotopic signature, which is represented by most samples plotting on the top right end of the evaporation line and is indicative of its source waters upstream in the Everglades. However, the Snapper Creek Canal samples have median δD and $\delta^{18}O$ values of 3.00‰ and 0.38‰, respectively, which indicates notably less enrichment than surface-water samples collected in the Everglades by Wilcox and others (2004), which had median δD and $\delta^{18}O$ values of 10.62‰ and 1.48‰, respectively (fig. 35). This finding indicates that, although the headwaters of the Snapper

Table 5. Description of discrete water-quality sampling events conducted in the Snapper Creek study area, July 2010–April 2011.

[NGVD 29, National Geodetic Vertical Datum of 1929; m^3/s, cubic meter per second]

Sampling event	Dates of sampling	Sites sampled (see fig. 1*B*)	Status of pumping wells	Canal stage (meters above NGVD 29)	Canal discharge (m^3/s)
1	July 26–28, 2010	All monitoring well clusters	Pumps OFF	0.96	6.68
2	November 17–18, 2010	Clusters 4 and 5, well S-3012, canal	S-3011 and S-3012 ON	1.00	2.54
3	November 30, 2010	Clusters 4 and 5, well S-3013, well S-3014, canal	S-3013 and S-3014 ON	0.98	1.94
4	April 13–15, 2011	All monitoring well clusters, canal	Pumps OFF	0.66	2.05

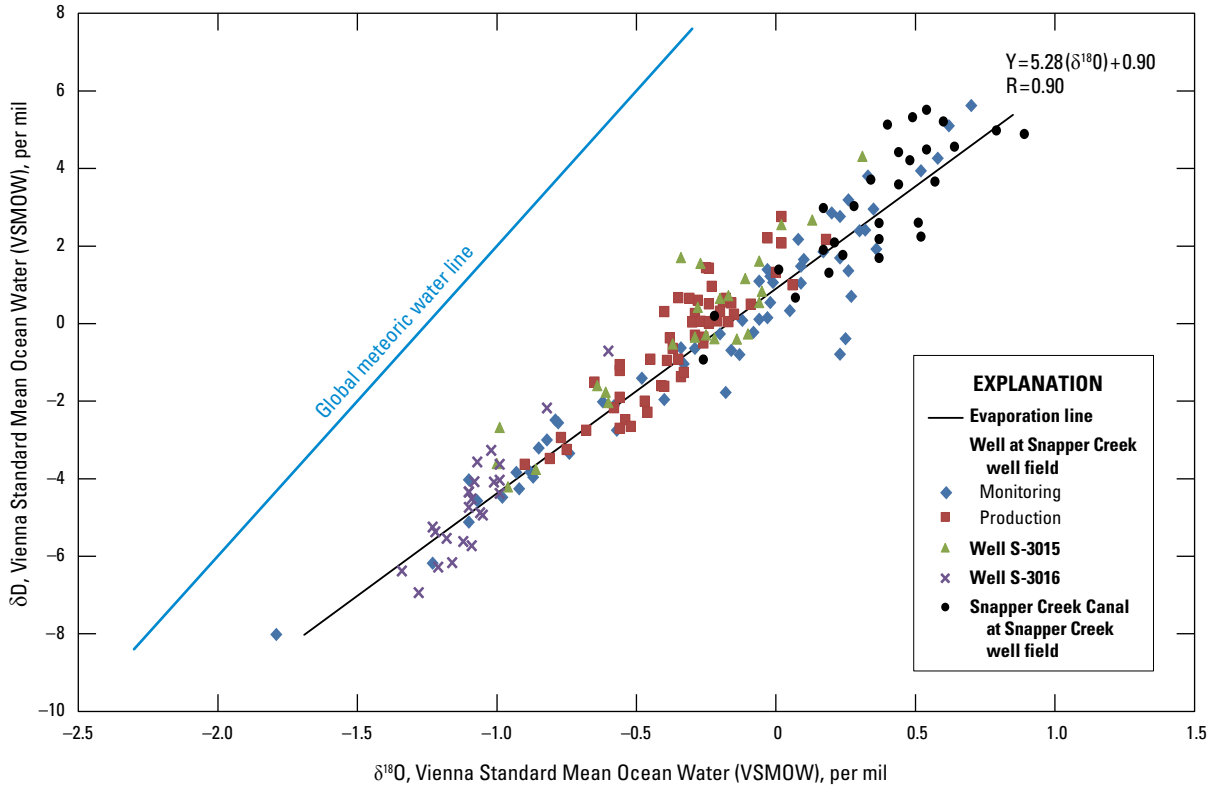

Figure 34. Relation between δD and $\delta^{18}O$ values for wells sampled within the study area in the Biscayne aquifer and Snapper Creek Canal in Miami-Dade County, Florida from October 2008 to April 2011. Global meteoric water line (GMWL) based on Craig (1961).

Creek Canal are in the Everglades, by the time the water flows through the study area, it has received a substantial amount of isotopically depleted recharge from local precipitation, runoff, and groundwater discharge from the Biscayne aquifer (Hughes and White, 2014).

The ambient median δD and $\delta^{18}O$ values for the monitoring well clusters seem to trend spatially across the study area from the southwest to northeast, where well clusters downgradient of the canal (clusters 5 and 6) generally had higher δD and $\delta^{18}O$ values than the other clusters (fig. 36). Lietz and others (2002) observed that the regional groundwater flow across the Miami-Dade County area was west to east at a water-level gradient of a fraction of a meter per kilometer. Throughout the first sampling event during the wet season, the southwestern side of the study area shows more uniform and relatively higher water levels (mean elevation of 0.94 m above NGVD 29) within the shallow flow zone of the aquifer when compared with the northeastern end of the study area, where groundwater levels are 0.03 m lower in cluster 5 (mean elevation of 0.90 m above NGVD 29) and nearly 0.15 m lower in cluster 6 (mean elevation of 0.81 m above NGVD 29) (fig. 37). This trend in water levels is consistent with the west-to-east groundwater flow that Lietz and others (2002) observed on a regional scale. The canal stage was 0.96 m above NGVD 29 during the wet season sampling, higher than all groundwater levels at the time, with a larger natural gradient on the northeast side of the study area, indicating a larger degree of canal recharge. The δD and $\delta^{18}O$ data appear to reflect the groundwater flow gradient during the wet season, when the lowest δD and $\delta^{18}O$ values are observed within the upgradient, southwest monitoring wells (clusters 1 and 2), and the most consistently high δD and $\delta^{18}O$ values (enriched) are observed in the furthest northeast wells within cluster 6. Thus, cluster 6 most closely reflects the isotopic signature of the canal. Note that some drawdown within cluster 6 may also be, in part, an effect of pumping operations from a nearby production well field to the northeast of the study area.

The clusters located closest to the canal, clusters 3, 4, and 5, have ambient median δD and $\delta^{18}O$ values that plot between the ranges of clusters 1 and 2 and cluster 6, with the exception of cluster 5 during the dry season (fig. 38). Clusters 3 and 4 located on the upgradient side of the canal have similar ambient water levels that have a relatively lower water-level gradient with the canal. Cluster 5, located on the downgradient side of the canal, has a relatively higher water-level gradient with the Snapper Creek Canal and is expected to have a larger component of the more enriched canal recharge than wells on the upgradient side; however, the isotopic data do not reflect this during the wet season.

During the dry season, the west-to-east water-level gradient does not appear to be as pronounced within the hydrologic data as observed during the wet season. Water

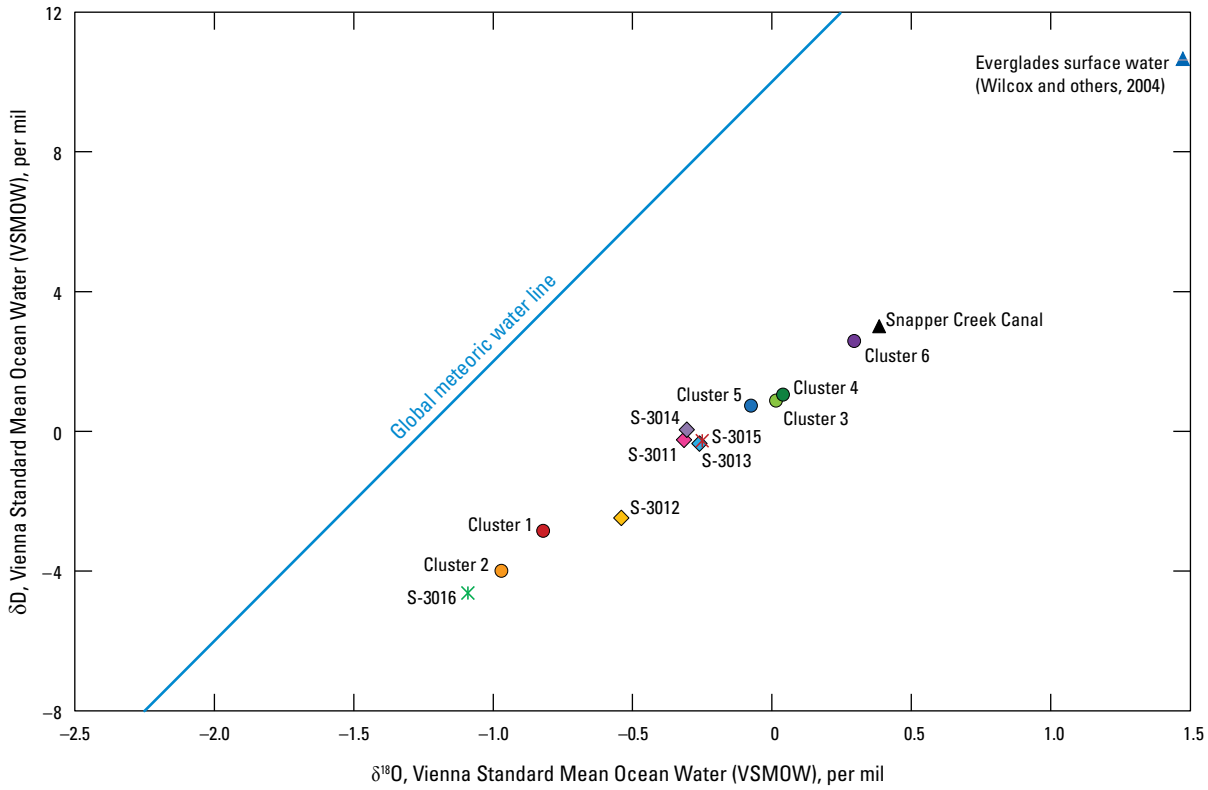

Figure 35. Relation between median δD and $\delta^{18}O$ values for sites sampled in the Biscayne aquifer and Snapper Creek Canal in Miami-Dade County, Florida from October 2008 to April 2011. Global meteoric water line (GMWL) based on Craig (1961).

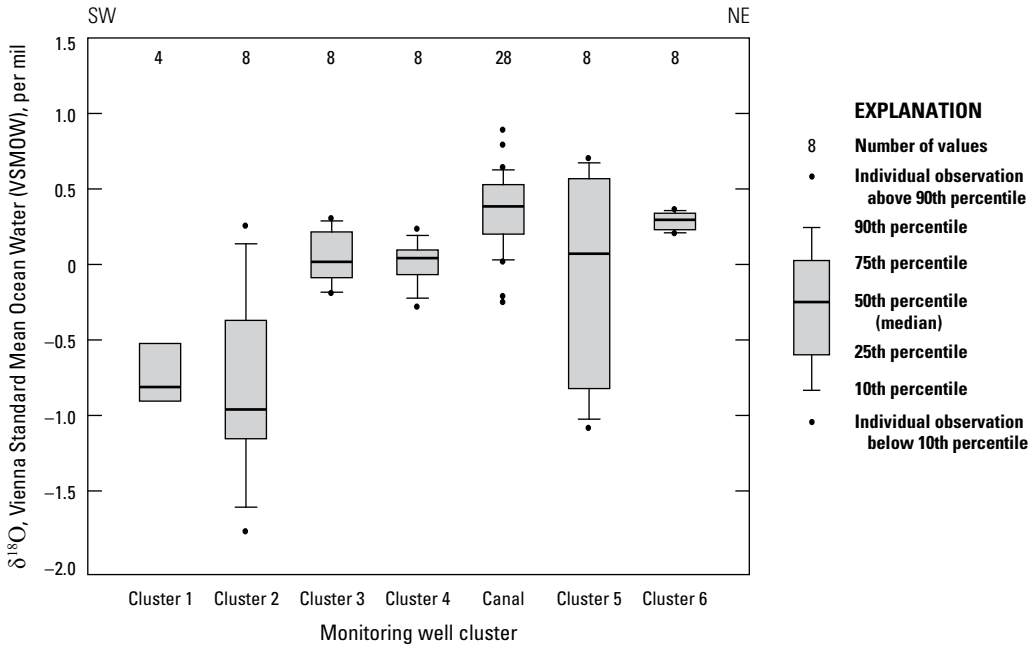

Figure 36. Range, median, and quartile statistical values for $\delta^{18}O$ composition at sites sampled in the Biscayne aquifer and Snapper Creek Canal in Miami-Dade County, Florida from October 2008 to April 2011.

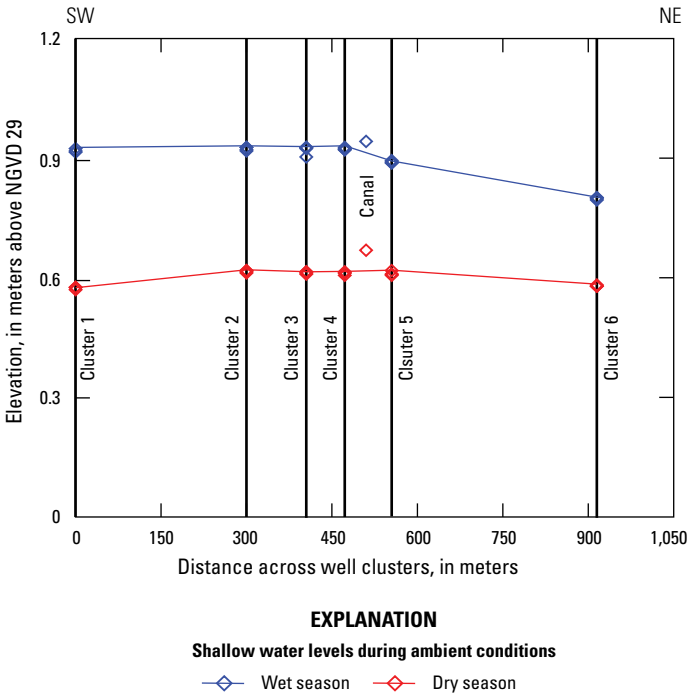

Figure 37. Water levels within the study area during the wet and dry season sampling events for the Biscayne aquifer and Snapper Creek Canal in Miami-Dade County, Florida from July 2010 to April 2011.

levels within the monitoring wells within the shallow zone closest to the canal are uniform, but with increasing distance from the canal, water levels decline slightly in wells, specifically within clusters 1 and 6. Though the canal stage was consistently higher than groundwater levels across the study area during all sampling events, the canal appears to have more influence on local groundwater recharge during the dry season when precipitation recharge is less than during the wet season. Though the regional groundwater gradient does not affect water levels during the dry season as much as during the wet season, it does affect isotopic composition of water samples during the dry season. The δD and $\delta^{18}O$ values increased across the study area, from west to east, during the dry season. This seasonal variation can be visualized within the δD and $\delta^{18}O$ data by plotting median values for both wet and dry season sampling events during ambient conditions (fig. 38). The overall trend is consistent, with δD and $\delta^{18}O$ values lower in samples from clusters 1 and 2 and δD and $\delta^{18}O$ values higher in samples from cluster 6. Groundwater samples from clusters 1 and 2 have noticeable variability in isotopic composition between seasons, more so than in samples from clusters 3, 4, and 6. Isotopic compositions in water samples from cluster 5 have considerable variability between the wet and dry seasons, with δD and $\delta^{18}O$ values that are comparable to those in clusters 1 and 2 during the wet season and the highest δD and $\delta^{18}O$ values sampled during the dry season. A possible explanation for the very low isotopic values during

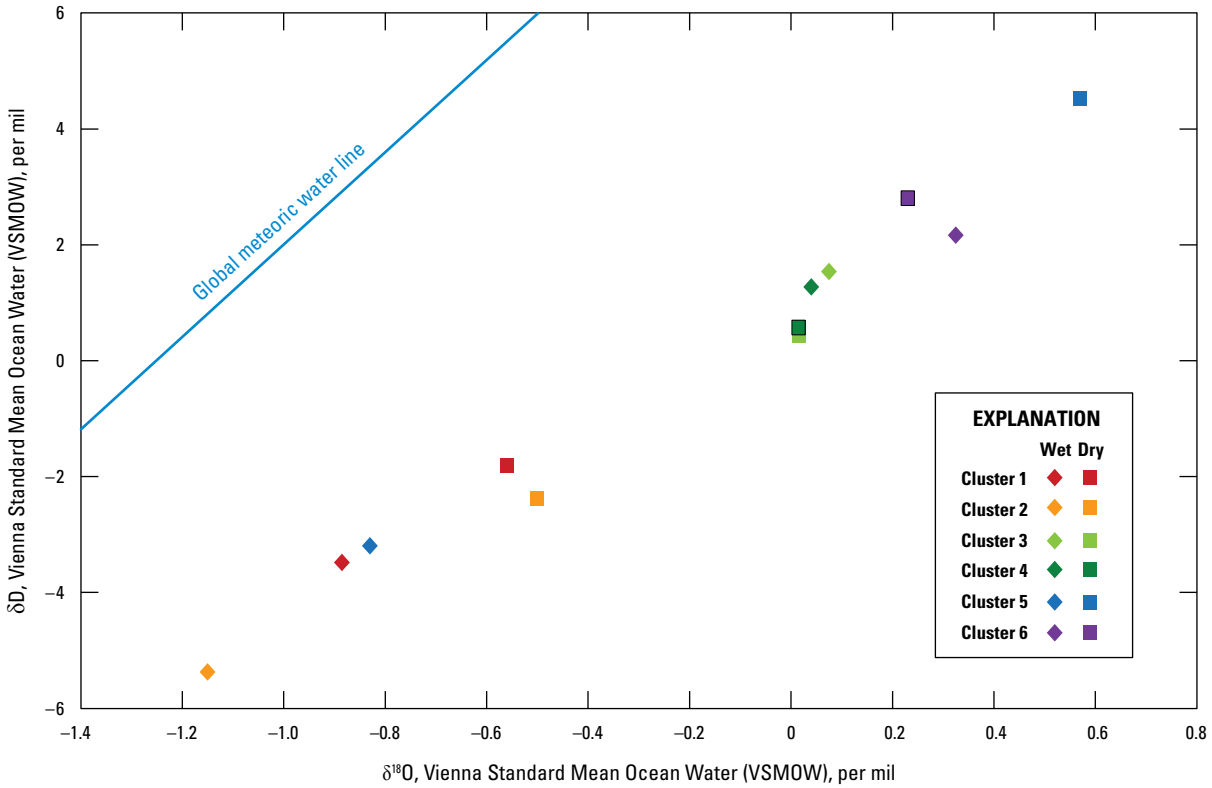

Figure 38. Relation between median δD and $\delta^{18}O$ values for sites sampled during the wet and dry season sampling events (July 2010 and April 2011, respectively) within the Biscayne aquifer and Snapper Creek Canal in Miami-Dade County, Florida. Global meteoric water line (GMWL) based on Craig (1961).

the wet season may involve pump maintenance within nearby production well S-3012, which was conducted earlier during the week of the wet season sampling event. Large volumes of groundwater were removed during maintenance and discharged into the field near cluster 5. Because the area may have numerous vertical dissolution cavities observed on the surface and in borehole geophysical data (Wacker and others, 2014), groundwater with an isotopically depleted composition from well S-3012 could have rapidly infiltrated and mixed with groundwater that may naturally receive a larger component of the enriched canal recharge. Despite the isotopically depleted compositions of water samples collected from cluster 5 during the wet season, the samples with the most enriched isotope compositions were collected from the shallow flow zone within cluster 5 during the dry season.

Cross sections showing generalized qualitative contours for $\delta^{18}O$ values from the ambient sampling events during the wet and dry seasons were created to show the vertical distribution of water quality across the study area (figs. 39 and 40, respectively). During the wet season sampling event, the more ^{18}O-depleted samples within each well cluster were from the deeper wells across most of the study area (fig. 39). Though more depleted in ^{18}O, the deeper zones within each cluster somewhat follow the isotopic trend of the wells in the shallower zones. The largest isotopic ranges within a well cluster were in clusters 2 and 5 where the shallow zone was noticeably more enriched than the deeper sampled zones. This enrichment may be indicative of canal recharge mixing with local groundwater within the shallow flow zone and not evident at depth within the aquifer. Samples from across the study area were generally enriched with the heavier isotopes during the dry season, with most enrichment in samples from within the shallow zones (fig. 40). Exceptions include cluster 2 and, to a lesser degree, cluster 3, where the isotopic trend is reversed and the shallow wells within the cluster have the most depleted signatures, indicating that the influence of canal recharge may have less influence on the shallow flow zones further upgradient from the canal than those near the canal. The trend reversal may also indicate small amounts of groundwater mixing in a deeper, interconnected flow zone located about 16.5 to 21 m below NGVD 29 within clusters 2, 3, and 4, which also coincides with the production zone of the nearby S-3013 production well.

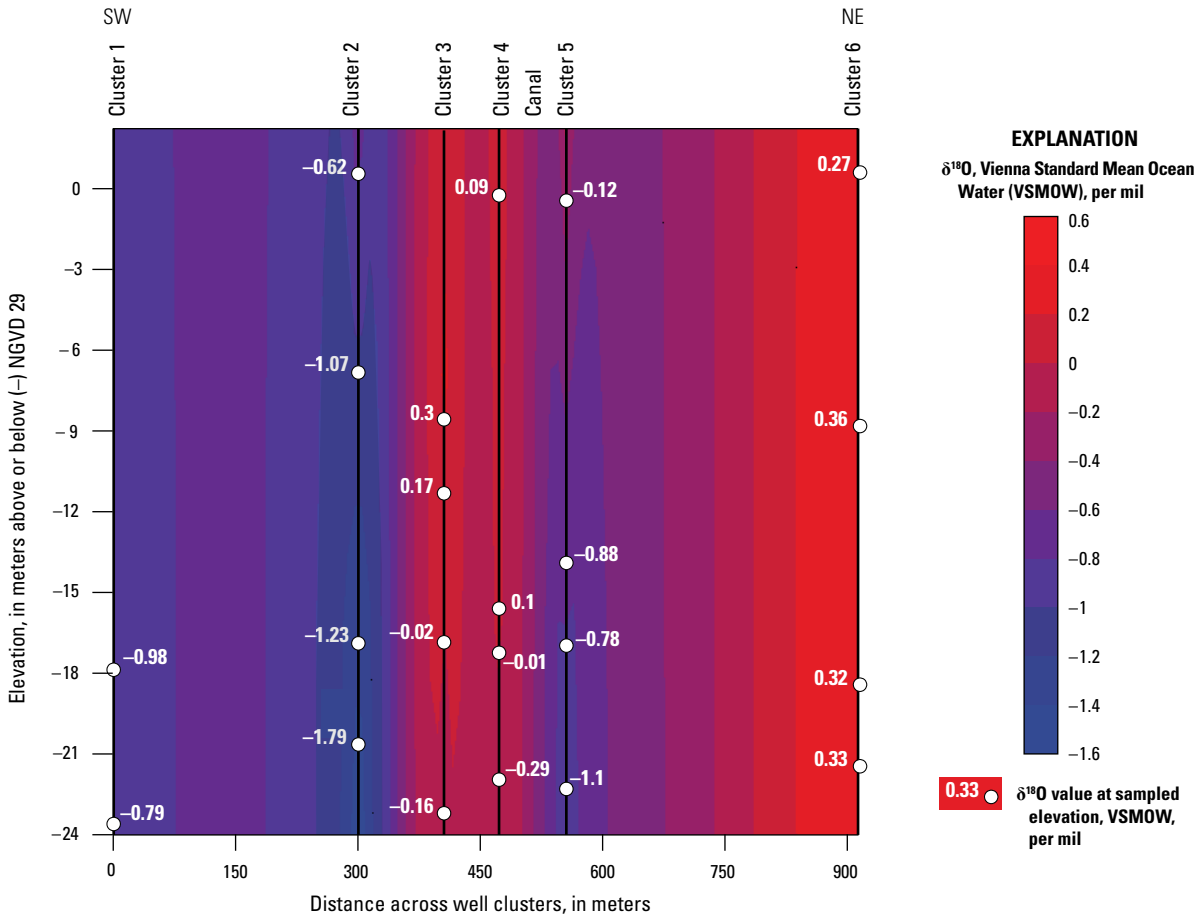

Figure 39. Study area cross-section $\delta^{18}O$ values for sites sampled during the 2010 wet season in the Biscayne aquifer and Snapper Creek Canal in Miami-Dade County, Florida.

Groundwater Sources and Mixing

Pumping drawdown within the study area enhances natural gradients, including the regional groundwater flow direction and the vertical gradient existing between the canal and the shallow groundwater, and introduces additional local gradients not present under ambient conditions. While making cross-hole flowmeter measurements within the monitoring well clusters, Wacker and others (2014) generally observed inflow to the borehole within the shallow flow zone and outflow from the borehole in the deeper flow zone under production well pumping conditions. The production wells are cased to 15.2 m and are open boreholes within the aquifer to a depth of 32.9 m. Because the production zone for the wells includes most of the deeper flow zone, groundwater outflow within this region of the aquifer would be expected under pumping conditions.

When production wells S-3011 and S-3012, located on the north side of the Snapper Creek Canal, were pumped, the natural southwest-northeast groundwater flow direction was enhanced; therefore, water levels within the monitoring wells decreased by 0.06 to 0.91 m below ambient water levels in clusters 1 and 5, respectively (fig. 41). The isotopic composition of the groundwater samples from wells within cluster 5 was more enriched than the samples from wells within cluster 4, as was seen during ambient conditions (except for the wet season sampling due to maintenance disturbances previously discussed). In particular, water from the shallow zone within cluster 5 had the highest $\delta^{18}O$ values in the study area (figs. 40 and 42). Isotopic enrichment increases slightly with depth within cluster 4, which may be indicative of the higher volume of upgradient, isotopically depleted groundwater inflow within the shallow zone under pumping conditions. The sample collected from production well S-3012 during pumping has an isotopic composition similar to the median isotopic composition values for the shallow wells in cluster 4 (fig. 43). The S-3012 groundwater sample isotopic composition indicates that the well likely is not receiving a substantial component of isotopically enriched water from the canal. The lowest water-level elevation measured during either set of pumping conditions was in well S-3012, with almost a 1.2-m difference from water levels measured in the other production wells during pumping (fig. 41). Production well S-3012 could be drawing from a less connected, deeper flow zone of the aquifer, resulting in the observed drawdown.

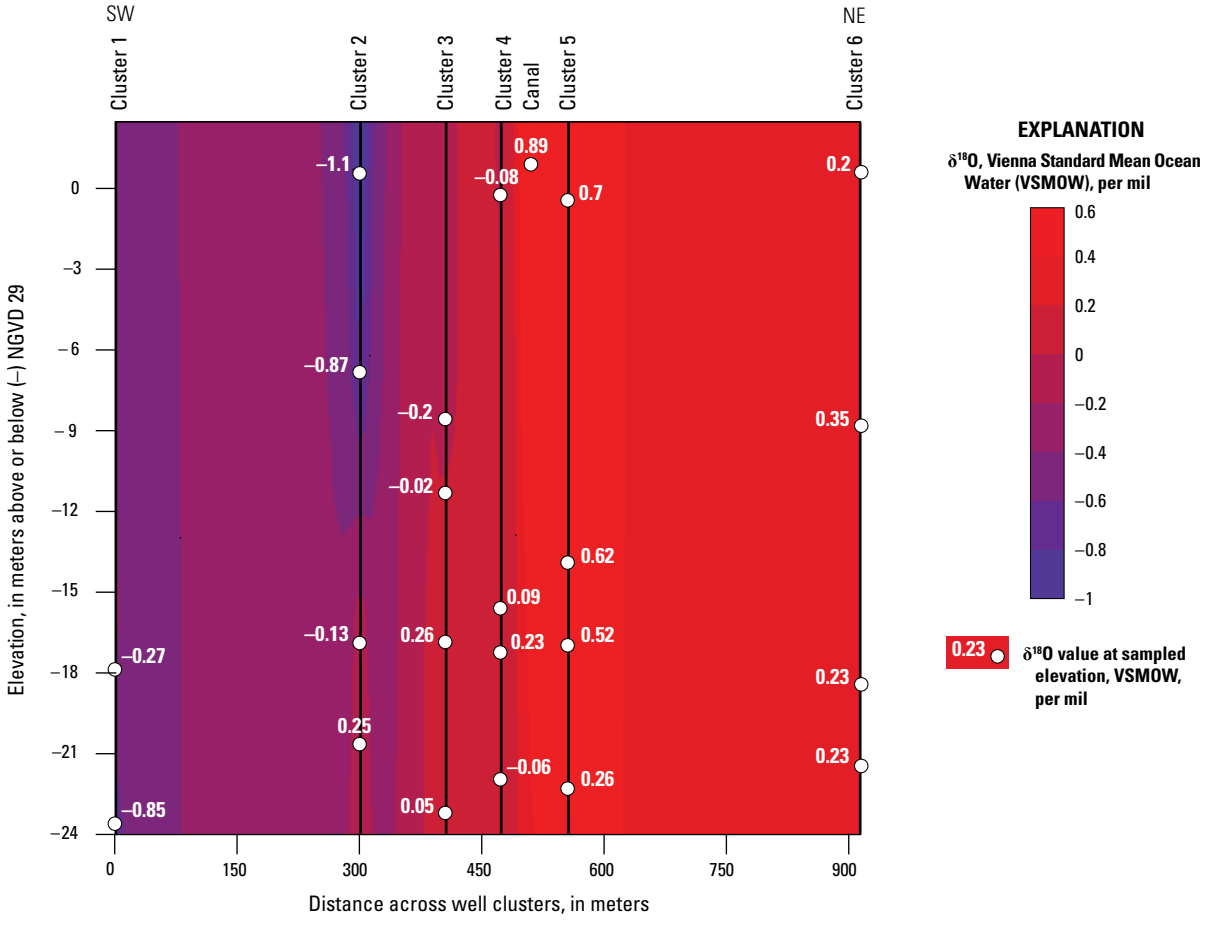

Figure 40. Study area cross-section $\delta^{18}O$ values for sites sampled during the 2011 dry season in the Biscayne aquifer and Snapper Creek Canal in Miami-Dade County, Florida.

When production wells S-3013 and S-3014, located south of the Snapper Creek Canal, were pumped, water levels within the monitoring wells were drawn below ambient water levels by a minimum of 0.15 m in cluster 6 to a maximum of 4.57 m in cluster 3 (fig. 41). The water levels indicated that the natural flow gradient between the shallow flow zone and the canal was enhanced toward cluster 4 but that the natural flow gradient observed under ambient conditions was reversed on the northeast side of the canal near cluster 5. The sample from the shallow well in cluster 4 had the isotopic signature of the canal water when the production wells south of the canal were being pumped, and, similar to the results from the previous pumping event, isotopic enrichment increased slightly with depth within the deeper wells in cluster 4 (figs. 42 and 44). Water samples from cluster 5 wells were generally more isotopically depleted when production wells south of the canal were pumped than when production wells north of the canal were pumped, with more enriched water observed within the shallow flow zone. The groundwater sample from production well S-3014 had an isotopic composition comparable to the samples taken from the deeper flow zone within cluster 4 (fig. 45). This finding is compatible with production wells open to the deeper flow zone within the aquifer, which is the likely groundwater source for the deeper wells within clusters 4 and 5. Water from production well S-3013 has an enriched isotopic composition relative to water from well S-3014, with a composition within the range of compositions of samples from shallow and deeper flow zones (fig. 45).

Water-level observations across the study area during both pumping events indicate that the canal may act as a "buffer" by minimizing pumping drawdown for any monitoring wells located on the opposite side of the canal. The $\delta^{18}O$ values were higher within the shallow flow zone of cluster 4 when the production wells south of the canal were being pumped than within the shallow flow zone of cluster 5 when the production wells north of the canal were pumped. If production well pumping enhances natural gradients between the shallow groundwater and the canal, similar or higher δD and $\delta^{18}O$ values would be expected in water from the shallow zone on the north side of the canal when these northern production wells were operating. A probable explanation for this result is that cluster 4 is located 40 m northeast from production well S-3013, whereas cluster 5 is located 75 m to the southeast from production well S-3012 (fig. 1*B*).

An approximate mixing line can be inferred from the median δD and $\delta^{18}O$ values from the study area production wells, monitoring well clusters, and the Snapper Creek Canal by treating the samples collected from regionally upgradient monitoring well clusters 1 and 2 as the most isotopically depleted samples and the local groundwater and the canal as the isotopically enriched end-member (fig. 35). In most instances, groundwater generally consists of some mixture of recharge from precipitation and recharge from surface-water bodies, so a simple mixing analysis typically includes those sources as end-members. By using the median δD and

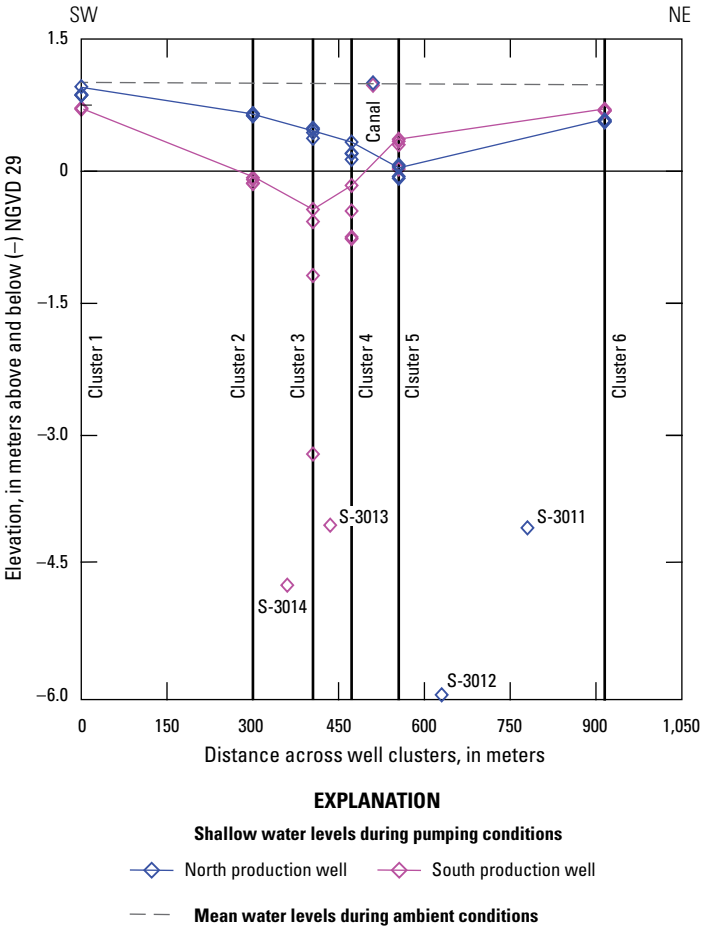

Figure 41. Water levels within the study area during pumping events in November 2010 for the Biscayne aquifer and Snapper Creek Canal in Miami-Dade County, Florida.

$\delta^{18}O$ values from the constructed mixing line, simple mixing proportions can be estimated (table 6). For this analysis, end-members representative of local groundwater and canal water were chosen to estimate contributions of those sources to production well water.

The mixing proportions appear to reflect and summarize the trends in the isotopic data that have been previously discussed. Within the study area, the highest proportion of isotopically enriched water was observed in the cluster 6 monitoring wells on the regionally downgradient side of the Snapper Creek Canal, where these wells are likely receiving a large component of canal recharge. All production wells had lower proportions of isotopically enriched water when compared to all monitoring well sites sampled. Production well S-3012 has a notably large component of local groundwater. Though well S-3012 is also located on the regionally downgradient side of the canal, aquifer heterogeneity may explain why this well is not as connected to the shallow flow zone and the canal that intersects it.

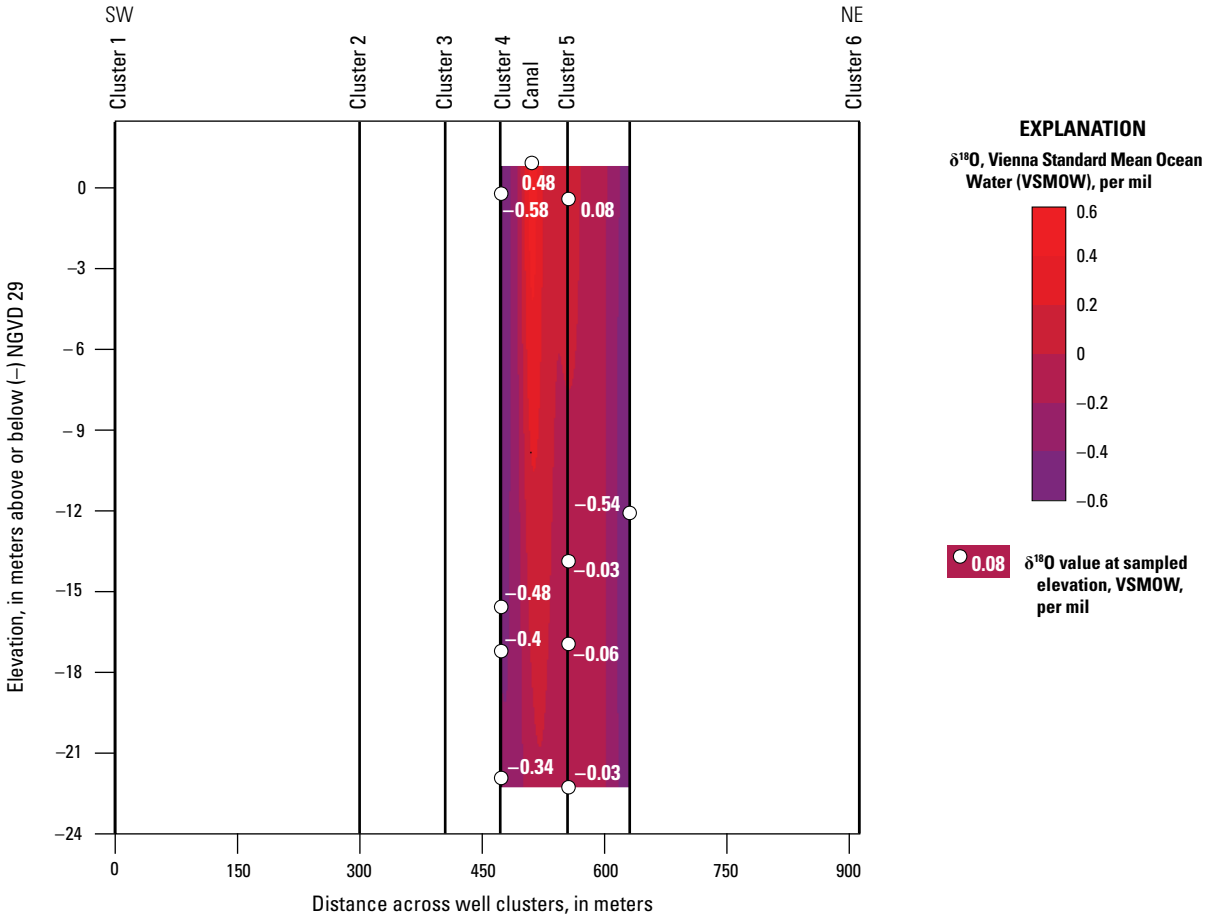

Figure 42. $\delta^{18}O$ values for sites sampled while northern production wells were pumped in November 2010 in the Biscayne aquifer and Snapper Creek Canal in Miami-Dade County, Florida.

Table 6. Simple mixing proportions for stable isotope data in the Snapper Creek study area, October 2008–April 2011.

Sample location	Description	δD percent depleted	$\delta^{18}O$ percent depleted	δD percent enriched	$\delta^{18}O$ percent enriched	Number of samples
Clusters 1 and 2	Southwest monitoring wells	100	100	0	0	12
Cluster 3	Southwest monitoring wells	32	27	68	73	8
Cluster 4	Southwest monitoring wells	30	25	70	75	8
Cluster 5	Northeast monitoring wells	34	34	66	66	8
Cluster 6	Northeast monitoring wells	6	7	94	93	8
Well S-3011	North production well	49	52	51	48	26
Well S-3012	North production well	83	68	17	32	1
Well S-3013	South production well	51	48	49	52	1
Well S-3014	South production well	45	51	55	49	26
Well S-3015	Offsite production well	50	47	50	53	25
Canal	Snapper Creek Canal	0	0	100	100	28

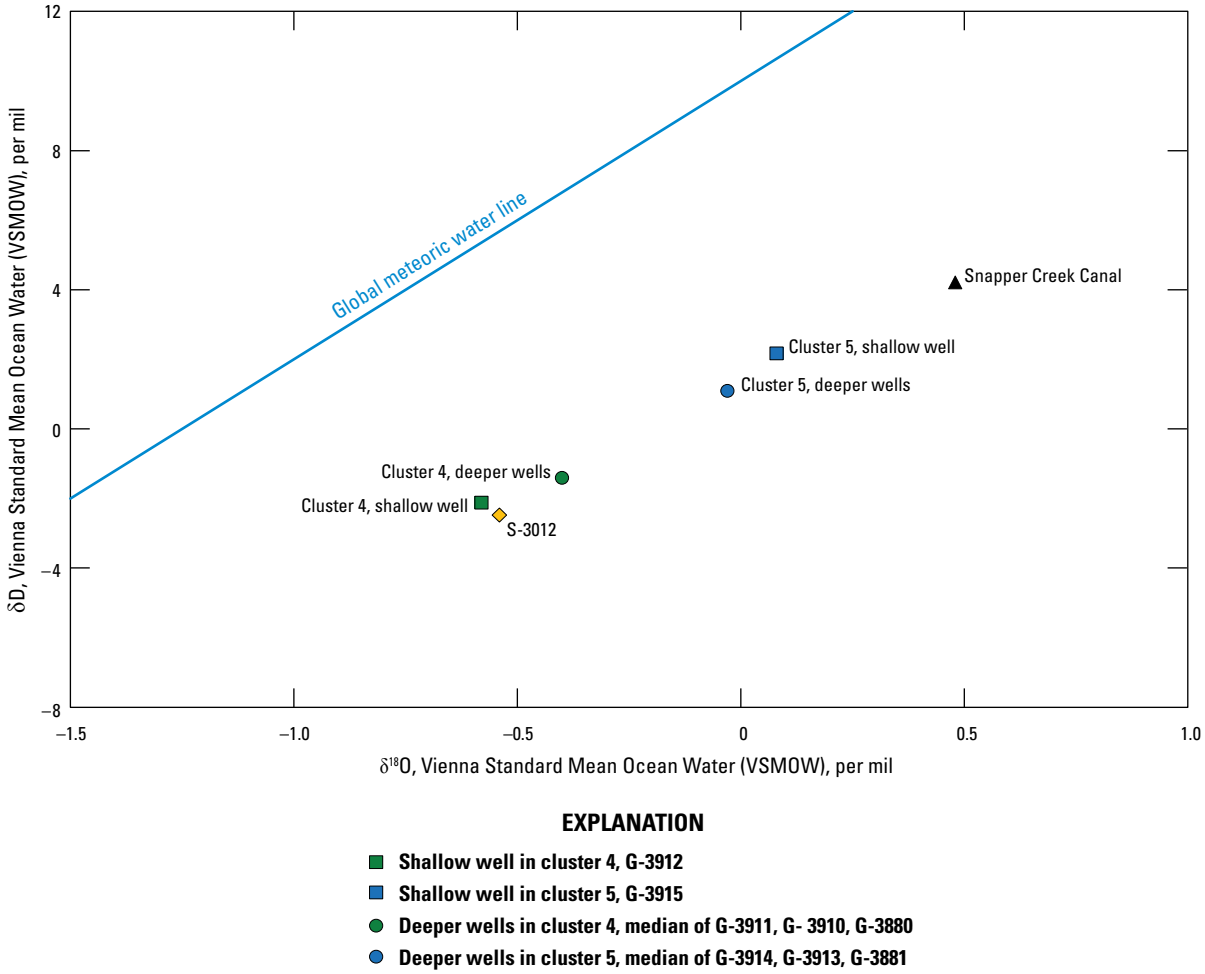

Figure 43. Relation between median δD and $\delta^{18}O$ values for sites sampled while northern production wells were pumped on November 17–18, 2010, in the Biscayne aquifer and Snapper Creek Canal in Miami-Dade County, Florida. Global meteoric water line (GMWL) based on Craig (1961).

Collectively, the production well samples within the study area are similar compositionally to those of production well S-3015 located 3.2 km west of the canal (figs. 34 and 7). The proximity of the study area production wells to the canal supports the assumption that some component of enriched water should be sourced from the nearby canal; however, similar isotopic signatures within well S-3015 suggest an enriched component aside from the canal. No surface-water bodies are close enough to provide enriched recharge to well S-3015, and water treatment discharge pits to the east of nearby well S-3016 seem to provide depleted recharge, as is evident within the isotopic composition of well S-3016 (fig. 34).

Enriched groundwater, originally recharged from surface water in the Everglades, flows within the deeper flow zone of the Biscayne aquifer and was detected in monitoring wells about 8 km west of production well S-3015 (Wilcox and others, 2004). The general groundwater flow direction is west to east within Miami-Dade County, and isotopic depletion has been detected along the groundwater flow path (Wilcox and others, 2004). By the time the groundwater reached well S-3015 and the study area, mixing with groundwater derived from local precipitation along the flow path likely depleted the isotopic composition to some degree. Aquifer heterogeneity may still provide zones where more enriched water is somewhat isolated from precipitation recharge and mobilized during pumping conditions, which could explain why enriched samples from well S-3015 have a similar isotopic composition to those of the study area production wells without receiving any nearby surface-water recharge.

The limitations of the mixing proportions must be considered because the mixing calculation is simple and heavily based on (1) the assumptions of the conceptual model that regional groundwater becomes more isotopically depleted as it mixes with precipitation recharge along the flow path, (2) the assumption that canal recharge is the sole source of isotopic enrichment in the study area, and (3) the assumption that the number of samples collected to compute the medians is enough to be representative of the groundwater at each well site.

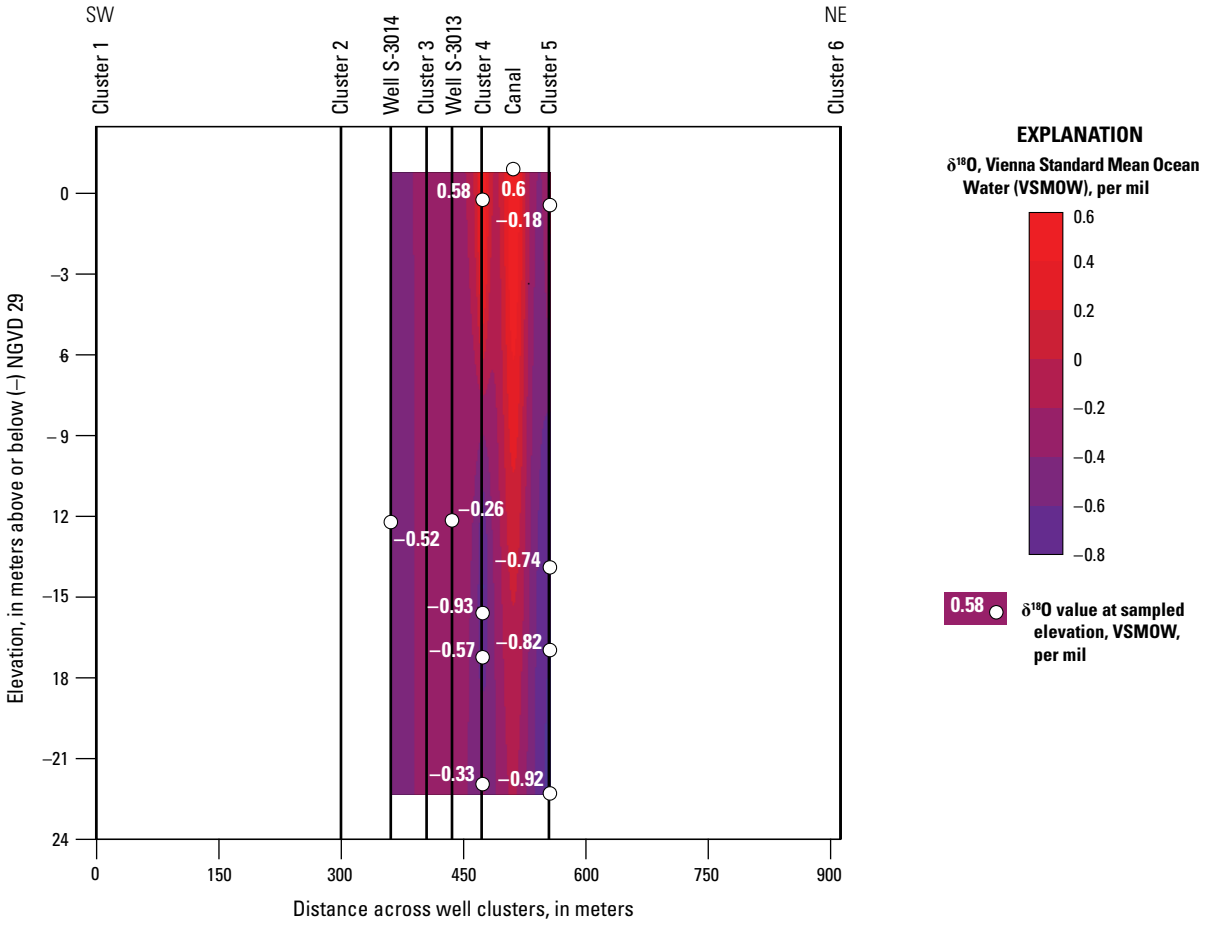

Figure 44. $\delta^{18}O$ values for sites sampled while southern production wells were pumped in November 2010 in the Biscayne aquifer and Snapper Creek Canal in Miami-Dade County, Florida.

Relations Between Canal Leakage and Pumping

The groundwater flow model and stable isotope data provide independent lines of evidence to evaluate the effects of production well pumping on canal leakage. These analyses were used to develop a conceptual model of the local exchange between groundwater and surface water.

While the hydrologic and isotopic analyses are independent, the findings are consistent. Results from both analyses indicated that the majority of the canal leakage enters the aquifer through the north side of the canal. The groundwater model indicates that 50 percent of the canal leakage flows laterally into the shallow flow zone on the northeast side of the canal. The groundwater samples collected from northeast of the canal show the greatest isotopic enrichment within the sampled monitoring well clusters. Additionally, the groundwater levels during the ambient wet season indicate a flow gradient to the northeast. This finding is also consistent with the regional Biscayne aquifer potentiometric gradient (Prinos, 2014) and the Biscayne aquifer groundwater simulations of Miami-Dade County (Hughes and White, 2014).

Furthermore, the groundwater model and the isotope data indicate that more leakage flows laterally into the shallow flow zone than vertically into the matrix flow zone. In the groundwater model flow budget, 96 percent of the canal leakage flows laterally into the shallow flow zone on either side of the canal, and only 4 percent flows vertically into the matrix flow zone beneath the canal. Generally, groundwater has a decreasing amount of δD and $\delta^{18}O$ enrichment with increasing depth in clusters across the study area, with the most enriched samples collected from the shallow monitoring wells. During pumping conditions, the greatest degree of isotopic enrichment is seen in the direction of production well pumping within the shallow flow zone wells nearest the canal. Hydrologic data also indicate that the shallow flow zone has the greatest permeability of all the Biscayne aquifer flow zones in the study area (Wacker and others, 2014), and that the underlying matrix flow zone has lower permeability than other flow zones.

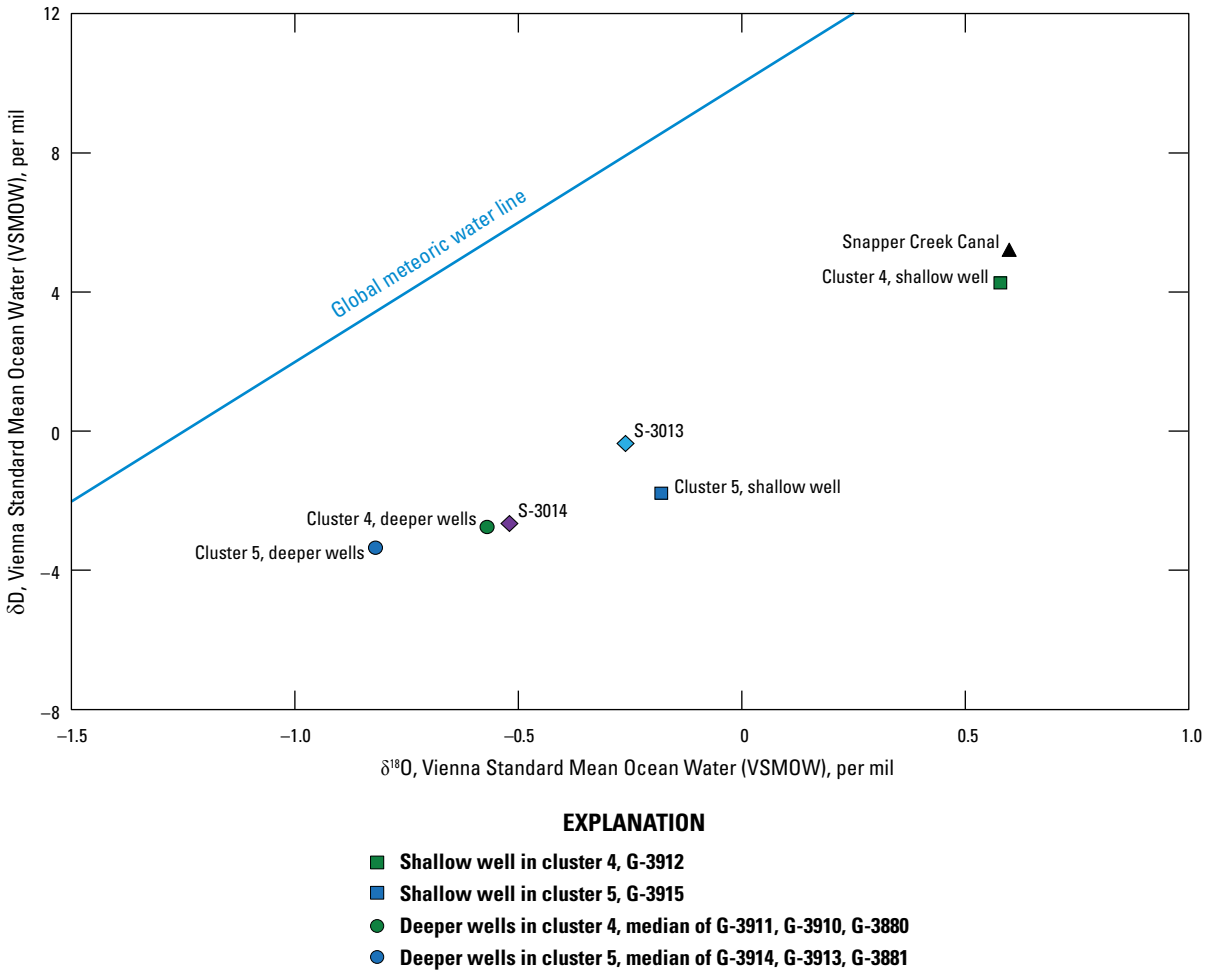

Figure 45. Relation between median δD and $\delta^{18}O$ values for sites sampled while southern production wells were pumped on November 30, 2010, in the Biscayne aquifer and Snapper Creek Canal in Miami-Dade County, Florida. Global meteoric water line (GMWL) based on Craig (1961).

Results from both analyses indicated that the groundwater withdrawals from the production wells are a mixture of local groundwater and canal water. The isotopic data indicate that the water in the production wells is likely some mixture of local groundwater and canal water; the mixing proportions estimating about 40 to 50 percent of production well water contains an isotopic composition similar to that of the canal. The model results show a fractional increase in canal leakage with pumping, but leakage varies with pumping magnitude and is not volumetrically equivalent to the amount withdrawn from the production wells. Additionally, leakage is likely related to pumping in neighboring well fields and cannot be solely attributed to local pumping.

The dominant controls on canal leakage in the study area were examined by using the groundwater model and results of isotopic analyses. Because the canal bisects a production well field, local pumping likely promotes leakage of canal water. In addition to local pumping, regional pumping to the northeast and southeast of the study area may promote leakage of canal water locally. Regional pumping caused lowered heads at the model boundaries, which in turn caused some of the simulated canal leakage. Some simulated canal leakage occurs even without pumping due to the local vertical head gradient. Local head gradients may be the result of regional pumping, or may simply be the result of seasonal regional lowering of the potentiometric surface. Geologic heterogeneity in the Biscayne aquifer is a substantive control on the pathways of canal water. Vertical and lateral differences in water levels and hydraulic testing data support the assignment of a non-uniform distribution of hydraulic properties. The shallow flow zone is particularly permeable and has a distinctly different permeability than the underlying matrix flow zone.

The isotopic composition of surface water in the Snapper Creek Canal is not as enriched as are the headwaters in the Everglades, indicating that substantial input from direct precipitation recharge and relatively depleted groundwater discharge likely occurs along the canal system. The isotopic composition of the local groundwater within the study area is

distinct and ranges between the composition of precipitation and canal water, indicating some mixture of the two sources. Leakage from the canal is primarily into the shallow flow zone, which serves as storage for the deeper production flow zones, but also can serve as storage for the canal, releasing groundwater seepage into the canal. The matrix flow zone generally prevents a direct connection between the canal and the production wells; however, the matrix flow zone is leaky, and a small amount of recharge from precipitation and the canal into the shallow flow zone does recharge the deeper flow zones. Recharge from the canal to the aquifer is also enhanced by proximity to other production wells. While groundwater recharge is enhanced locally and seasonally by the canal system, the aquifer is discharging to the canal system regionally and over longer time scales (Hughes and White, 2014).

Limitations

All hydrologic analyses are subject to limitations, and the results from the numerical model and isotope analysis presented in this report should be interpreted in light of these limitations. Generally, results of numerical models are subject to assumptions about the processes simulated, the system configuration, and the data used to represent the system, calibrate the model, and check model accuracy. Interpretations of groundwater sources and mixing using stable isotope data are limited by the number of samples and the temporal and spatial distribution of data. The groundwater flow model documented herein is limited by (1) the degree of uncertainty in representing heterogeneities associated with karst in the Biscayne aquifer, (2) a limited time period containing only a relatively dry year of precipitation, (3) uncertainty in leakage measurements and associated error, (4) the exclusion of runoff in the recharge calculations, and (5) uncertainty associated with the representation of boundary conditions.

The karstic nature of the Biscayne aquifer introduces uncertainties in model representation of the flow system. Karst aquifers are characterized by small-scale heterogeneities such as the horizontal and vertical solution cavities found in the Biscayne aquifer. Small-scale heterogeneities have the potential to greatly influence regional groundwater flow in karstic environments. In the Snapper Creek study area, the location and effect of vertical solution pipes are largely unknown; although some solution pipes have been observed, their full extent has not been determined. The semi-confining layer of the aquifer could be breached by these vertical solution pipes, which would introduce preferential pathways for canal water to leak into the well-field production zone. Without knowledge of the complete extent of vertical solution pipes, the model may not account for recharge through the semi-confining matrix flow zone into the deeper production zone. As a result, additional water may be pulled out of the canal reach when the pumps are operating, causing a slight overestimation of induced canal leakage due to pumping.

Rainfall in the Snapper Creek study area during the simulation period (about 125 cm during August 2010 to July 2011) was below the annual average for southeast Florida (127 to 158 cm [Renken and others, 2005]). Pumping likely induces a greater proportion of leakage during dry conditions than during a period of average or above-average rainfall. During a wet year, there would be larger amounts of groundwater recharge than during a dry year. The additional local recharge would contribute more water to storage and increase the potential for additional regional flow into the study area. With the increased availability of water in the system, the proportion of induced leakage due to pumping would likely be reduced during a wet year.

Some error is associated with measurements of pumping used during the simulation period. Pump curves, which are head-versus-discharges curves at a given pump speed (Crowe and others, 2009), are used to determine the amount of water withdrawn from the production wells, and errors are related to this process. Sunderland and Krupa (2007) estimated a ±30-percent error in withdrawal rates. This measurement error could affect simulated canal leakage that is correlated with pumping. Higher withdrawal rates than those used in the simulation would likely lead to higher simulated values for induced canal leakage, whereas lower withdrawal rates would reduce simulated canal leakage.

To calculate recharge to the study area, runoff was assumed to be negligible, and only rainfall and evapotranspiration were considered. Although runoff was not included in the recharge calculations, impervious surfaces (15–20 percent of the study area) could contribute substantially to runoff during large storm events (Hughes and White, 2014). The sensitivity of simulated groundwater levels and canal leakage to recharge changes was tested; recharge to the groundwater model was reduced by 20 percent during the testing. The absolute average difference between the simulated groundwater levels using the observed recharge and the reduced recharge was negligible (6.13×10^{-4} m). The absolute average difference between the simulated canal leakage values using the observed recharge and reduced recharge was also negligible (1.7×10^{-3} m^3/s). The composite-scaled sensitivity for recharge was 0.75, which is more than an order of magnitude less than the most sensitive parameters. Therefore, although runoff likely occurs at the study area and could affect the simulated model results, the effect on simulated values is expected to be small.

Uncertainty associated with the development and representation of the model boundary conditions likely had an effect on the groundwater model results. Calibrated models using different head distributions applied to the head-dependent flux boundaries at the lateral edges of the model resulted in a substantial difference in canal leakage, as well as internal fluxes. Additionally, the proximity of the perimeter boundary to the canal and well field introduces uncertainty into the analysis. Extending the model boundary further outward, however, would result in interferences from neighboring well fields that would have to be accounted for explicitly. Natural hydrologic boundaries are located so far away from

the study area that the groundwater model would need to be substantially larger or embedded into a larger model in order to account for regional groundwater fluxes that occur around the study area.

Interpretation of the isotope data is limited by (1) the frequency of the sampling dataset, (2) the collection of representative samples for end-member mixing analysis, (3) the location of sampling points, and (4) the influence of background regional groundwater flow on the isotope signatures. These limitations should be considered in the certainty of the interpretation of this stable isotope analysis or use of the analysis results.

The monthly stable isotope data collected for the two production wells and the canal within the study area, as well as the two offsite background production wells, cover a period of about 2 years. This timeframe provides data representative of a range of hydrologic conditions, including seasonal fluctuations and changes in groundwater withdrawals. Data from the monitoring wells are limited to two discrete samples during different seasons under non-pumping conditions. Without monthly data from the monitoring wells, it is difficult to attribute the observed variation to seasonal effects or discrete events. For example, the wet season isotope values for cluster 5 may represent a discrete event due to an anomalous recharge event (pump maintenance discharge) and may not be representative of the average isotopic signatures for the wet season. Using data from small datasets can skew and lower confidence in conceptual model interpretation. Additionally, a sufficient database of background groundwater isotopic composition is not available.

Finding an appropriate regional groundwater end-member for the estimation of mixing proportions in the study area is uncertain because the hydrologic system is characterized by a shallow, highly permeable aquifer in which groundwater is likely to readily mix with recharge. Also, because of the heterogeneity of the aquifer and large pumping stresses within well fields across the region, groundwater residence times can be quite variable. Therefore, groundwater chemistry within the Biscayne aquifer can range somewhat depending on the local influences at any given well location.

The distribution of sampling points within the study area may have limited the geochemical interpretation of canal recharge to the shallow flow zone. The construction of the monitoring wells across the study area provided for the well clusters to be organized perpendicular to the regional groundwater flow, but did not provide for the well clusters to be equidistant to the production wells. Groundwater sampling points spaced at shorter and more equal intervals between the canal and zone of production well drawdown could provide better quantitative control on the geochemical data with regard to pumping effects on canal recharge to the aquifer, especially within the shallow flow zone.

In spite of numerous limitations, the combination of the stable isotope data and the groundwater model is a useful tool for gaining an understanding of the complex relations between canal leakage and pumping at the study area. Both analysis techniques provide insight on these relations by examining different aspects of the flow system, and they yield similar and consistent interpretations of directions of flow and evaluations of canal water contribution to local pumping wells. Both methods also stress the importance of considering heterogeneity in a system dominated by discontinuous flow zones with large groundwater withdrawals. For the groundwater model, the use of two different types of calibration data constrains the calibration for each realization. The model does not overfit the available observation data. Interpretations based on the model results and isotopic data presented here are relevant to the particular hydrologic conditions during the study, and extending the interpretations for other conditions should be made with caution.

Summary and Conclusions

A groundwater flow model and stable isotope data were used to characterize the relations between production well pumping and canal leakage. The groundwater flow model was developed and calibrated to assess relations between pumping at the study area and the Snapper Creek Canal leakage in Miami-Dade County, Florida, from June 2010 to July 2011. The model extent is 2.19 square kilometers surrounding the canal and production wells.

The groundwater flow model, MODFLOW-NWT, was used to construct the model. Rainfall and evapotranspiration data were used in the Recharge Package to estimate groundwater recharge. Groundwater flux between the Snapper Creek Canal and the Biscayne aquifer was represented with the Constant-Head Boundary Package. Pumping stresses were represented by using the Multi-Nodal Well Package. The head-dependent model boundary was represented by using the General Head Boundary Package.

Trial-and-error and inverse methods were used to calibrate the model. Model sensitivities to geologic heterogeneity, non-laminar flow, and controlling boundary heads were evaluated. The calibrated model was used to estimate background and induced canal leakage. Background canal leakage was defined as the canal leakage that occurs without pumping and in response to processes such as rainfall and changes in canal stage. Induced leakage was defined as the canal leakage caused by pumping in the study area.

Canal leakage induced by pumping was quantified as a percentage of total canal leakage during pumping events. The percentage of leakage during pumping increased non-linearly with pumping rate. For example, when pumping was about 0.5 and 1.9 cubic meters per second, canal leakage increased by about 15 and 33 percent, respectively.

The model results likely serve as an upper limit for well-field interaction with surface-water features in Miami-Dade County, given the proximity of the pumping wells to the Snapper Creek Canal (about 50 meters). Moreover, the amount of induced leakage is likely affected not only by local pumping but also by pumping at neighboring well fields because

water demand is presumably area-wide during the dry season and contributes to widespread lowering of groundwater levels along the model boundaries.

The model results are limited by the uncertainty associated with the representation of the heterogeneous karstic aquifer as well as the perimeter boundary conditions. In addition, the time period simulated for this study was relatively dry, and correlations between canal leakage and well-field operations could be lower in a wet year with higher rainfall and similar well-field operations. Uncertainty is also introduced into the groundwater model by leakage measurement error and the exclusion of runoff in the recharge calculations.

Beginning in October 2008, monthly water-quality samples were collected from four production wells (S-3011, S-3014, S-3015, and S-3016) and the Snapper Creek Canal for the analysis of stable isotopes of water (δ^2H and $\delta^{18}O$). In addition, four discrete water-quality sampling events were conducted during the summer and fall of 2010 and during the spring of 2011, spanning a range of pumping rates.

Water-level and isotope data from the monitoring wells closest to the canal indicate that groundwater/surface-water interactions have a substantial influence on flow patterns within the study area, especially within the shallow flow zone of the Biscayne aquifer, which is intersected by the Snapper Creek Canal. The highest proportion of isotopically enriched water was measured in the shallow monitoring wells near the banks of the canal.

Isotopic compositions within the study area indicate that the shallow, high transmissivity preferential flow zone receives recharge from the canal and precipitation, but is not well connected with the deeper flow zones throughout the study area. At production well S-3012, the mixing of isotopically enriched water is minimal when compared to mixing in other production wells in the area, indicating a limited connection with the shallow flow zone and the canal that intersects it. Moreover, the isotopic signature of the canal water indicates a regional input of flow from the Everglades, adding further complexity to interpretation of the isotope data. The groundwater sampled at production well S-3015 may be some mixture of enriched groundwater from the Everglades with locally recharged waters. The production well is open to the lower flow zone within the Tamiami Formation, which is often separated from the upper flow zones by a semi-confining limestone matrix. Evidence from USGS borehole imagery suggests that vertical solution pipes may be connecting the flow zones in the near vicinity of well S-3015 and could facilitate mixing under pumping conditions.

Results from the groundwater model and the isotope data analysis were consistent and demonstrate the importance of groundwater/surface-water interactions in the shallow flow zone. Results also indicate that pumping in the local well field and in neighboring well fields influences canal leakage, causing the water in the production wells to be a mix of local groundwater and water from the canal. Both sets of results confirm that geologic heterogeneity in the study area controls the pathways of flow.

References

Baldocchi, D.D., Hicks, B.B., and Meyers, T.P., 1988, Measuring biosphere–atmosphere exchanges of biologically related gases with micrometeorological methods: Ecology, v. 69, no. 5, p. 1331–1340.

Bouwer, Herman, 1965, Theoretical aspects of seepage from open channels: American Society of Civil Engineers Journal of the Hydraulics Division, v. 91, no. HY3, p. 37–59.

Chin, D.A., 1990, A method to estimate canal leakage to the Biscayne aquifer, Dade County, Florida: U.S. Geological Survey Water-Resources Investigations Report 90–4135, 32 p.

Clark, I.D., and Fritz, Peter, 1997, Environmental isotopes in hydrogeology: New York, Lewis Publishers, 328 p.

Coplen, T.B., 1994, Reporting of stable hydrogen, carbon, and oxygen isotopic abundances: Pure and Applied Chemistry, v. 66, p. 273–276.

Coplen, T.B., Wildman, J.D., and Chen, Julie, 1991, Improvements in the gaseous hydrogen–water equilibration technique for hydrogen isotope ratio analysis: Analytical Chemistry, v. 63, no. 9, p. 910–912.

Craig, Harmon, 1961, Isotopic variations in meteoric waters: Science, v. 133, p. 1702–1703.

Crowe, C.T., Elger, D.F., Williams, B.C., and Roberson, J.A., 2009, Engineering Fluid Mechanics (9th ed.): Jefferson City, Mo., John Wiley & Sons, Inc., 553 p.

Cunningham, K.J., Renken, R.A., Wacker, M.A., Zygnerski, M.R., Robinson, Edward, Shapiro, A.M., and Wingard, G.L., 2006a, Application of carbonate cyclostratigraphy and borehole geophysics to delineate porosity and preferential flow in the karst limestone of the Biscayne aquifer, SE Florida: Geological Society of America Special Papers, v. 404, p. 191–208. [Also available at http://dx.doi.org/10.1130/2006.2404(16).]

Cunningham, K.J., Sukop, M.C., Huang, Haibo, Alvarez, P.F., Curran, H.A., Renken, R.A., and Dixon, J.F., 2009, Prominence of ichnologically influenced macroporosity in the karst Biscayne Aquifer: Stratiform“super-K” zones: Geological Society of America Bulletin, v. 121, p. 164–180.

DiFrenna, V.J., Price, R.M., and Savabi, M.R., 2008, Identification of a hydrodynamic threshold in karst rocks from the Biscayne Aquifer, south Florida, USA: Hydrogeology Journal, v. 16, no. 1, p. 31–42.

Epstein, S., and Mayeda, T., 1953, Variation of O18 content of waters from natural sources: Geochimica et Cosmochimica Acta, v. 4, no. 5, p. 213–224.

Florea, L.J., and McGee, D.K., 2010, Stable isotopic and geochemical variability within shallow groundwater beneath a hardwood hammock and surface water in an adjoining slough (Everglades National Park, Florida, USA): Isotopes in Environmental and Health Studies, v. 46, no. 2, p. 190–209. [Also available at http://dx.doi.org/10.1080/10256016.2010.494770.]

Gibson, J.J., Edwards, T.W.D., Birks, S.J., St Amour, N.A., Buhay, W.M., McEachern, P.M.,Wolfe, B.B., and Peters, D.L., 2005, Progress in isotope tracer hydrology in Canada: Hydrological Processes, v. 19, no. 1, p. 303–327.

Harbaugh, A.W., 2005, MODFLOW-2005, The U.S. Geological Survey modular ground-water model—The ground-water flow process: U.S. Geological Survey Techniques and Methods 6-A16 [variously paged].

Hill, M.C., Banta, E.R., Harbaugh, A.W., and Anderman, E.R., 2000, MODFLOW-2000, the U.S. Geological Survey modular ground-water model—User guide to the observation, sensitivity, and parameter-estimation processes and three post-processing programs: U.S. Geological Survey Open-File Report 00–184, 210 p.

Hill, M.C., and Tiedeman, C.R., 2007, Effective groundwater model calibration—With analysis of data, sensitivities, predictions, and uncertainty: Hoboken, New Jersey, John Wiley & Sons, Inc., 480 p.

Hughes, J.D., and White, J.T., 2014, Hydrologic conditions in urban Miami-Dade County, Florida, and the effect of groundwater pumpage and increased sea level on canal leakage and regional groundwater flow: U.S. Geological Survey Scientific Investigations Report 2014–5162, 175 p. [Also available at http://pubs.usgs.gov/sir/2014/5162/.]

Jones, L.E., and, Torak, L.J., 2006, Simulated effects of seasonal ground-water pumpage for irrigation on hydrologic conditions in the lower Apalachicola–Chattahoochee–Flint River Basin, southwestern Georgia and parts of Alabama and Florida, 1999–2002: U.S. Geological Survey Scientific Investigations Report 2006–5234, 115 p., a Web-only publication at http://pubs.usgs.gov/sir/2006/5234/.

Kendall, Carol, and McDonnell, J.J. (Eds.), 1998, Isotope tracers in catchment hydrology, Amsterdam: Elsevier Science.

Konikow, L.F., Hornberger, G.Z., Halford, K.J., and Hanson, R.T., 2009, Revised Multi-Node Well (MNW2) Package for MODFLOW ground-water flow model: U.S. Geological Survey Techniques and Methods 6–A30, 67 p.

Leak, S.A., and Prudic, D.E., 1991, Documentation of a computer program to simulate aquifer-system compaction using the modular finite-difference ground-water flow model: U.S. Geological Survey Techniques of Water-Resources Investigations, book 6, chap. A2, 68 p.

Lietz, A.C., Dixon, J.F., and Byrne, M.J., 2002, Average altitude of the water table (1990–99) and frequency analysis of water levels (1974–99) in the Biscayne aquifer, Miami-Dade County, Florida: U.S. Geological Survey Open-File Report 02–91.

Meyer, F.W., 1971, Seepage beneath the Hoover Dike southern shore of Lake Okeechobee Florida: Florida Bureau of Geology Report of Investigations 58, 98 p.

Niswonger, R.G., Panday, Sorab, and Ibaraki, Motomu, 2011, MODFLOW-NWT, A Newton formulation for MODFLOW-2005: U.S. Geological Survey Techniques and Methods 6–A37, 44 p.

Paillet, F.L., and Reese, R.S., 2000, Integrating borehole logs and aquifer tests in aquifer characterization: Ground Water, v. 38, no. 5, p. 713–725.

Parker, G.G., and Glass, W.A., 1951, Geologic and hydrologic factors in the perennial yield of the Biscayne aquifer: Journal of the American Water Works Association, v. 43, no. 10, p. 817–835.

Poeter, E.P., Hill, M.C., Banta, E.R., Mehl, Steffen, and Christensen, Steen, 2005, UCODE_2005 and six other computer codes for universal sensitivity analysis, calibration, and uncertainty evaluation: U.S. Geological Survey Techniques and Methods, book 6, chap. 11, section A, 283 p. [Also available at http://pubs.usgs.gov/tm/2006/tm6a11/.]

Prinos, S.T., Wacker, M.A., Cunningham, K.J., and Fitterman, D.V., 2014, Origins and delineation of saltwater intrusion in the Biscayne aquifer and changes in the distribution of saltwater in Miami-Dade County, Florida: U.S. Geological Survey Scientific Investigations Report 2014–5025, 101 p. [Also available at http://dx.doi.org/10.3133/sir20145025.]

Reese, R.S., and Cunningham, K.J., 2000, Hydrogeology of the gray limestone aquifer in southern Florida: U.S. Geological Survey Water-Resources Investigations Report 99–4213, 244 p.

Renken, R.A., Cunningham, K.J., Shapiro, A.M., Harvey, R.W., Zygnerski, M.R., Metge, D.W., and Wacker, M.A., 2008, Pathogen and chemical transport in the karst limestone of the Biscayne aquifer: 1. Revised conceptualization of groundwater flow: Water Resources Research, v. 44, no. 8, W08429. [Also available at http://dx.doi.org/10.1029/2007WR006058.]

Renken, R.A., Dixon, Joann, Koehmstedt, John, Ishman, Scott, Lietz, A.C., Marella, R.L., Telis, Pamela, Rodgers, Jeff, and Memberg, Steven, 2005, Impact of anthropogenic development on coastal ground-water hydrology in southeastern Florida, 1900–2000: U.S. Geological Survey Circular 1275, 77 p. [Also available at http://pubs.usgs.gov/circ/2005/circ1275/.]

SAS Institute Inc., 2010, SAS/GRAPH® 9.2—Statistical graphics procedures guide (2d ed.): Cary, North Carolina, SAS Institute Inc., 324 p.

Sepúlveda, Nicasio, Tiedeman, C.R., O'Reilly, A.M., Davis, J.B., and Burger, Patrick, 2012, Groundwater flow and water budget in the surficial and Floridan aquifer systems in east-central Florida: U.S. Geological Survey Scientific Investigations Report 2012–5161, 214 p.

Sherwood, C.B., and Leach, S.D., 1962, Hydrologic studies in the Snapper Creek Canal area, Dade County, Florida: Florida Geological Survey Report of Investigations 24, part 2, 32 p.

Sunderland, R.S.A., and Krupa S.L., 2007, Groundwater–surface water interaction along the C-2 Canal, Miami-Dade County, Florida: South Florida Water Management District Technical Publication WS-22, 94 p.

Swayze, L.J., 1988, Ground-water flow beneath levee 35A from conservation area 2B, Broward County, Florida: U.S. Geological Survey Water Resources Investigations Report 87–4280, 22 p.

U.S. Environmental Protection Agency, 2013, Sole source aquifers in the Southeast, accessed March 29, 2013, at http://www.epa.gov/region4/water/groundwater/r4ssa.html.

U.S. Geological Survey, variously dated, National field manual for the collection of water-quality data: U.S. Geological Survey Techniques of Water-Resources Investigations, book 9, chaps. A1–A9. [Also available at http://pubs.water.usgs.gov/twri9A.]

Wacker, M.A., Cunningham, K.J., and Williams, J.H., 2014, Geologic and hydrogeologic frameworks of the Biscayne aquifer in central Miami-Dade County, Florida: U.S. Geological Survey Scientific Investigations Report 2014–5138, 66 p., accessed January 22, 2015, at http://dx.doi.org/10.3133/sir20145138.

Wilcox, W.M., Solo-Gabriele, H.M., and Sternberg, L.O., 2004, Use of stable isotopes to quantify flows between the Everglades and urban areas in Miami-Dade County Florida: Journal of Hydrology, v. 293, no. 1–4, p. 1–19.

Appendix 1. Monitoring Well Construction and Location Information, Weather, Groundwater-Level, and Canal Leakage Data from Snapper Creek Well Field, June 2010–July 2011, and Water-Quality Data from the Snapper Creek Canal Area, October 2008–April 2011

Table 1–1. Monitoring well construction information at the Snapper Creek well field.

[USGS, U.S. Geological Survey; End date is the date when coring was completed in the test coreholes or the date the open interval was drilled in the monitoring wells. Top of screen depth in parentheses is bottom of grout or top of limestone. Casing was not fully installed to the bottom of the borehole, so some grout was drilled through during construction of the open hole; NAD 83, North American Datum of 1983; NGVD 29, National Geodetic Vertical Datum of 1929; m, meter; cm, centimeter; —, no data]

Monitoring well cluster	USGS local well number	USGS site identifier	End date of coring or drilling of open hole	Latitude (north)	Longitude (west)	Elevation of ground surface	Elevation of top of casing
				(in degrees, minutes, seconds NAD 83)		(m above NGVD 29)	
Cluster 1	G-3877	254150080215501	04/03/2009	25°41'50.74"	80°21'55.03"	2.72	2.58
	G-3902	254150080215502	01/25/2010	25°41'50.66"	80°21'54.99"	2.69	2.58
	G-3903	254150080215503	01/26/2010	25°41'50.67"	80°21'54.90"	2.72	2.58
Cluster 2	G-3878	254151080214301	04/09/2009	25°41'51.78"	80°21'43.23"	2.17	2.04
	G-3904	254151080214302	01/29/2010	25°41'51.94"	80°21'43.20"	2.18	2.08
	G-3905	254151080214303	01/14/2010	25°41'51.87"	80°21'43.14"	2.15	2.06
	G-3906	254151080214304	01/15/2010	25°41'51.86"	80°21'43.23"	2.16	2.06
Cluster 3	G-3879	254153080213901	03/25/2009	25°41'53.47"	80°21'39.93"	2.14	2.07
	G-3907	254153080213902	01/04/2010	25°41'53.42"	80°21'39.91"	2.17	2.06
	G-3908	254153080213903	01/06/2010	25°41'53.51"	80°21'39.95"	2.21	2.10
	G-3909	254153080213904	01/06/2010	25°41'53.55"	80°21'39.98"	2.19	2.03
Cluster 4	G-3880	254154080213704	05/06/2009	25°41'54.68"	80°21'37.71"	2.48	2.32
	G-3910	254154080213702	02/09/2010	25°41'54.71"	80°21'37.74"	2.52	2.33
	G-3911	254154080213703	02/08/2010	25°41'54.75"	80°21'37.77"	2.46	2.32
	G-3912	254154080213701	02/02/2010	25°41'54.67"	80°21'37.70"	2.47	2.30
Cluster 5	G-3881	254155080243501	04/16/2009	25°41'55.88"	80°21'34.96"	2.20	2.04
	G-3913	254155080243502	03/08/2010	25°41'55.88"	80°21'35.04"	2.27	2.12
	G-3914	254155080243503	03/05/2010	25°41'55.96"	80°21'35.04"	2.19	2.04
	G-3915	254155080243504	03/08/2010	25°41'55.96"	80°21'34.96"	2.19	1.99
Cluster 6	G-3882	254158080212201	03/19/2009	25°41'58.33"	80°21'22.26"	2.27	2.10
	G-3916	254158080212202	03/23/2010	25°41'58.55"	80°21'22.26"	2.39	2.16
	G-3917	254158080212203	02/25/2010	25°41'58.49"	80°21'22.26"	2.30	2.17
	G-3918	254158080212204	02/19/2010	25°41'58.44"	80°21'22.26"	2.33	2.14

Table 1–1. Monitoring well construction information at the Snapper Creek well field.—Continued

[USGS, U.S. Geological Survey; End date is the date when coring was completed in the test coreholes or the date the open interval was drilled in the monitoring wells. Top of screen depth in parentheses is bottom of grout or top of limestone. Casing was not fully installed to the bottom of the borehole, so some grout was drilled through during construction of the open hole; NAD 83, North American Datum of 1983; NGVD 29, National Geodetic Vertical Datum of 1929; m, meter; cm, centimeter; —, no data]

Monitoring well cluster	USGS local well number	Total depth cored from surface (m)	Base of Biscayne aquifer from land surface (m)	Open hole or screen slot size (cm)	Casing internal diameter (cm)	Top of screen or open hole from land surface (m)	Bottom of screen or open hole from land surface (m)
Cluster 1	G-3877	32.31	27.93	0.05	10.16	26.55	28.07
	G-3902	—	—	Open	10.16	20.73	23.01
	G-3903	—	—	0.03	7.62	1.83	5.94
Cluster 2	G-3878	30.78	26.33	0.05	10.16	22.40	24.54
	G-3904	—	—	Open	10.16	19.23	22.04
	G-3905	—	—	Open	10.16	8.99	10.24
	G-3906	—	—	Open	10.16	1.49	4.39
Cluster 3	G-3879	30.78	26.09	0.05	10.16	25.63	28.68
	G-3907	—	—	Open	10.16	19.17	22.74
	G-3908	—	—	Open	10.16	13.59 (13.75)	17.25
	G-3909	—	—	Open	10.16	10.73 (11.40)	11.92
Cluster 4	G-3880	31.09	26.94	Open	10.16	2.56	4.30
	G-3910	—	—	Open	10.16	19.84	23.84
	G-3911	—	—	Open	10.16	18.17	19.05
	G-3912	—	—	0.05	10.16	24.60	26.73
Cluster 5	G-3881	32.16	26.76	0.05	10.16	24.44	29.02
	G-3913	—	—	Open	10.16	19.29	22.89
	G-3914	—	—	Open	10.16	16.06	18.41
	G-3915	—	—	Open	10.16	2.35	5.43
Cluster 6	G-3882	30.48	25.91	0.05	10.16	23.90	27.55
	G-3916	—	—	Open	10.16	20.88 (20.97)	23.56
	G-3917	—	—	Open	10.16	11.09	13.38
	G-3918	—	—	Open	10.16	2.32	5.58

Table 1–2. Production well construction information at Snapper Creek well field.

[USGS, U.S. Geological Survey; NGVD 29, National Geodetic Vertical Datum of 1929; m, meter; cm, centimeter; gal/min, gallon per minute; —, no data]

USGS local well number	End date of coring or drilling of open hole	Elevation of top of casing (m above NGVD 29)	Estimated base of Biscayne aquifer from land surface (m)	Total depth of well from land surface (m)	Casing depth from land surface (m)	Casing internal diameter (cm)	Pump type	Pump or flow capacity (gal/min)
S-3011	1976	2.93	22.86	32.92	15.24	60.96	Turbine	8,300
S-3012	1976	2.94	22.86	32.92	15.24	60.96	Turbine	8,300
S-3013	1976	2.90	22.86	32.92	15.24	60.96	Turbine	8,300
S-3014	1976	2.83	22.86	32.92	15.24	60.96	Turbine	8,300
S-3015	1953	—	21.34	30.48	12.19	50.80	Turbine	4,900
S-3016	1953	—	18.29	30.48	12.19	50.80	Turbine	4,900

Table 1–3. Rainfall, evapotranspiration, pumping withdrawals, and canal stage by stress period for the Snapper Creek Canal study area groundwater flow model, June 2010–July 2011.

[m, meter]

Stress period	Month and year	Rainfall (m)	Evapo-transpiration (m)	S-3011 withdrawals	S-3012 withdrawals	S-3013 withdrawals	S-3014 withdrawals	Canal stage (meter above NGVD 29)
				(cubic meters per second)				
1	June 2010	0.26	0.11	0.43	0.34	0.42	0.42	0.90
2	July 2010	0.13	0.19	0.31	0.13	0.13	0.31	0.95
3	August 2010	0.25	0.14	0.13	0.22	0	0	0.95
4	September 2010	0.29	0.12	0.27	0.32	0	0	0.96
5	October 2010	0.04	0.08	0	0.07	0.10	0	0.96
6	November 2010	0.04	0.06	0.10	0.10	0.11	0.21	1.00
7	December 2010	0.03	0.05	0.11	0.42	0.11	0.11	0.93
8	January 2011	0.07	0.05	0.07	0.40	0.01	0.05	0.92
9	February 2011	0.01	0.06	0.08	0.38	0	0	0.89
10	March 2011	0.03	0.08	0.13	0.28	0.03	0.03	0.76
11	April 2011	0.13	0.09	0.14	0.14	0.14	0.14	0.67
12	May 2011	0.03	0.10	0.42	0.42	0.22	0.22	0.58
13	June 2011	0.11	0.08	0.44	0.44	0.44	0.44	0.45
14	July 2011	0.22	0.05	0.47	0.47	0.47	0.47	0.85

Table 1–4. Measured average groundwater-level data at the Snapper Creek well field, June 2010–July 2011.

Stress period	Month and year	USGS local well number	Head elevation (meter above or below [–] NGVD 29)
1	June 2010	G-3877	0.75
		G-3878	–0.42
		G-3879	–0.18
		G-3881	–0.86
		G-3882	0.53
		G-3902	0.76
		G-3903	0.75
		G-3904	–0.42
		G-3905	–0.35
		G-3906	–0.32
		G-3907	–1.64
		G-3908	–0.84
		G-3909	–0.90
		G-3913	–0.80
		G-3914	–0.77
		G-3915	–0.68
		G-3916	0.60
		G-3918	0.51
2	July 2010	G-3877	0.80
		G-3878	0.27
		G-3879	0.33
		G-3881	–0.01
		G-3882	0.61
		G-3902	0.81
		G-3903	0.80
		G-3904	0.27
		G-3905	0.30
		G-3906	0.31
		G-3907	–0.16
		G-3908	0.02
		G-3909	0.07
		G-3913	0.02
		G-3914	0.13
		G-3915	0.19
		G-3916	0.64
		G-3918	0.59
3	August 2010	G-3877	0.95
		G-3878	0.85
		G-3879	0.76
		G-3881	0.59
		G-3882	0.81
		G-3902	0.95
		G-3903	0.95
		G-3904	0.85
		G-3905	0.86
		G-3906	0.87
		G-3907	0.77
		G-3908	0.79
		G-3909	0.79
		G-3913	0.60
		G-3914	0.64
		G-3915	0.65
		G-3916	0.83
		G-3918	0.82
4	September 2010	G-3877	0.97
		G-3878	0.81
		G-3879	0.67
		G-3881	0.44
		G-3882	0.77
		G-3902	0.97
		G-3903	0.97
		G-3904	0.81
		G-3905	0.82
		G-3906	0.83
		G-3907	0.71
		G-3908	0.73
		G-3909	0.74
		G-3913	0.45
		G-3914	0.51
		G-3915	0.52
		G-3916	0.77
		G-3918	0.77

Table 1–4. Measured average groundwater-level data at the Snapper Creek well field, June 2010–July 2011.—Continued

Stress period	Month and year	USGS local well number	Head elevation (meter above or below [–] NGVD 29)
5	October 2010	G-3877	0.94
		G-3878	0.85
		G-3879	0.22
		G-3881	0.79
		G-3882	0.88
		G-3902	0.94
		G-3903	0.95
		G-3904	0.85
		G-3905	0.87
		G-3906	0.87
		G-3907	0.66
		G-3908	0.78
		G-3909	0.81
		G-3913	0.80
		G-3914	0.84
		G-3915	0.84
		G-3916	0.88
		G-3918	0.87
6	November 2010	G-3877	0.89
		G-3878	0.62
		G-3879	–0.13
		G-3881	0.53
		G-3882	0.80
		G-3902	0.89
		G-3903	0.89
		G-3904	0.61
		G-3905	0.63
		G-3906	0.64
		G-3907	0.32
		G-3908	0.47
		G-3909	0.51
		G-3913	0.54
		G-3914	0.62
		G-3915	0.64
		G-3916	0.80
		G-3917	0.70
		G-3918	0.79
6	December 2010	G-3877	0.77
		G-3878	0.44
		G-3879	–0.36
		G-3881	0.05
		G-3882	0.66
		G-3902	0.78
		G-3903	0.77
		G-3904	0.44
		G-3905	0.45
		G-3906	0.46
		G-3907	0.08
		G-3908	0.22
		G-3909	0.28
		G-3913	0.07
		G-3914	0.19
		G-3915	0.22
		G-3916	0.65
		G-3917	0.64
		G-3918	0.64
8	January 2011	G-3877	0.81
		G-3878	0.68
		G-3879	0.52
		G-3881	0.32
		G-3882	0.69
		G-3902	0.82
		G-3903	0.82
		G-3904	0.69
		G-3905	0.70
		G-3906	0.71
		G-3907	0.57
		G-3908	0.61
		G-3909	0.63
		G-3913	0.32
		G-3914	0.41
		G-3915	0.44
		G-3916	0.69
		G-3917	0.68
		G-3918	0.68

Table 1–4. Measured average groundwater-level data at the Snapper Creek well field, June 2010–July 2011.—Continued

Stress period	Month and year	USGS local well number	Head elevation (meter above or below [–] NGVD 29)
9	February 2011	G-3877	0.80
		G-3878	0.71
		G-3879	0.59
		G-3881	0.40
		G-3882	0.71
		G-3902	0.80
		G-3903	0.80
		G-3904	0.71
		G-3905	0.72
		G-3906	0.72
		G-3907	0.62
		G-3908	0.65
		G-3909	0.65
		G-3913	0.40
		G-3914	0.47
		G-3915	0.51
		G-3916	0.70
		G-3917	0.70
		G-3918	0.69
10	March 2011	G-3877	0.66
		G-3878	0.58
		G-3879	0.48
		G-3881	0.31
		G-3882	0.56
		G-3902	0.65
		G-3903	0.66
		G-3904	0.59
		G-3905	0.58
		G-3906	0.58
		G-3907	0.50
		G-3908	0.53
		G-3909	0.52
		G-3913	0.32
		G-3914	0.36
		G-3915	0.39
		G-3916	0.56
		G-3917	0.55
		G-3918	0.55
11	April 2011	G-3877	0.48
		G-3878	0.08
		G-3879	–0.97
		G-3881	–0.25
		G-3882	0.40
		G-3902	0.48
		G-3903	0.47
		G-3904	0.09
		G-3905	0.09
		G-3906	0.10
		G-3907	–0.38
		G-3908	–0.17
		G-3909	–0.14
		G-3913	–0.22
		G-3914	–0.09
		G-3915	–0.09
		G-3916	0.41
		G-3917	0.39
		G-3918	0.38
12	May 2011	G-3877	0.33
		G-3878	–0.42
		G-3879	–2.19
		G-3881	–1.23
		G-3882	0.09
		G-3902	0.34
		G-3903	0.33
		G-3904	–0.42
		G-3905	–0.39
		G-3906	–0.38
		G-3907	–1.11
		G-3908	–0.87
		G-3909	–0.54
		G-3913	–1.20
		G-3914	–0.94
		G-3915	–0.80
		G-3916	0.10
		G-3917	0.08
		G-3918	0.07

Table 1–4. Measured average groundwater-level data at the Snapper Creek well field, June 2010–July 2011.—Continued

Stress period	Month and year	USGS local well number	Head elevation (meter above or below [–] NGVD 29)
13	June 2011	G-3877	0.04
		G-3878	–1.44
		G-3879	–5.63
		G-3881	–2.60
		G-3882	–0.34
		G-3902	0.04
		G-3903	0.03
		G-3904	–1.45
		G-3905	–1.35
		G-3906	–1.33
		G-3908	–2.34
		G-3913	–2.49
		G-3914	–2.11
		G-3916	–0.33
		G-3917	–0.40
		G-3918	–0.39
14	July 2011	G-3877	0.54
		G-3878	–0.94
		G-3879	–5.15
		G-3881	–1.91
		G-3882	0.21
		G-3902	0.53
		G-3903	0.52
		G-3904	–0.95
		G-3905	–0.85
		G-3906	–0.82
		G-3907	–2.45
		G-3908	–1.75
		G-3909	–1.36
		G-3913	–1.80
		G-3914	–1.40
		G-3915	–1.36
		G-3916	0.21
		G-3917	0.19
		G-3918	0.19

Table 1–5. Measured canal leakage values at Snapper Creek well field, June 2010–July 2011.

[m^3/s, cubic meter per second; —, no data]

Stress period	Month and year	Canal leakage (m^3/s)
1	June 2010	—
2	July 2010	—
3	August 2010	0.92
4	September 2010	0.63
5	October 2010	1.55
6	November 2010	1.03
7	December 2010	0.46
8	January 2011	0.45
9	February 2011	—
10	March 2011	0.61
11	April 2011	0.68
12	May 2011	1.05
13	June 2011	1.60
14	July 2011	1.99

Table 1–6. Summary of water-level and water-quality results for visited sites in Miami-Dade County, Florida, October 2008 through April 2011.

Table 1–6 available in Excel format at http://dx.doi.org/10.3133/sir20155095.

Appendix 2. Conceptual Model Testing

In addition to the construction and calibration of the groundwater model, other realizations were simulated to evaluate the consequences of uncertainty associated with the hydrogeologic framework and boundary conditions. Evaluating the sensitivity of the groundwater model to different hydrogeologic constructions informed the decisions leading to the final calibrated model construction. The sensitivities indicated conceptual areas in which further complexity was or was not needed to better represent the groundwater flow. All of the conceptual realizations were also calibrated to obtain the most realistic parameter set for each model construction.

Effects of Heterogeneity of Hydraulic Properties

Modified realizations of the model were used to test the effects of heterogeneity of hydraulic properties on model calibration and to gage the degree of complexity required to represent the system. Results from two model realizations, homogeneous and simplified heterogeneous realizations, were compared with results from the calibrated model. The homogeneous model realization represents the simplest distribution of hydraulic properties at the study area. Hydraulic conductivity is homogeneous and isotropic with laminar groundwater flow. The calibrated hydraulic conductivity of the homogeneous realization was about 150 meters per day (m/d). Specific storage and specific yield were set to 0.00001 m^{-1} and 0.2, respectively, based on the results of aquifer hydraulic testing (Paillet and Reese, 2000; Bolster and others, 2001; R.S. Reese, U.S. Geological Survey, written commun., 2011). A uniform value of 50 square meters per day (m^2/d) was assigned for the perimeter conductance within the GHB. The vertically heterogeneous model represents preferential and matrix flow with different properties, but with uniform properties within each flow zone. The calibrated hydraulic conductivity values for the preferential and matrix flow zones were about 2,100 and 9 m/d, respectively. Specific storage, specific yield, and perimeter conductance values were consistent with those used in the homogeneous realization. These realizations were compared with the more complex calibrated model, which uses a variable distribution of hydraulic properties within each preferential flow zone and a uniform value of hydraulic conductivity in the matrix flow zone.

The homogeneous realization resulted in observed and simulated values that were more disparate than values from either the vertically heterogeneous realization or the calibrated model with vertical and lateral heterogeneity in the flow zones (fig. 2–1). The vertically heterogeneous model realization shows a tighter cluster of observed and simulated values than the homogeneous model realization, but also shows a substantial bias away from the slope of the line y=x (fig. 2–1). The linear bias was not removed by calibration of the vertically heterogeneous model, but it was removed when lateral heterogeneity was allowed within each preferential flow zone. Allowing complexity in the distribution of hydraulic properties is supported by field data, which indicate variability in hydraulic conductivity of more than three orders of magnitude vertically between matrix preferential flow zones and variability in hydraulic conductivity of more than two orders of magnitude within preferential flow zones.

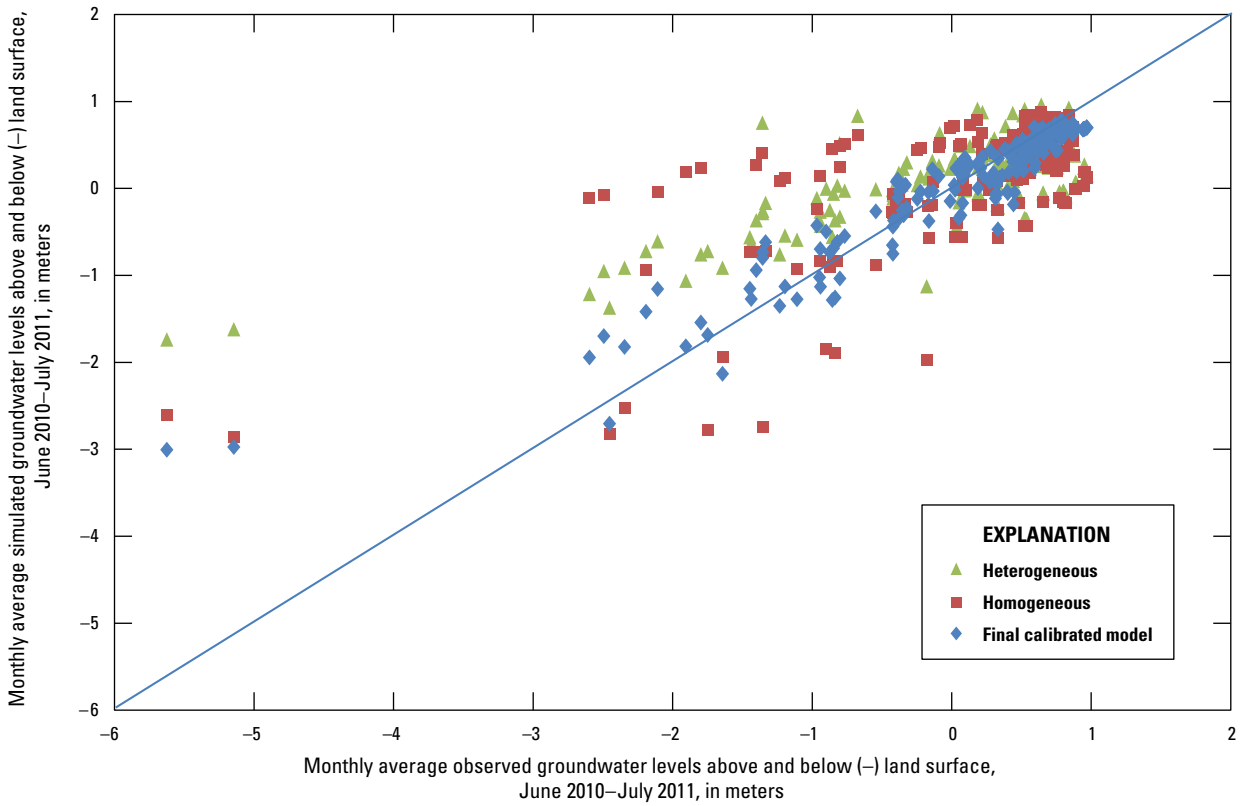

Figure 2-1. Groundwater levels observed and simulated by using the heterogeneous and homogeneous models for the Snapper Creek Canal study area, Miami-Dade County, Florida, June 2010–July 2011.

For more information, contact:
Director, USGS Caribbean-Florida Water Science Center
4446 Pet Lane, Suite 108
Lutz, FL 33559
http://fl.water.usgs.gov

USGS

Nemec and others—**Relations Between Well-Field Pumping and Induced Canal Leakage, Miami-Dade County, Florida, 2010–2011**— Scientific Investigations Report 2015–5095

ISSN 2328-0328 (online)
http://dx.doi.org/10.3133/sir20155095